

Scalar Field Theories with Polynomial Shift Symmetries

Tom Griffin^a, Kevin T. Grosvenor^{b,c}, Petr Hořava^{b,c} and Ziqi Yan^{b,c}

^a*Blackett Laboratory, Department of Physics
Imperial College, London, SW7 2AZ, UK*

^b*Berkeley Center for Theoretical Physics and Department of Physics
University of California, Berkeley, CA, 94720-7300, USA*

^c*Theoretical Physics Group, Lawrence Berkeley National Laboratory
Berkeley, CA 94720-8162, USA*

ABSTRACT: We continue our study of naturalness in nonrelativistic QFTs of the Lifshitz type, focusing on scalar fields that can play the role of Nambu-Goldstone (NG) modes associated with spontaneous symmetry breaking. Such systems allow for an extension of the constant shift symmetry to a shift by a polynomial of degree P in spatial coordinates. These “polynomial shift symmetries” in turn protect the technical naturalness of modes with a higher-order dispersion relation, and lead to a refinement of the proposed classification of infrared Gaussian fixed points available to describe NG modes in nonrelativistic theories. Generic interactions in such theories break the polynomial shift symmetry explicitly to the constant shift. It is thus natural to ask: Given a Gaussian fixed point with polynomial shift symmetry of degree P , what are the lowest-dimension operators that preserve this symmetry, and deform the theory into a self-interacting scalar field theory with the shift symmetry of degree P ? To answer this (essentially cohomological) question, we develop a new graph-theoretical technique, and use it to prove several classification theorems. First, in the special case of $P = 1$ (essentially equivalent to Galileons), we reproduce the known Galileon N -point invariants, and find their novel interpretation in terms of graph theory, as an equal-weight sum over all labeled trees with N vertices. Then we extend the classification to $P > 1$ and find a whole host of new invariants, including those that represent the most relevant (or least irrelevant) deformations of the corresponding Gaussian fixed points, and we study their uniqueness.

Contents

1. Introduction: Landscapes of Naturalness	1
2. Multicritical Nambu-Goldstone Bosons and Polynomial Shift Symmetries	4
2.1. Geometry of the Spacetime with Lifshitz Symmetries	4
2.2. Effective Field Theories of Type A and B Nambu-Goldstone Bosons	5
2.3. Naturalness of Slow Nambu-Goldstone Modes	7
2.4. Polynomial Shift Symmetries	7
2.5. Refinement of the Goldstone Theorem in the Nonrelativistic Regime	9
2.6. Infrared Behavior and the Nonrelativistic CHMW Theorem	10
2.7. Cascading Multicriticality	12
2.8. Polynomial Shift Symmetries as Exact Symmetries	13
3. Galileon Invariants	14
3.1. The Graphical Representation	14
3.2. Galileon Invariants as Equal-Weight Sums of Trees	15
4. Beyond the Galileons	17
4.1. Brute-force Examples	18
4.1.1. $(P, N, \Delta) = (1, 3, 2)$	18
4.1.2. $(P, N, \Delta) = (3, 3, 4)$	18
4.2. Introduction to the Graphical Representation	19
4.2.1. $(P, N, \Delta) = (1, 3, 2)$	19
4.2.2. $(P, N, \Delta) = (3, 3, 4)$	20
4.3. New Invariants via the Graphical Approach	21
4.3.1. The Minimal Invariant: $(P, N, \Delta) = (2, 4, 5)$	22
4.3.2. The Minimal Invariant: $(P, N, \Delta) = (3, 4, 6)$	23
4.3.3. Medusas and Total Derivative Relations	25
4.4. Superposition of Graphs	26
4.4.1. Quadratic Shift ($P=2$)	27
4.4.2. Cubic Shift ($P=3$)	29
4.4.3. Quartic Shift ($P=4$)	30
4.4.4. Quintic Shift ($P=5$)	31
5. Conclusions and Outlook	32
A. Glossary of Graph Theory	33

B. Theorems and Proofs	35
B.1. The Graphical Representation	35
B.1.1. Types of Graphs and Vector Spaces	37
B.1.2. Maps	37
B.1.3. Relations	38
B.1.4. The Consistency Equation and Associations	39
B.2. Building Blocks for Consistency Equations	40
B.2.1. The Loopless Realization of \mathcal{L}/\mathcal{R}	41
B.2.2. Medusas and Spiders	42
B.2.3. Constructing Loopless \times -Relations	45
B.2.4. A Basis for $\mathcal{R}_{\text{loopless}}^\times$	47
B.2.5. Lower Bound on Vertex Degree	52
B.3. Linear Shift Symmetry, Trees and Galileons	53
B.3.1. Minimal Invariants	54
B.3.2. Non-minimal Invariants	56
B.4. Invariants from Superpositions	58
B.4.1. Superposition of a P -invariant and an Exact Invariant	59
B.4.2. Superposition of Minimal Loopless 1-invariants	60
B.5. Unlabeled Invariants	63
C. Coset Construction	64

1. Introduction: Landscapes of Naturalness

Some of the most fundamental questions of modern theoretical physics can be formulated as puzzles of naturalness [1]. Why is the observed cosmological constant so small compared to the Planck scale? Why is the observed Higgs mass so small compared to any high particle-physics scale (be it the quantum gravity scale, or the scale of grand unification, or some other scale of new physics)? In both cases, the expected quantum corrections estimated in the framework of relativistic effective field theory (EFT) predict natural values at a much higher scale, many orders of magnitude larger than the observed ones. The principle of naturalness is rooted in the time-honored physical principles of causality and the hierarchy of energy scales from the microscopic to the macroscopic. It is conceivable that some puzzles of naturalness may only have environmental explanations, based on the landscape of many vacua in the multiverse. However, before we give up naturalness as our guiding principle, it is important to investigate more systematically the “landscape of naturalness”: To map out the various quantum systems and scenarios in which technical naturalness does hold, identifying possible surprises and new pieces of the puzzle that might help restore the power of naturalness in fundamental physics.

One area in which naturalness has not yet been fully explored is nonrelativistic gravity theory [2, 3]. This approach to quantum gravity has attracted a lot of attention in

recent years, largely because of its improved quantum behavior at short distances, novel phenomenology at long distances [4], its connection to the nonperturbative Causal Dynamical Triangulations approach to quantum gravity [5–7], as well as for its applications to holography and the AdS/CFT correspondence of nonrelativistic systems [8–10]. This area of research in quantum gravity is still developing rapidly, with new surprises already encountered and other ones presumably still awaiting discovery. Mapping out the quantum structure of nonrelativistic gravity theories, and in particular investigating the role of naturalness, represents an intriguing and largely outstanding challenge.

Before embarking on a systematic study of the quantum properties of nonrelativistic gravity, one can probe some of the new conceptual features of quantum field theories (QFTs) with Lifshitz-type symmetries in simpler systems, without gauge symmetry, dynamical gravity and fluctuating spacetime geometry. In [11], we considered one of the ubiquitous themes of modern physics: The phenomenon of spontaneous symmetry breaking, in the simplest case of global, continuous internal symmetries. According to Goldstone’s theorem, spontaneous breaking of such symmetries implies the existence of a gapless Nambu-Goldstone (NG) mode in the system. For Lorentz invariant systems, the relativistic version of Goldstone’s theorem is stronger, and we know more: There is a one-to-one correspondence between broken symmetry generators and the NG modes, whose gaplessness implies that they all share the same dispersion relation $\omega = ck$. On the other hand, nonrelativistic systems are phenomenologically known to exhibit a more complex pattern: Sometimes, the number of NG modes is smaller than the number of broken symmetry generators, and sometimes they disperse quadratically instead of linearly. This rich phenomenology opens up the question of a full classification of possible NG modes. A natural and elegant approach to this problem has been pursued in [12]: In order to classify NG modes, one classifies the low-energy EFTs available to control their dynamics.

In the case of systems with nonrelativistic Lifshitz symmetries, this approach suggests a classification of NG modes into two categories [12]: Type A, and Type B NG modes. Each Type A mode is associated with a single broken symmetry generator, and each Type B mode with a pair. Upon closer inspection [11], it turns out that even such simple examples of Lifshitz-type QFTs exhibit rich and surprising features, often contrasting or contradicting the intuition developed in relativistic QFTs. Our analysis of naturalness in the patterns of spontaneous symmetry breaking in systems with Lifshitz symmetries has revealed a refined hierarchy of the Type A and B universality classes of NG dynamics, with rich low-energy phenomenology dominated by multicritical NG modes whose dispersion is of higher degree in momentum. These results shed some new, and perhaps surprising, light on the concept of naturalness in nonrelativistic quantum field theory. However, as usual, the naturalness of the multicritical dispersion relation turns out to be protected by a symmetry. This new kind of symmetry is generated by the shifts of the NG fields by a polynomial in spatial coordinates.¹

In this paper, we continue our investigation of scalar field theories with such polynomial

¹This symmetry is a natural generalization of two types of symmetries well-known in the literature: The famous constant shift symmetry observed in systems with relativistic NG modes, and the shift linear in the spacetime coordinates known from the relativistic theory of Galileons [13].

shift symmetries of degree P . The paper is organized into several relatively self-contained blocks. In §2, we review the physics background and discuss the structure of multicritical symmetry breaking in nonrelativistic systems of the Lifshitz type, summarizing and expanding on the findings of [11, 14]. We discuss the Goldstone theorem in the nonrelativistic regime, and give the refined classification of Nambu-Goldstone modes for systems with Lifshitz symmetries into two hierarchies of multicritical fixed points of Type A_n and B_{2n} , with $n = 1, 2, \dots$. We present the nonrelativistic analog of the Coleman-Hohenberg-Mermin-Wagner (CHMW) theorem, and discuss its implications for the dynamics of the multicritical NG modes. Throughout, we stress the role played by the polynomial shift symmetry, as an approximate symmetry restored at the Gaussian infrared fixed points. In many general examples of multicritical symmetry breaking, the polynomial shift symmetry is broken by the self-interactions of the NG modes. It is then natural to ask: What if we impose the polynomial shift symmetry as an exact symmetry? What is the lowest-dimension operator that can be added to the action while preserving the symmetry? This is the task we address in the remainder of the paper.

The classification of Lagrangians invariant under the polynomial shift of degree P up to a total derivative (which we will refer to as “ P -invariants” for short) is essentially a cohomological problem. In §3, we consider the polynomial-shift invariants in the simplest case of linear shifts (i.e., “1-invariants”). In order to prepare for the general case of $P > 1$, we develop a novel technique, based on graph theory. Having rephrased the defining relation for the invariants into the language of graphs, we can address the classification problem using the abstract mathematical machinery of graph theory. The basic ingredients of this technique are explained as needed in §3 and §4. However, we relegate all the technicalities of the graphical technique into a self-contained Appendix B (preceded by Appendix A, in which we offer a glossary of the basic terms from graph theory). Appendix B is rather mathematical in nature, as it contains a systematic exposition of all our definitions, theorems and proofs that we found useful in the process of generating the invariants discussed in the body of the paper. The good news is that Appendix B is not required for the understanding of the results presented in §3 and §4: Once the invariants have been found using the techniques in Appendix B, their actual invariance can be checked by explicit calculation (for example, on a computer). In this sense, the bulk of the paper (§3 and §4) is also self-contained, and can be read independently of the Appendices.

The N -point 1-invariants discussed in §3 are known in the literature, where they have been generated in the closely related context of the relativistic Galileon theories [13]. While it is reassuring to see that our graph-theoretical technique easily reproduces these known 1-invariants, the novelty of our results presented in §3 lies elsewhere: We find a surprisingly simple and elegant interpretation of the known N -point 1-invariants in the language of graphs. They are simply given by the equal-weight sum over all labeled trees with N vertices!

In §4 we move beyond the 1-invariants, and initiate a systematic study of P -invariants with $P > 1$, organized in the order of their scaling dimension. We find several series of invariants; some of them we prove to be the unique and most relevant (or, more accurately, least irrelevant) N -point P -invariants, while others represent hierarchies of P -invariants of

higher dimensions. We also show how to construct higher P -invariants from superposing several graphs that represent invariants of lower P . Appendix C contains a brief discussion of the connection between our invariant Lagrangians and the Chevalley-Eilenberg Lie algebra cohomology theory. In §5 we present our conclusions.

2. Multicritical Nambu-Goldstone Bosons and Polynomial Shift Symmetries

Some surprising features of naturalness in the regime of nonrelativistic field theories are illustrated by considering one of the classic problems in physics: The classification of NG modes associated with possible patterns of spontaneous breaking of continuous global internal symmetries. In this section, we summarize and explain the results found in [11, 14], which lead to a refinement in the classification of NG modes in systems with Lifshitz symmetries, characterized by a multicritical behavior which is technically natural, and protected by a symmetry.

2.1. Geometry of the Spacetime with Lifshitz Symmetries

For clarity and simplicity, as in [11], in this paper we focus on systems on the flat spacetime with Lifshitz spacetime symmetries. We define this spacetime to be $M = \mathbf{R}^{D+1}$ with a preferred foliation \mathcal{F} by fixed spatial slices \mathbf{R}^D , and equipped with a flat metric. Such a spacetime with the preferred foliation \mathcal{F} would for example appear as a ground-state solution of nonrelativistic gravity [2] whose gauge symmetry is given by the group of foliation-preserving spacetime diffeomorphisms, $\text{Diff}(M, \mathcal{F})$ (or a nonrelativistic extension thereof [15]). It is useful to parametrize M by coordinates $(t, \mathbf{x} = \{x^i, i = 1, \dots, D\})$, such that the leaves of \mathcal{F} are the leaves of constant t , and the metric has the canonical form

$$g_{ij}(t, \mathbf{x}) = \delta_{ij}, \quad \mathcal{N}(t, \mathbf{x}) = 1, \quad \mathcal{N}_i(t, \mathbf{x}) = 0 \quad (2.1)$$

(here g_{ij} is the spatial metric on the leaves of \mathcal{F} , \mathcal{N} is the lapse function, and \mathcal{N}_i the shift vector).

The isometries of this spacetime are, by definition, those elements of $\text{Diff}(M, \mathcal{F})$ that preserve this flat metric [16]. Explicitly, the connected component of this isometry group is generated by infinitesimal spatial rotations and spacetime translations,

$$\delta t = b, \quad \delta x^i = \omega^i_j x^j + b^i, \quad \omega_{ij} = -\omega_{ji}. \quad (2.2)$$

At fixed points of the renormalization group, systems with Lifshitz isometries develop an additional scaling symmetry, generated by

$$\delta x^i = \lambda x^i, \quad \delta t = z \lambda t. \quad (2.3)$$

The dynamical critical exponent z is an important observable associated with the fixed point, and characterizes the degree of anisotropy between space and time at the fixed point.

The connected component of the group of isometries of our spacetime M with the flat metric (2.1) is generated by (2.2), and we will refer to it as the ‘‘Lifshitz symmetry’’ group.² The full isometry group of this spacetime has four disconnected components, which can be obtained by combining the Lifshitz symmetry group generated by (2.2) with two discrete symmetries: The time-reversal symmetry \mathcal{T} , and a discrete symmetry \mathcal{P} that reverses the orientation of space. In this paper, we shall be interested in systems that are invariant under the Lifshitz symmetry group. Note that this mandatory Lifshitz symmetry does not contain either the discrete symmetries \mathcal{T} and \mathcal{P} , or the anisotropic scaling symmetry (2.3).

2.2. Effective Field Theories of Type A and B Nambu-Goldstone Bosons

We are interested in the patterns of spontaneous symmetry breaking of global continuous internal symmetries in the flat spacetime with the Lifshitz symmetries, as defined in the previous paragraph. Our analysis gives an example of phenomena that are novel to Goldstone’s theorem in nonrelativistic settings, and can in principle be generalized to nonrelativistic systems with even less symmetry.

An elegant strategy has been proposed in [12]: In order to classify Nambu-Goldstone modes, we can classify the corresponding EFTs available to describe their low-energy dynamics. In this EFT approach, we organize the terms in the effective action by their increasing dimension. Such dimensions are defined close enough to the infrared fixed point. However, until we identify the infrared fixed point, we don’t a priori know the value of the dynamical critical exponent, and hence the relative dimension of the time and space derivatives – it is then natural to count the time derivatives and spatial derivatives separately. Consider first the ‘‘potential terms’’ in the action, i.e., terms with no time derivatives. The general statement of Goldstone’s theorem implies that non-derivative terms will be absent, and the spatial rotational symmetry further implies that (for $D > 1$) all derivatives will appear in pairs contracted with the flat spatial metric. Hence, we can write the general ‘‘potential term’’ in the action as

$$S_{\text{eff},V} = \int dt d\mathbf{x} \left\{ \frac{1}{2} g_{IJ}(\pi) \partial_i \pi^I \partial_i \pi^J + \dots \right\} \quad (2.4)$$

where $g_{IJ}(\pi)$ is the most general metric on the vacuum manifold which is compatible with all the global symmetries, and \dots stand for all the terms of higher order in spatial derivatives.

If the system is also invariant under the primitive version \mathcal{T} of time reversal, defined as the transformation that acts trivially on fields,

$$\mathcal{T} : \begin{cases} t \rightarrow -t, \\ \pi^I \rightarrow \pi^I, \end{cases} \quad (2.5)$$

²It would be natural to refer to M with the flat metric (2.1) as the ‘‘Lifshitz spacetime’’. Unfortunately, this term already has another widely accepted meaning in the holography literature, where it denotes the curved spacetime geometry in one dimension higher, whose isometries realize the Lifshitz symmetries (2.2) plus the Lifshitz scaling symmetry (2.3) for some fixed value of z [17].

the time derivatives will similarly have to appear in pairs, and the kinetic term will be given by

$$S_{\text{eff},K} = \int dt d\mathbf{x} \left\{ \frac{1}{2} h_{IJ}(\pi) \dot{\pi}^I \dot{\pi}^J + \dots \right\}, \quad (2.6)$$

where again h_{IJ} is a general metric on the vacuum manifold compatible with all symmetries, but not necessarily equal to the g_{IJ} that appeared in (2.4); and \dots are higher-derivative terms.

However, invariance under \mathcal{T} is not mandated by the Lifshitz symmetry. If it is absent, the Lifshitz symmetries allow a new, more relevant kinetic term,

$$\tilde{S}_{\text{eff},K} = \int dt d\mathbf{x} \left\{ \Omega_I(\pi) \dot{\pi}^I + \dots \right\}, \quad (2.7)$$

assuming one can define the suitable object $\Omega_I(\pi)$ on the vacuum manifold so that all the symmetry requirements are satisfied, and $\Omega_I(\pi) \dot{\pi}^I$ is not a total derivative. Since $\Omega_I(\pi)$ plays the role of the canonical momentum conjugate to π^I , if such Ω -terms are present in the action, they induce a natural canonical pairing on an even-dimensional subset of the coordinates on the vacuum manifold.

In specific dimensions, new terms in the effective action that are odd under spatial parity \mathcal{P} may exist. For example, in $D = 2$ spatial dimensions, we can add new terms to the “potential” part of the action, of the form

$$\tilde{S}_{\text{eff},V} = \int dt d\mathbf{x} \left\{ \frac{1}{2} \Omega_{IJ}(\pi) \varepsilon_{ij} \partial_i \pi^I \partial_j \pi^J + \dots \right\}, \quad (2.8)$$

where Ω_{IJ} is any two-form on the vacuum manifold that respects all the symmetries.³ In the interest of simplicity, we wish to forbid such terms, and will do so by imposing the \mathcal{P} invariance of the action, focusing on the symmetry breaking patterns that respect spatial parity. This condition can of course be easily relaxed, without changing our conclusions significantly.

This structure of low-energy effective theories suggests the following classification of NG modes, into two general types:

- Type A: One NG mode per broken symmetry generator (not paired by Ω_I). The low-energy dispersion relation is linear, $\omega \propto k$.
- Type B: One NG mode per each pair of broken symmetry generators (paired by Ω_I). The low-energy dispersion relation is quadratic, $\omega \propto k^2$.

In general, Type A and Type B NG modes may coexist in one system. Some examples from condensed matter theory can be found in [12].

Based on the intuition developed in the context of relativistic quantum field theory, one might be tempted to conclude that everything else would be fine tuning, as quantum corrections would be likely to generate large terms of the form (2.4) in the effective action if we attempted to tune them to zero.

³For example, if $\Omega_I(\pi)$ suitable for (2.7) exist, one can take $\Omega_{IJ} = \partial_{[I} \Omega_{J]}$.

2.3. Naturalness of Slow Nambu-Goldstone Modes

Our careful study of a number of explicit examples revealed [11] that the naive intuition about fine-tuning summarized in the previous paragraph is incorrect. It turns out that the leading spatial-derivative term in (2.4) can be naturally small (or even zero), as we illustrated in [11] by explicit calculations of loop corrections in a series of examples. The leading contribution to $S_{\text{eff},V}$ then comes at fourth order in spatial derivatives; schematically,

$$S_{\text{eff},V} = \int dt d\mathbf{x} \left\{ \frac{1}{2} g_{IJ}(\pi) \partial^2 \pi^I \partial^2 \pi^J + \dots \right\}, \quad (2.9)$$

where the “...” stand for all other terms of order four and higher in ∂_i . The dispersion relation of this NG mode at the Gaussian infrared fixed point is then $\omega \propto k^2$ (or $\omega \propto k^4$), if the kinetic term is of Type A as in (2.6) (or of Type B as in (2.7)). The reason why this behavior does not require fine tuning is simple [11]: As we approach this new Gaussian infrared fixed point, the theory develops a new enhanced symmetry. Specifically, the symmetry that protects the Type A NG modes with the quadratic dispersion relation is a generalization of the constant shift symmetry of conventional NG modes: The generators of the new symmetry act by shifting each field component π^I by a quadratic polynomial in spatial coordinates,

$$\delta \pi^I(t, \mathbf{x}) = a_{ij}^I x^i x^j + a_i^I x^i + a_0^I. \quad (2.10)$$

The leading, quadratic part of this symmetry forbids the term (2.4) allowing only terms of fourth order in ∂_i and higher to appear in the action in the free-field limit. The subleading linear and constant terms have been included in (2.10) because they would be generated anyway by the action of spatial translations and rotations, which are a part of the assumed Lifshitz symmetry of the system. Similarly, quadratic shift symmetries can also be extended to the Gaussian limit of Type B NG modes. At the Gaussian fixed point, $\Omega_I(\pi)$ of (2.7) reduces to a linear function of π , such that $\tilde{S}_{\text{eff},K}$ is invariant under the quadratic shift up to a total derivative, and the extra shift symmetry yields Type B NG modes with a quartic dispersion relation.

This construction can obviously be iterated. The quadratic shift symmetry (2.10) can be promoted to a polynomial shift symmetry by polynomials of degree $P = 2, 3, \dots$, leading to a natural protection of higher-order dispersion relations $\omega \propto k^n$ (or $\omega \propto k^{2n}$) for Type A (or Type B) NG modes.

2.4. Polynomial Shift Symmetries

Since the polynomial shift symmetries act on the fields $\pi^I(t, \mathbf{x})$ separately component by component, from now on we shall focus on just one field component, and rename it $\phi(t, \mathbf{x})$.

The generators of the polynomial shift symmetry of degree P act on ϕ by

$$\delta_P \phi = a_{i_1 \dots i_P} x^{i_1} \dots x^{i_P} + \dots + a_i x^i + a. \quad (2.11)$$

The multicritical Gaussian fixed point with dynamical exponent $z = n$ is described by

$$S_n = \int dt d\mathbf{x} \left\{ \frac{1}{2} \dot{\phi}^2 - \frac{1}{2} c_n^2 (\partial_{i_1} \dots \partial_{i_n} \phi) (\partial_{i_1} \dots \partial_{i_n} \phi) \right\}. \quad (2.12)$$

In fact, it is a one-parameter family of fixed points, parametrized by the real positive coupling ζ_n^2 . (Sometimes it is convenient to absorb ζ_n into the rescaling of space, and we will often do so when there is no competition between different fixed points.)

The action S_n is invariant under polynomial shift symmetries (2.11) of degree $P \leq 2n - 1$: It is strictly invariant under the symmetries of degree $P < n$, and invariant up to a total derivative for degrees $n \leq P \leq 2n - 1$.

Morally, this infinite hierarchy of symmetries can be viewed as a natural generalization of the Galileon symmetry, proposed in [13] and much studied since, mostly in the cosmological literature. In the case of the Galileons, the theory is relativistic, and the symmetry is linear in space-time coordinates. The requirement of relativistic invariance is presumably the main reason that has precluded the generalization of the Galileon symmetries past the linear shift: The higher polynomial shift symmetries in spacetime coordinates would lead to actions dominated by higher time derivatives, endangering perturbative unitarity.

So far, we considered shifts by generic polynomials of degree P , whose coefficients $a_{i_1 \dots i_\ell}$ are arbitrary symmetric real tensors of rank ℓ for $\ell = 0, \dots, P$. We note here in passing that for degrees $P \geq 2$, the polynomial shift symmetries allow an interesting refinement. To illustrate this feature, we use the example of the quadratic shift,

$$\delta_2 \phi = a_{ij} x^i x^j + a_i x^i + a_0. \quad (2.13)$$

The coefficient a_{ij} of the quadratic part is a general symmetric 2-tensor. It can be decomposed into its traceless part \tilde{a}_{ij} and the trace part a_{ii} ,

$$a_{ij} = \tilde{a}_{ij} + \frac{1}{D} a_{kk} \delta_{ij}. \quad (2.14)$$

Since this decomposition is compatible with the spacetime Lifshitz symmetries (2.2), one can restrict the symmetry group to be generated by a strictly smaller invariant subalgebra in the original algebra generated by a_{ij} . For example, setting the traceless part \tilde{a}_{ij} of the quadratic shift symmetry to zero reduces the number of independent generators from $(D+2)(D+1)/2$ to $D+2$, but it is still sufficient to prevent $\partial_i \phi \partial_i \phi$ from being an invariant under the smaller symmetry. This intriguing pattern extends to $P > 2$, leading to intricate hierarchies of polynomial shift symmetries whose coefficients $a_{i_1 \dots i_\ell}$ have been restricted by various invariant conditions. As another example, invariance under the traceless part has been studied in [18]. In the interest of simplicity, we concentrate in the rest of this paper on the maximal case of polynomial shift symmetries with arbitrary unrestricted real coefficients $a_{i_1 \dots i_\ell}$.

The invariance of the action under each polynomial shift leads to a conserved Noether current. Each such current then implies a set of Ward identities on the correlation functions and the effective action. Take, for example, the case of $n = 2$ in (2.12): The currents for the infinitesimal shift by a general function $a(\mathbf{x})$ of the spatial coordinates x^i are collectively given by

$$\mathcal{J}_t = a(\mathbf{x}) \dot{\phi}, \quad \mathcal{J}_i = a(\mathbf{x}) \partial_i \partial^2 \phi - \partial_j a(\mathbf{x}) \partial_i \partial_j \phi + \partial_i \partial_j a(\mathbf{x}) \partial_j \phi - \partial_i \partial^2 a(\mathbf{x}) \phi, \quad (2.15)$$

and their conservation requires

$$\dot{\mathcal{J}}_t + \partial_i \mathcal{J}_i \equiv a(\mathbf{x}) \left\{ \ddot{\phi} + (\partial^2)^2 \phi \right\} - (\partial^2)^2 a(\mathbf{x}) \phi = 0. \quad (2.16)$$

The term in the curly brackets is zero on shell, and the current conservation thus reduces to the condition $(\partial^2)^2 a(\mathbf{x}) \phi = 0$, which is certainly satisfied by a polynomial of degree three,

$$a(\mathbf{x}) = a_{ijk} x^i x^j x^k + a_{ij} x^i x^j + a_i x^i + a. \quad (2.17)$$

Note that if we start instead with the equivalent form of the classical action

$$\tilde{S}_2 = \int dt d\mathbf{x} \left\{ \frac{1}{2} \dot{\phi}^2 - \frac{1}{2} (\partial_i \partial_i \phi)^2 \right\}, \quad (2.18)$$

the Noether currents will be related, as expected, by

$$\begin{aligned} \tilde{\mathcal{J}}_t &= \mathcal{J}_t, \\ \tilde{\mathcal{J}}_i &= a(\mathbf{x}) \partial_i \partial^2 \phi - \partial_i a(\mathbf{x}) \partial^2 \phi + \partial^2 a(\mathbf{x}) \partial_i \phi - \partial_i \partial^2 a(\mathbf{x}) \phi \\ &= \mathcal{J}_i + \partial_j [\partial_i a(\mathbf{x}) \partial_j \phi - \partial_j a(\mathbf{x}) \partial_i \phi]. \end{aligned} \quad (2.19)$$

From these conserved currents, one can formally define the charges

$$Q[a] = \int_{\Sigma} d\mathbf{x} \mathcal{J}_t. \quad (2.20)$$

However, for infinite spatial slices $\Sigma = \mathbf{R}^D$, such charges are all zero on the entire Hilbert space of states generated by the normalizable excitations of the fields ϕ . This behavior is quite analogous to the standard case of NG modes invariant under the constant shifts, and it simply indicates that the polynomial shift symmetry is being spontaneously broken by the vacuum.

2.5. Refinement of the Goldstone Theorem in the Nonrelativistic Regime

In its original form, Goldstone's theorem guarantees the existence of a gapless mode when a global continuous internal symmetry is spontaneously broken. However, in the absence of Lorentz symmetry, it does not predict the number of such modes, or their low-energy dispersion relation.

The classification of the effective field theories which are available to describe the low-energy limit of the Nambu-Goldstone mode dynamics leads to a natural refinement of the Goldstone theorem in the nonrelativistic regime. In the specific case of spacetimes with Lifshitz symmetry, we get two hierarchies of NG modes:

- Type A: One NG mode per broken symmetry generator (not paired by Ω_I) The low-energy dispersion relation is $\omega \propto k^n$, where $n = 1, 2, 3, \dots$
- Type B: One NG mode per each pair of broken symmetry generators (paired by Ω_I). The low-energy dispersion relation is $\omega \propto k^{2n}$, where $n = 1, 2, 3, \dots$

It is natural to label the members of these two hierarchies by the value of the dynamical critical exponent of their corresponding Gaussian fixed point. From now on, we will refer to these multicritical universality classes of Nambu-Goldstone modes as “Type A_n ” and “Type B_{2n} ”, respectively.

The following few comments may be useful:

- (1) While Type B NG modes represent a true infinite hierarchy of consistent fixed points, the Type A NG modes hit against the nonrelativistic analog of the Coleman-Hohenberg-Mermin-Wagner (CHMW) theorem: At the critical value of $n = D$, they develop infrared singularities and cease to exist as well-defined quantum fields. We comment on this behavior further in §2.6.
- (2) Type A preserve \mathcal{T} invariance, while Type B break \mathcal{T} . (This does not mean that a suitable time reversal invariance cannot be defined on Type B modes, but it would have to extend \mathcal{T} of (2.5) to act nontrivially on the fields.)
- (3) Our classification shows the existence of A_n and B_{2n} hierarchies of NG modes described by Gaussian fixed points, and therefore represents a refinement of the classifications studied in the literature so far. However, it does not pretend to completeness: We find it plausible that nontrivial fixed points (and fixed points at non-integer values of n) suitable for describing NG modes may also exist. In this sense, the full classification of all possible types of nonrelativistic NG dynamics – even under the assumption of Lifshitz symmetries – still remains a fascinating open question.
- (4) For simplicity, we worked under the assumption of spacetime Lifshitz symmetry. Obviously, this simplifying restriction can be removed, and the classification of multicritical NG modes in principle extended to cases whereby some of the the spacetime symmetries are further broken by additional features of the system – such as spatial anisotropy, layers, an underlying lattice structure, etc. We also expect that the classification can be naturally extended to Nambu-Goldstone fermions associated with spontaneous breaking of symmetries associated with supergroups. Such generalizations, however, are beyond the scope of this paper.

2.6. Infrared Behavior and the Nonrelativistic CHMW Theorem

In this section, we consider the Type A_n and Type B_{2n} hierarchies of NG modes, and their infrared behavior. For simplicity, we will focus on theories that consist of Type A_n (or Type B_n) NG modes with a fixed n , and leave the generalizations to interacting systems that mix different types of NG modes for future studies.

In relativistic systems, all NG bosons – if they exist – are Type A_1 . However, whether or not the corresponding symmetry is spontaneously broken famously depends on the spacetime dimension. This phenomenon is controlled by the celebrated theorem discovered independently in condensed matter by Mermin and Wagner [19] and by Hohenberg [20], and in high-energy physics by Coleman [21]; we therefore refer to it, in the alphabetical order, as the Coleman-Hohenberg-Mermin-Wagner (CHMW) theorem.

This famous CHMW theorem states that no spontaneous breaking of global continuous internal symmetries is possible in $1 + 1$ spacetime dimensions. The proof is beautifully simple: $1 + 1$ represents the “lower critical dimension” of the massless scalar field ϕ , defined as the dimension where ϕ is formally dimensionless at the Gaussian fixed point. Quantum mechanically, this means that its propagator is logarithmically divergent, and we need to regulate it by introducing an infrared regulator μ_{IR} :

$$\langle \phi(x)\phi(0) \rangle = \int \frac{d^2k}{(2\pi)^2} \frac{e^{ik \cdot x}}{k^2 + \mu_{\text{IR}}^2} \approx -\frac{1}{2\pi} \log(\mu_{\text{IR}}|x|) + \text{const.} + \mathcal{O}(\mu_{\text{IR}}|x|). \quad (2.21)$$

The asymptotic expansion in (2.21), valid in the regime $\mu_{\text{IR}}|x| \ll 1$, clearly shows that as we try to take $\mu_{\text{IR}} \rightarrow 0$ the propagator stays sensitive at long scales to the infrared regulator μ_{IR} . We can still construct various composite operators out of derivatives and exponentials of ϕ , yielding consistent and finite renormalized correlation functions in the $\mu_{\text{IR}} \rightarrow 0$ limit, but the field ϕ itself does not exist as a quantum object. And since the candidate NG mode ϕ does not exist, the corresponding symmetry could never have been broken in the first place, which concludes the proof.

Going back to the general class of Type A_n NG modes, we find an intriguing nonrelativistic analog of the CHMW theorem. The dimension of $\phi(t, \mathbf{x})$ at the A_n Gaussian fixed point in $D + 1$ dimensions – measured in the units of spatial momentum – is

$$[\phi(t, \mathbf{x})]_{A_n} = \frac{D - n}{2}. \quad (2.22)$$

The Type A_n field ϕ is at its lower critical dimension when $D = n$. Its propagator also requires an infrared regulator. There are many ways how to introduce μ_{IR} in this case, for example by

$$\langle \phi(t, \mathbf{x})\phi(0) \rangle = \int \frac{d\omega d^D\mathbf{k}}{(2\pi)^{D+1}} \frac{e^{i\mathbf{k} \cdot \mathbf{x} - i\omega t}}{\omega^2 + k^{2D} + \mu_{\text{IR}}^{2D}}, \quad (2.23)$$

or by

$$\langle \phi(t, \mathbf{x})\phi(0) \rangle = \int \frac{d\omega d^D\mathbf{k}}{(2\pi)^{D+1}} \frac{e^{i\mathbf{k} \cdot \mathbf{x} - i\omega t}}{\omega^2 + (k^2 + \mu_{\text{IR}}^2)^D}. \quad (2.24)$$

Either way, as we try to take $\mu_{\text{IR}} \rightarrow 0$, the asymptotics of the propagator again behaves logarithmically, both in space

$$\langle \phi(t, \mathbf{x})\phi(0) \rangle \approx -\frac{1}{(4\pi)^{D/2}\Gamma(D/2)} \log(\mu_{\text{IR}}|\mathbf{x}|) + \dots \quad \text{for } |\mathbf{x}|^D \gg t \quad (2.25)$$

and in time,

$$\langle \phi(t, \mathbf{x})\phi(0) \rangle \approx -\frac{1}{(4\pi)^{D/2}D\Gamma(D/2)} \log(\mu_{\text{IR}}^D t) + \dots \quad \text{for } |\mathbf{x}|^D \ll t. \quad (2.26)$$

Most importantly, the propagator remains sensitive to the infrared regulator μ_{IR} . Consequently, we obtain the nonrelativistic, multicritical version of the CHMW theorem for Type A NG modes and their associated symmetry breaking:

The Type A_n would-be NG mode $\phi(t, \mathbf{x})$ at its lower critical dimension $D = n$ exhibits a propagator which is logarithmically sensitive to the infrared regulator μ_{IR} , and therefore $\phi(t, \mathbf{x})$ does not exist as a quantum mechanical object. Consequently, no spontaneous symmetry breaking with Type A_n NG modes is possible in $D = n$ dimensions.

By extension, this also invalidates all Type A_n would-be NG modes with $n > D$: Their propagator grows polynomially at long distances, destabilizing the would-be condensate and disallowing the associated symmetry breaking pattern.

In contrast, in the Type B_n case (and assuming that all the NG field components are assigned the same dimension), we have

$$[\phi(t, \mathbf{x})]_{B_{2n}} = \frac{D}{2},$$

and the lower critical dimension is $D = 0$. Hence, in all dimensions $D > 0$, the Type B_{2n} NG modes are free of infrared divergences and well-defined quantum mechanically for all $n = 1, 2, \dots$, and the Type B nonrelativistic, multicritical CHMW theorem is limited to the following statement:

The Type B_{2n} symmetry breaking is possible in any $D > 0$ and for any $n = 1, 2, \dots$

In the special cases for Type A_2 and Type B_2 NG modes, the multicritical CHMW theorems stated above reproduce the results reported in [22].

2.7. Cascading Multicriticality

The conclusions of the nonrelativistic CHMW theorem appear rather unfavorable for Type A_n NG modes with $n \geq D$. However, unlike in the relativistic case of $n = 1$ in $1 + 1$ dimensions, the nonrelativistic systems offer an intriguing way out [14], as we now illustrate for the case of the lower critical dimension $D = n$, with $D > 1$.

At this Gaussian fixed point, the propagator for ϕ is logarithmically sensitive to the infrared regulator. However, all is not lost – unlike in the relativistic case, the system can now provide its own natural infrared regulator, and flow under the influence of some of the relevant terms to another infrared fixed point of Type $A_{n'}$, with a lower value of $n' < n$. And we know that this phenomenon can be arranged to happen hierarchically, in a pattern protected by the hierarchical breaking of the polynomial symmetries. Thus, we can break the polynomial shift symmetry at a high energy scale μ only partially, to a polynomial symmetry of a lower degree which is then broken at a lower energy scale μ' . This process can continue until at some low scale μ'' the symmetry is broken all the way to the constant shift and $n'' = 1$.⁴ This process of consecutive partial symmetry breaking opens up a hierarchy of energy scales

$$\mu \gg \mu' \gg \dots \gg \mu'', \quad (2.27)$$

⁴In the case of pseudo-NG modes, even the constant shift symmetry can be broken explicitly at some scale.

over which the propagator for ϕ exhibits a cascading behavior: First it appears logarithmic and the formation of a condensate seems precluded, and then it undergoes a series of crossovers to lower values of $z < D$ until in the far infrared the condensate is no longer destabilized by infrared fluctuations. The separation between two consecutive scales μ and μ' can be kept large, as a result of the symmetry that is given by a larger-degree polynomial at scale μ than at scale μ' . All in all, whether or not the original continuous global internal symmetry (for which the field is the NG mode) is spontaneously broken is now a question about the competition of various scales in the system.

2.8. Polynomial Shift Symmetries as Exact Symmetries

We have established a new infinite sequence of symmetries in scalar field theories, and have shown that they can protect the smallness of quantum mechanical corrections to their low-energy dispersion relations near the Gaussian fixed points. The symmetries are exact at the infrared Gaussian fixed point, and turning on interactions typically breaks them explicitly – as we have seen in the series of examples in [11]. Yet, the polynomial shift symmetry at the Gaussian fixed point is useful for the interacting theory as well: It controls the interaction terms, allowing them to be naturally small, parametrized by the amount ε of the explicit polynomial symmetry breaking near the fixed point.

Generally, this explicit breaking by interactions breaks the polynomial shift symmetries of NG modes all the way to the constant shift, which remains mandated by the original form of the Goldstone theorem (guaranteeing the existence of gapless modes).⁵ However, one can now turn the argument around, and ask the following question: Starting at a given Type A_n or B_{2n} fixed point, what are the lowest-dimension scalar composite operators that involve N fields ϕ and respect the polynomial shift symmetry of degree P exactly, up to a total derivative? Such operators can be added to the action, and for $N = 3, 4, \dots$ they represent self-interactions of the system, invariant under the polynomial shift of degree P . More generally, one can attempt to classify all independent composite operators invariant under the polynomial shift symmetry of degree P , organized in the order of their increasing dimensions.

These are the questions on which we focus in the rest of this paper. In order to provide some answers, we will first translate this classification problem into a more precise mathematical language, and then we will develop techniques – largely based on abstract graph theory – that lead us to systematic answers. For some low values of the degree P of the polynomial symmetry and of the number N of fields involved, we can even find the most relevant invariants and prove their uniqueness.

⁵Strictly speaking, moving away from the Gaussian fixed point by turning on the self-interactions generally yields additional corrections to the constant shift symmetries, if the underlying symmetry group of the interacting theory is non-Abelian. Such non-Abelian corrections vanish at the Gaussian fixed point, and each NG component effectively becomes an Abelian field with its own constant shift symmetry. In this paper, we will concentrate solely on the simplest Abelian case, with one Type A NG field ϕ and the symmetry group $U(1)$.

3. Galileon Invariants

Consider a quantum field theory of a single scalar field $\phi(t, \mathbf{x})$ in D spatial dimensions and one time dimension. Consider the transformation of the field which is linear in spatial coordinates: $\delta\phi = a_i x^i + a_0$, where a_i and a_0 are arbitrary real coefficients. Other than the split between time and space and the exclusion of the time coordinate from the linear shift transformation, this is the same as the theory of the Galileon [13].

The goal is to find Lagrangian terms which are invariant (up to a total derivative) under this linear shift transformation. We will classify the Lagrangian terms by their numbers of fields N and derivatives 2Δ . Imposing spatial rotation invariance requires that spatial derivatives be contracted in pairs by the flat metric δ_{ij} . Thus Δ counts the number of contracted pairs of derivatives. It is easy to find Lagrangian terms which are exactly invariant (i.e., not just up to a total derivative): Let $\Delta \geq N$ and let at least two spatial derivatives act on every ϕ . For the linear shift case, all terms with at least twice as many derivatives as there are fields are equal to exact invariants, up to total derivatives (Theorem 4). However, it is possible for a term to have fewer derivatives than this and still be invariant up to a non-vanishing total derivative. For fixed N , the terms with the lowest Δ are more relevant in the sense of the renormalization group. Therefore, we will focus on invariant terms with the lowest number of derivatives, which we refer to as *minimal invariants*.

These minimal invariants have already been classified for the case of the linear shift. There is a unique (up to total derivatives and an overall constant prefactor) N -point minimal invariant, which contains $2(N - 1)$ derivatives (i.e., $\Delta = N - 1$). These are listed below up to $N = 5$.

$$L_{1\text{-pt}} = \phi, \tag{3.1a}$$

$$L_{2\text{-pt}} = \partial_i \phi \partial_i \phi, \tag{3.1b}$$

$$L_{3\text{-pt}} = 3 \partial_i \phi \partial_j \phi \partial_i \partial_j \phi, \tag{3.1c}$$

$$L_{4\text{-pt}} = 12 \partial_i \phi \partial_i \partial_j \phi \partial_j \partial_k \phi \partial_k \phi + 4 \partial_i \phi \partial_j \phi \partial_k \phi \partial_i \partial_j \partial_k \phi, \tag{3.1d}$$

$$L_{5\text{-pt}} = 60 \partial_i \phi \partial_i \partial_j \phi \partial_j \partial_k \phi \partial_k \partial_\ell \phi \partial_\ell \phi + 60 \partial_i \phi \partial_i \partial_j \phi \partial_j \partial_k \partial_\ell \phi \partial_k \phi \partial_\ell \phi + 5 \partial_i \phi \partial_j \phi \partial_k \phi \partial_\ell \phi \partial_i \partial_j \partial_j \partial_k \partial_\ell \phi. \tag{3.1e}$$

These are not identical to the usual expressions (e.g., in [13]), but one can easily check that they are equivalent.

3.1. The Graphical Representation

We can represent the terms in (3.1) as formal linear combinations of graphs. In these graphs, ϕ is represented by a \bullet -vertex. An edge joining two vertices represents a pair of contracted derivatives, one derivative acting on each of the ϕ 's representing the endpoints

of the edge. The graphical representations of the above terms are given below:

$$L_{1\text{-pt}} = \bullet, \tag{3.2a}$$

$$L_{2\text{-pt}} = \bullet\text{---}\bullet, \tag{3.2b}$$

$$L_{3\text{-pt}} = 3 \begin{array}{c} \bullet \\ / \\ \bullet\text{---}\bullet \end{array}, \tag{3.2c}$$

$$L_{4\text{-pt}} = 12 \begin{array}{c} \bullet \quad \bullet \\ | \quad | \\ \bullet\text{---}\bullet \end{array} + 4 \begin{array}{c} \bullet \quad \bullet \\ / \quad | \\ \bullet\text{---}\bullet \end{array}, \tag{3.2d}$$

$$L_{5\text{-pt}} = 60 \begin{array}{c} \bullet \quad \bullet \\ / \quad \backslash \\ \bullet\text{---}\bullet \end{array} + 60 \begin{array}{c} \bullet \quad \bullet \\ / \quad / \\ \bullet\text{---}\bullet \end{array} + 5 \begin{array}{c} \bullet \\ / \quad \backslash \\ \bullet \quad \bullet \\ | \quad | \\ \bullet\text{---}\bullet \end{array}. \tag{3.2e}$$

The structure of the graph (i.e., the connectivity of the vertices) is what distinguishes graphs; the placement of the vertices is immaterial. This reflects the fact that the order of the ϕ 's in the algebraic expressions is immaterial and the only thing that matters is which contracted pairs of derivatives act on which pairs of ϕ 's. Therefore, for example, the graphs below all represent the same algebraic expression.

$$\begin{array}{ccc} \begin{array}{c} \bullet \\ / \\ \bullet\text{---}\bullet \end{array} & \begin{array}{c} \bullet \\ \backslash \\ \bullet\text{---}\bullet \end{array} & \begin{array}{c} \bullet \\ / \quad \backslash \\ \bullet \quad \bullet \\ | \quad | \\ \bullet\text{---}\bullet \end{array} \end{array} \tag{3.3}$$

Similarly, the four graphs below represent the same algebraic expression.

$$\begin{array}{cccc} \begin{array}{c} \bullet \quad \bullet \\ / \quad | \\ \bullet\text{---}\bullet \end{array} & \begin{array}{c} \bullet \quad \bullet \\ \backslash \quad | \\ \bullet\text{---}\bullet \end{array} & \begin{array}{c} \bullet \quad \bullet \\ / \quad / \\ \bullet\text{---}\bullet \end{array} & \begin{array}{c} \bullet \quad \bullet \\ / \quad \backslash \\ \bullet \quad \bullet \\ | \quad | \\ \bullet\text{---}\bullet \end{array} \end{array} \tag{3.4}$$

A more nontrivial example is given by the following twelve graphs, which all represent the same algebraic expression.

$$\begin{array}{cccc} \begin{array}{c} \bullet \quad \bullet \\ | \quad | \\ \bullet\text{---}\bullet \end{array} & \begin{array}{c} \bullet \quad \bullet \\ \text{---} \quad \text{---} \\ | \quad | \\ \bullet\text{---}\bullet \end{array} & \begin{array}{c} \bullet \quad \bullet \\ \text{---} \quad \text{---} \\ | \quad | \\ \bullet\text{---}\bullet \end{array} & \begin{array}{c} \bullet \quad \bullet \\ \text{---} \quad \text{---} \\ | \quad | \\ \bullet\text{---}\bullet \end{array} \\ \begin{array}{c} \bullet \quad \bullet \\ / \quad \backslash \\ \bullet \quad \bullet \\ | \quad | \\ \bullet\text{---}\bullet \end{array} & \begin{array}{c} \bullet \quad \bullet \\ / \quad / \\ \bullet \quad \bullet \\ | \quad | \\ \bullet\text{---}\bullet \end{array} & \begin{array}{c} \bullet \quad \bullet \\ / \quad \backslash \\ \bullet \quad \bullet \\ | \quad | \\ \bullet\text{---}\bullet \end{array} & \begin{array}{c} \bullet \quad \bullet \\ / \quad \backslash \\ \bullet \quad \bullet \\ | \quad | \\ \bullet\text{---}\bullet \end{array} \\ \begin{array}{c} \bullet \quad \bullet \\ / \quad | \\ \bullet\text{---}\bullet \end{array} & \begin{array}{c} \bullet \quad \bullet \\ \backslash \quad | \\ \bullet\text{---}\bullet \end{array} & \begin{array}{c} \bullet \quad \bullet \\ / \quad / \\ \bullet\text{---}\bullet \end{array} & \begin{array}{c} \bullet \quad \bullet \\ / \quad \backslash \\ \bullet \quad \bullet \\ | \quad | \\ \bullet\text{---}\bullet \end{array} \end{array} \tag{3.5}$$

The graphs in the second line above appear to have intersecting edges. However, since there is no \bullet -vertex at the would-be intersection, these edges do not actually intersect.

3.2. Galileon Invariants as Equal-Weight Sums of Trees

There are three times as many graphs in (3.5) as there are in (3.4). It so happens that the coefficient with which the first graph in (3.5) appears in $L_{4\text{-pt}}$ (3.2d) is also three times the coefficient with which the first graph in (3.4) appears in $L_{4\text{-pt}}$. This suggests that the coefficient with which a graph appears in a minimal term is precisely the number of

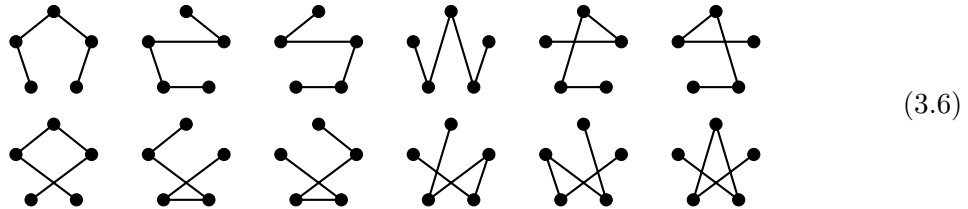
graphs with the exact same structure (i.e., isomorphic), just with various vertices and edges permuted.

One simple way to state this is to actually label the vertices in the graphs. If the vertices were labeled, and thus distinguished from each other, then all of the graphs in each one of (3.3), (3.4) and (3.5) would actually be distinct graphs. Of course, this means that the corresponding algebraic expressions have ϕ 's similarly labeled, but this labeling is fiducial and may be removed afterwards. Note the simplicity that this labeled convention introduces: $L_{4\text{-pt}}$ is the sum of all of the graphs in (3.4) and (3.5) with unit coefficients.

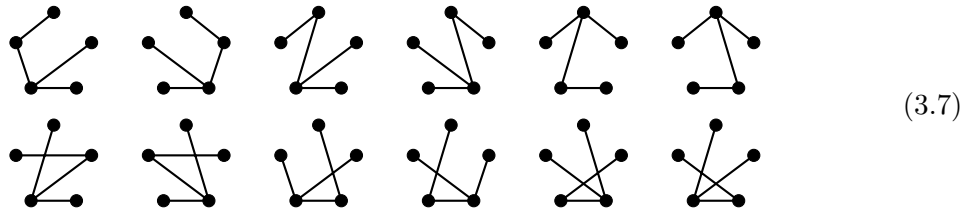
The graphs in (3.4) and (3.5) have an elegant and unified interpretation in graph theory. These graphs are called *trees*. A tree is a graph which is connected (i.e., cannot be split into two or more separate graphs without cutting an edge), and contains no loops (edges joining a vertex to itself) or cycles (edges joining vertices in a closed cyclic manner). One can check that there are exactly 16 trees with four vertices and they are given by (3.4) and (3.5). Cayley's formula, a well-known result in graph theory, says that the number of trees with N vertices is N^{N-2} .

For $N = 3$, the $3^{3-2} = 3$ trees are in (3.3), and we indeed find that $L_{3\text{-pt}}$ is the sum of all three graphs with unit coefficients. The same can be said for $L_{2\text{-pt}}$ and $L_{1\text{-pt}}$. Therefore, the minimal terms for $N = 1, 2, 3$ and 4 are represented graphically as a sum of trees with unit coefficients (an equal-weight sum of trees). If this were to hold for the $N = 5$ case, it would strongly suggest that this may hold for all N .

There are $5^3 = 125$ trees for $N = 5$. They can be divided into three sets such that the trees in each set are isomorphic to one of the three graphs appearing in $L_{5\text{-pt}}$ (3.2e). There are 60 graphs which are isomorphic to the first graph appearing in $L_{5\text{-pt}}$; 12 of these are listed below and the rest are given by the five rotations acting on each of these 12 graphs:



There are 60 graphs which are isomorphic to the second graph appearing in $L_{5\text{-pt}}$; 12 of these are listed below and the rest are given by their rotations:



Finally, there are five graphs which are isomorphic to the third graph appearing in $L_{5\text{-pt}}$, which are simply the five rotations acting on that graph. Therefore, $L_{5\text{-pt}}$ is indeed the sum with unit coefficients of all trees with five vertices!

Thus, we arrive at the main result of this section (proven in Appendix B.3):

The unique minimal N -point linear shift-invariant Lagrangian term is represented graphically as a sum with unit coefficients of all labeled trees with N vertices.

4. Beyond the Galileons

Now, we extend the linear shift transformation to polynomials of higher degree. We will need to develop the graphical approach further in order to tackle this problem and numerous technicalities will arise. However, a rather elegant and beautiful description of these polynomial shift invariants will emerge.

Consider the problem of determining all possible terms in a Lagrangian that are invariant under the polynomial shift symmetry:

$$\phi(t, x^i) \rightarrow \phi(t, x^i) + \delta_P \phi, \quad \delta_P \phi = a_{i_1 \dots i_P} x^{i_1} \dots x^{i_P} + \dots + a_i x^i + a. \quad (4.1)$$

The a 's are arbitrary real coefficients that parametrize the symmetry transformation, and are symmetric in any pair of indices. $P = 0, 1, 2, \dots$ corresponds to constant shift, linear shift, quadratic shift, and so on. Obviously, if a term is invariant under a polynomial shift of order P , then it is also invariant under a polynomial shift of order P' with $0 \leq P' \leq P$.

We will call a term with N fields and 2Δ derivatives an (N, Δ) term. We are interested in interaction terms, for which $N \geq 3$. As previously mentioned, terms with the lowest possible value of Δ are of greatest interest. It is straightforward to write down invariant terms with $\Delta \geq \frac{1}{2}N(P+1)$ since, if each ϕ has more than P derivatives acting on it, then the term is exactly invariant. Are there any invariant terms with lower values of Δ ? If so, then these invariant terms will be more relevant than the exact invariants.

To be invariant, a term must transform into a total derivative under the polynomial shift symmetry. In other words, for a specific P and given (N, Δ) , we are searching for terms L such that

$$\delta_P L = \partial_i(L_i). \quad (4.2)$$

Here L is a linear combination of terms with N ϕ 's and 2Δ ∂ 's, and L_i is a linear combination of terms with $N-1$ ϕ 's. Such L 's are called *P -invariants*.

How might we determine such invariant terms in general? For a given (N, Δ) , the most brute-force method for determining invariant terms can be described as follows. First, write down all possible terms in the Lagrangian with a given (N, Δ) and ensure that they are independent up to integration by parts. Next, take the variation of all these terms under the polynomial shift. There may exist linear combinations of these variations which are equal to a total derivative, which we call *total derivative relations*. If we use these total derivative relations to maximally reduce the number of variation terms, then the required P -invariants form the kernel of the map from the independent Lagrangian terms to the independent variation terms (Corollary 6). Let us consider some examples of this brute-force procedure in action.

4.1. Brute-force Examples

4.1.1. $(P, N, \Delta) = (1, 3, 2)$

In this case, a general Lagrangian is made up of two independent terms, after integrating by parts, given by

$$L_1 = \partial_i \phi \partial_j \phi \partial_i \partial_j \phi, \quad L_2 = \phi \partial_i \partial_j \phi \partial_i \partial_j \phi.$$

The variation under the linear shift symmetry (for $P = 1$) of these terms is given by

$$\delta_1(L_1) = 2L_a^\times, \quad \delta_1(L_2) = L_b^\times,$$

where $L_a^\times = a_i \partial_j \phi \partial_i \partial_j \phi$ and $L_b^\times = (a_k x^k + a) \partial_i \partial_j \phi \partial_i \partial_j \phi$. There is only one total derivative that can be formed from these terms, namely

$$\partial_i (a_i \partial_j \phi \partial_j \phi) = 2L_a^\times.$$

Therefore, there is a single invariant term for $(P, N, \Delta) = (1, 3, 2)$, given by

$$L_1 = \partial_i \phi \partial_j \phi \partial_i \partial_j \phi.$$

4.1.2. $(P, N, \Delta) = (3, 3, 4)$

In this case, a general Lagrangian is made up of four independent terms, after integrating by parts, given by

$$\begin{aligned} L_1 &= \partial_i \partial_j \phi \partial_k \partial_l \phi \partial_i \partial_j \partial_k \partial_l \phi, & L_2 &= \partial_i \partial_j \phi \partial_i \partial_k \partial_l \phi \partial_j \partial_k \partial_l \phi, \\ L_3 &= \partial_i \phi \partial_j \partial_k \partial_l \phi \partial_i \partial_j \partial_k \partial_l \phi, & L_4 &= \phi \partial_i \partial_j \partial_k \partial_l \phi \partial_i \partial_j \partial_k \partial_l \phi. \end{aligned}$$

The variation under the cubic shift symmetry (for $P = 3$) of these terms is given by

$$\begin{aligned} \delta_3(L_1) &= 2L_a^\times, & \delta_3(L_2) &= L_b^\times + 2L_c^\times, \\ \delta_3(L_3) &= L_d^\times + L_e^\times, & \delta_3(L_4) &= L_f^\times. \end{aligned}$$

where

$$\begin{aligned} L_a^\times &= (6a_{ijm}x^m + 2a_{ij})\partial_k \partial_l \phi \partial_i \partial_j \partial_k \partial_l \phi \\ L_b^\times &= (6a_{ijm}x^m + 2a_{ij})\partial_i \partial_k \partial_l \phi \partial_j \partial_k \partial_l \phi \\ L_c^\times &= 6a_{ikl}\partial_i \partial_j \phi \partial_j \partial_k \partial_l \phi \\ L_d^\times &= (3a_{imn}x^m x^n + 2a_{im}x^m + a_i)\partial_i \phi \partial_j \partial_k \partial_l \phi \partial_i \partial_j \partial_k \partial_l \phi \\ L_e^\times &= 6a_{jkl}\partial_i \phi \partial_i \partial_j \partial_k \partial_l \phi \\ L_f^\times &= (a_{mnp}x^m x^n x^p + a_{mn}x^m x^n + a_m x^m + a)\partial_i \partial_j \partial_k \partial_l \phi \partial_i \partial_j \partial_k \partial_l \phi. \end{aligned}$$

There are three independent total derivatives that can be formed out of these:

$$\begin{aligned} \partial_i [2(6a_{ijm}x^m + 2a_{ij})\partial_k \partial_l \phi \partial_j \partial_k \partial_l \phi - 6a_{ijj}\partial_k \partial_l \phi \partial_k \partial_l \phi] &= 2(L_a^\times + L_b^\times), \\ \partial_i [6a_{ijk}\partial_j \partial_l \phi \partial_k \partial_l \phi] &= 2L_c^\times, \\ \partial_i [6a_{ijk}\partial_j \partial_k \partial_l \phi \partial_l \phi] &= L_c^\times + L_e^\times. \end{aligned}$$

It is a non-trivial exercise to find and verify this, and a more systematic way of finding the total derivative relations will be introduced later.

Applying these relations, one finds a single invariant for $(P, N, \Delta) = (3, 3, 4)$:

$$L_1 + 2L_2 = \partial_i \partial_j \phi \partial_k \partial_l \phi \partial_i \partial_j \partial_k \partial_l \phi + 2 \partial_i \partial_j \phi \partial_i \partial_k \partial_l \phi \partial_j \partial_k \partial_l \phi.$$

Note that $\delta_3(L_1 + 2L_2) = 2(L_a^\times + L_b^\times) + 2(2L_c^\times)$, which is a total derivative.

4.2. Introduction to the Graphical Representation

It is clear that even for these simple examples, the calculations quickly become unwieldy, and it becomes increasingly difficult to classify all of the total derivative relations. At this point we will rewrite these results in a graphical notation which will make it easier to keep track of the contractions of indices in the partial derivatives. Full details about this graphical approach can be found in Appendix B, but we will summarize them here. In addition to the \bullet -vertex and edges we introduced in §3, we represent $\delta_P \phi$ by a \otimes (a \times -vertex). Note that there are at most P edges incident to a \times -vertex since $P+1$ derivatives acting on $\delta_P \phi$ yields zero, whereas an arbitrary number of edges can be incident to a \bullet -vertex. Moreover, we introduce another vertex, called a \star -vertex, which will be used to represent terms that are total derivatives. We require that a \star -vertex always be incident to exactly one edge, and that this edge be incident to a \bullet -vertex or \times -vertex. This edge represents a derivative acting on the entire term as a whole, and the index of that derivative is contracted with the index of another derivative acting on the ϕ or $\delta_P \phi$ of the \bullet - or \times -vertex, respectively, to which the \star -vertex is adjacent. Therefore, directly from the definition, any graph with a \star -vertex represents a total derivative term. The expansion of this derivative using the Leibniz rule is graphically represented by the summation of the graphs formed by removing the \star -vertex and attaching the edge that was incident to the \star -vertex to each remaining vertex. This operation is denoted by the *derivative map* ρ . The symbols $N(\bullet)$, $N(\times)$ and $N(\star)$ represent the numbers of each type of vertex. Note that $N = N(\bullet) + N(\times)$ does not include $N(\star)$ since \star -vertices represent neither ϕ nor $\delta_P \phi$.

We define three special types of graphs: A *plain-graph* is a graph in which all vertices are \bullet -vertices. A *\times -graph* is a plain-graph with one \bullet -vertex replaced with a \times -vertex. A *\star -graph* is a graph with one \times -vertex and at least one \star -vertex.

Note that the variation δ_P of a plain-graph under the polynomial shift symmetry is given by summing over all graphs that have exactly one \bullet -vertex in the original graph replaced with a \times -vertex. To illustrate the graphical approach, we rewrite the examples from sections 4.1.1 and 4.1.2 using this new graphical notation. Since the algebraic expressions have unlabeled ϕ 's, the graphs in this section will be unlabeled.

4.2.1. $(P, N, \Delta) = (1, 3, 2)$

The two independent terms are written in the graphical notation as

$$L_1 = \begin{array}{c} \bullet \\ | \\ \bullet - \bullet \end{array} \qquad L_2 = \begin{array}{c} \bullet \\ \curvearrowright \\ \bullet - \bullet \end{array}$$

The variation under the linear shift symmetry (for $P = 1$) is given by

$$\delta_1 \left(\begin{array}{c} \bullet \\ | \\ \bullet \end{array} \begin{array}{c} \bullet \\ \text{---} \\ \bullet \end{array} \right) = 2 \begin{array}{c} \otimes \\ | \\ \bullet \end{array} \begin{array}{c} \bullet \\ \text{---} \\ \bullet \end{array} \quad \delta_1 \left(\begin{array}{c} \bullet \\ \text{---} \\ \bullet \end{array} \begin{array}{c} \bullet \\ \text{---} \\ \bullet \end{array} \right) = \begin{array}{c} \otimes \\ \text{---} \\ \bullet \end{array} \begin{array}{c} \bullet \\ \text{---} \\ \bullet \end{array}$$

The only independent total derivative that can be formed out of these terms is

$$\rho \left(\begin{array}{c} \otimes \text{---} \star \\ \text{---} \\ \bullet \end{array} \begin{array}{c} \bullet \\ \text{---} \\ \bullet \end{array} \right) = 2 \begin{array}{c} \otimes \\ | \\ \bullet \end{array} \begin{array}{c} \bullet \\ \text{---} \\ \bullet \end{array}$$

As before, there is a single invariant for $(P, N, \Delta) = (1, 3, 2)$ given by L_1 . In this case, the graphical version of (4.2) is given by

$$\delta_1 \left(\begin{array}{c} \bullet \\ | \\ \bullet \end{array} \begin{array}{c} \bullet \\ \text{---} \\ \bullet \end{array} \right) = 2 \begin{array}{c} \otimes \\ | \\ \bullet \end{array} \begin{array}{c} \bullet \\ \text{---} \\ \bullet \end{array} = \rho \left(\begin{array}{c} \otimes \text{---} \star \\ \text{---} \\ \bullet \end{array} \begin{array}{c} \bullet \\ \text{---} \\ \bullet \end{array} \right)$$

4.2.2. $(P, N, \Delta) = (3, 3, 4)$

The four independent terms are written in the graphical notation as

$$L_1 = \begin{array}{c} \bullet \\ \text{---} \\ \bullet \end{array} \begin{array}{c} \bullet \\ \text{---} \\ \bullet \end{array} \quad L_2 = \begin{array}{c} \bullet \\ \text{---} \\ \bullet \end{array} \begin{array}{c} \bullet \\ \text{---} \\ \bullet \end{array} \quad L_3 = \begin{array}{c} \bullet \\ | \\ \bullet \end{array} \begin{array}{c} \bullet \\ \text{---} \\ \bullet \end{array} \quad L_4 = \begin{array}{c} \bullet \\ \text{---} \\ \bullet \end{array} \begin{array}{c} \bullet \\ \text{---} \\ \bullet \end{array}$$

The variation under the cubic shift symmetry (for $P = 3$) is given by

$$\begin{aligned} \delta_3 \left(\begin{array}{c} \bullet \\ \text{---} \\ \bullet \end{array} \begin{array}{c} \bullet \\ \text{---} \\ \bullet \end{array} \right) &= 2 \begin{array}{c} \otimes \\ \text{---} \\ \bullet \end{array} \begin{array}{c} \bullet \\ \text{---} \\ \bullet \end{array} & \delta_3 \left(\begin{array}{c} \bullet \\ \text{---} \\ \bullet \end{array} \begin{array}{c} \bullet \\ \text{---} \\ \bullet \end{array} \right) &= \begin{array}{c} \otimes \\ \text{---} \\ \bullet \end{array} \begin{array}{c} \bullet \\ \text{---} \\ \bullet \end{array} + 2 \begin{array}{c} \bullet \\ \text{---} \\ \bullet \end{array} \begin{array}{c} \bullet \\ \text{---} \\ \bullet \end{array} \\ \delta_3 \left(\begin{array}{c} \bullet \\ | \\ \bullet \end{array} \begin{array}{c} \bullet \\ \text{---} \\ \bullet \end{array} \right) &= \begin{array}{c} \otimes \\ | \\ \bullet \end{array} \begin{array}{c} \bullet \\ \text{---} \\ \bullet \end{array} + \begin{array}{c} \otimes \\ | \\ \bullet \end{array} \begin{array}{c} \bullet \\ \text{---} \\ \bullet \end{array} & \delta_3 \left(\begin{array}{c} \bullet \\ \text{---} \\ \bullet \end{array} \begin{array}{c} \bullet \\ \text{---} \\ \bullet \end{array} \right) &= \begin{array}{c} \otimes \\ \text{---} \\ \bullet \end{array} \begin{array}{c} \bullet \\ \text{---} \\ \bullet \end{array} \end{aligned}$$

The independent total derivatives that can be formed out of these terms are

$$\begin{aligned} \rho \left(2 \begin{array}{c} \otimes \text{---} \star \\ \text{---} \\ \bullet \end{array} \begin{array}{c} \bullet \\ \text{---} \\ \bullet \end{array} - \begin{array}{c} \otimes \text{---} \star \\ \text{---} \\ \bullet \end{array} \begin{array}{c} \bullet \\ \text{---} \\ \bullet \end{array} \right) &= 2 \begin{array}{c} \otimes \\ \text{---} \\ \bullet \end{array} \begin{array}{c} \bullet \\ \text{---} \\ \bullet \end{array} + 2 \begin{array}{c} \otimes \\ \text{---} \\ \bullet \end{array} \begin{array}{c} \bullet \\ \text{---} \\ \bullet \end{array} \\ \rho \left(\begin{array}{c} \otimes \text{---} \star \\ \text{---} \\ \bullet \end{array} \begin{array}{c} \bullet \\ \text{---} \\ \bullet \end{array} \right) &= 2 \begin{array}{c} \bullet \\ \text{---} \\ \bullet \end{array} \begin{array}{c} \bullet \\ \text{---} \\ \bullet \end{array} \\ \rho \left(\begin{array}{c} \otimes \text{---} \star \\ \text{---} \\ \bullet \end{array} \begin{array}{c} \bullet \\ \text{---} \\ \bullet \end{array} \right) &= \begin{array}{c} \otimes \\ \text{---} \\ \bullet \end{array} \begin{array}{c} \bullet \\ \text{---} \\ \bullet \end{array} + \begin{array}{c} \otimes \\ | \\ \bullet \end{array} \begin{array}{c} \bullet \\ \text{---} \\ \bullet \end{array} \end{aligned}$$

Once again, there is a single invariant for $(P, N, \Delta) = (3, 4)$ given by $L_1 + 2L_2$. The graphical version of (4.2) is given by

$$\begin{aligned} \delta_3 \left(\begin{array}{c} \bullet \\ \text{---} \\ \bullet \end{array} \begin{array}{c} \bullet \\ \text{---} \\ \bullet \end{array} + 2 \begin{array}{c} \bullet \\ \text{---} \\ \bullet \end{array} \begin{array}{c} \bullet \\ \text{---} \\ \bullet \end{array} \right) &= 2 \begin{array}{c} \otimes \\ \text{---} \\ \bullet \end{array} \begin{array}{c} \bullet \\ \text{---} \\ \bullet \end{array} + 2 \begin{array}{c} \otimes \\ \text{---} \\ \bullet \end{array} \begin{array}{c} \bullet \\ \text{---} \\ \bullet \end{array} + 4 \begin{array}{c} \otimes \\ \text{---} \\ \bullet \end{array} \begin{array}{c} \bullet \\ \text{---} \\ \bullet \end{array} \\ &= \rho \left(2 \begin{array}{c} \otimes \text{---} \star \\ \text{---} \\ \bullet \end{array} \begin{array}{c} \bullet \\ \text{---} \\ \bullet \end{array} - \begin{array}{c} \otimes \text{---} \star \\ \text{---} \\ \bullet \end{array} \begin{array}{c} \bullet \\ \text{---} \\ \bullet \end{array} + 2 \begin{array}{c} \otimes \text{---} \star \\ \text{---} \\ \bullet \end{array} \begin{array}{c} \bullet \\ \text{---} \\ \bullet \end{array} \right) \end{aligned} \quad (4.3)$$

So far all we have done is rewrite our results in a new notation. But the graphical notation is more than just a succinct visual way of expressing the invariant terms. The following section illustrates the virtue of this approach.

4.3. New Invariants via the Graphical Approach

As shown in Appendix B, the graphical approach allows us to prove many general theorems. In particular, we have the following useful outcomes:

1. Without loss of generality, we can limit our search for invariants to graphs with very specific properties (Appendix B.2).
2. There is a simple procedure for obtaining all the independent total derivative relations between the variation terms for each P , N and Δ (Theorem 1).
3. The graphical method allows a complete classification of 1-invariants (Theorem 4).
4. The graphical method allows many higher P -invariant terms to be constructed from lower P invariants (Appendix B.4).

We will expound upon the above points by presenting explicit examples. These examples are generalizable and their invariance is proven in Appendix B. However, the reader can also check by brute force that the terms we present are indeed invariant. We will now summarize points 1 and 2 and will return to point 4 in §4.4. Point 3 was discussed in §3 with technical details in Appendix B.3.

When building invariants, we need only consider loopless plain-graphs (Proposition 2), since a loop represents $\partial_i \partial_i$ acting on a single ϕ and one can always integrate by parts to move one of the ∂_i 's to act on the remaining ϕ 's. We can also restrict to plain-graphs with vertices of degree no less than $\frac{1}{2}(P+1)$ (Proposition 7). This represents a significant simplification from the previous procedure (§4.2). For instance, in §4.2.2, the graphs L_3 and L_4 are immediately discarded.

Taking the variation of these terms yields \times -graphs and we need to determine the total derivative relations between them. Since all plain-graphs we are considering are loopless, any \times -graphs involved in these total derivative relations are also loopless. The total derivative relations that we need to consider can be obtained with the use of graphs called *Medusas* (Definition 10). A Medusa is a loopless \star -graph with all of its \star -vertices adjacent to the \times -vertex and such that the degree of the \times -vertex is given by:

$$\deg(\times) = P + 1 - N(\star), \quad (4.4)$$

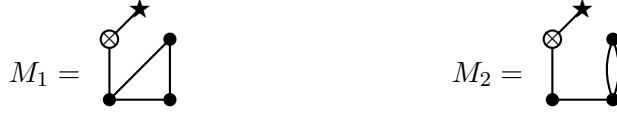
where, again, $N(\star)$ is the number of \star -vertices. Note that because $\deg(\times) \geq N(\star)$ for a Medusa, (4.4) implies that $N(\star) \leq \frac{1}{2}(P+1) \leq \deg(\times)$ for any Medusa. Furthermore, we need only consider Medusas with \times -vertex and \bullet -vertices of degree no less than $\frac{1}{2}(P+1)$ (Proposition 8). From each of these Medusas, we obtain a total derivative relation, containing only loopless \times -graphs, by applying the map ρ and then omitting all looped graphs (Proposition 4). This map is denoted as $\rho^{(0)}$ in Definition 13. In §4.3.3, we will give an

introduction to the construction of such total derivative relations from Medusas. Moreover, this procedure captures all relevant total derivative relations (Theorem 1). Appendix B.2 provides a systematic treatment of Medusas.

In general, for given N and P , we call an invariant consisting of graphs containing the lowest possible value of Δ a *minimal* invariant (Definition 16). Minimal invariants are of particular interest in a QFT, since they are the most relevant N -point interactions. In §4.3.1 and §4.3.2 we apply the graphical approach to classify all minimal invariants for $N = 4$ and $P = 2, 3$.

4.3.1. The Minimal Invariant: $(P, N, \Delta) = (2, 4, 5)$

As our first example, let us find the minimal 2-invariant for $N = 4$. For $P = 2$, any Medusa must have $N(\star) \leq \frac{1}{2}(P+1) = \frac{3}{2}$, and thus there is exactly one \star -vertex in a $P = 2$ Medusa. Furthermore, we need only consider Medusas in which each vertex has degree at least 2, since $\frac{1}{2}(P+1) = \frac{3}{2}$. Therefore, the counting implies that we need only consider $P = 2$ Medusas with $\Delta \geq N + 1$. In particular, when $N = 4$, the minimal Δ is 5 (representing terms with 10 derivatives). In the following we show that there is exactly one 2-invariant with $\Delta = 5$. The relevant Medusas are:

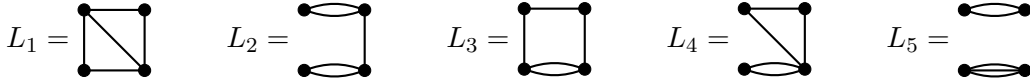


The resulting loopless total derivative relations are:

$$\begin{aligned} \rho^{(0)}(M_1) &= 2 \begin{array}{c} \circledast \\ \diagup \\ \square \\ \diagdown \\ \bullet \end{array} + \begin{array}{c} \circledast \\ \square \\ \diagdown \\ \bullet \end{array} \equiv 2L_a^\times + L_e^\times \\ \rho^{(0)}(M_2) &= \begin{array}{c} \circledast \\ \square \\ \bullet \end{array} + \begin{array}{c} \circledast \\ \square \\ \bullet \end{array} + \begin{array}{c} \circledast \\ \square \\ \bullet \end{array} \equiv L_b^\times + L_c^\times + L_d^\times \end{aligned} \quad (4.5)$$

Note that, when acting on these $P = 2$ Medusas, ρ and $\rho^{(0)}$ are in fact the same.

On the other hand, the invariants must be constructed out of plain-graphs containing vertices of degree no less than $\frac{1}{2}(P+1) = \frac{3}{2}$. The only possibilities are:



The invariant cannot be constructed out of L_5 since $\delta_2(L_5)$ is absent from the total derivative relations (4.5). Hence, we need only consider the variations of L_1 , L_2 , L_3 and L_4 .

We can now determine the 2-invariants. The total derivative relations allow us to identify $L_d^\times \sim -L_b^\times - L_c^\times$ and $L_e^\times \sim -2L_a^\times$. Up to total derivatives,

$$\delta_2 \begin{pmatrix} L_1 \\ L_2 \\ L_3 \\ L_4 \end{pmatrix} = \begin{pmatrix} 2 & 0 & 0 & 0 & 0 \\ 0 & 2 & 0 & 0 & 0 \\ 0 & 0 & 2 & 0 & 0 \\ 0 & 0 & 0 & 2 & 1 \end{pmatrix} \begin{pmatrix} L_a^\times \\ L_b^\times \\ L_c^\times \\ L_d^\times \\ L_e^\times \end{pmatrix} \sim \begin{pmatrix} 2 & 0 & 0 \\ 0 & 2 & 0 \\ 0 & 0 & 2 \\ -2 & -1 & -1 \end{pmatrix} \begin{pmatrix} L_a^\times \\ L_b^\times \\ L_c^\times \end{pmatrix} \quad (4.6)$$

The invariants form the nullspace of the transpose of the final 4×3 matrix in (4.6). The nullspace is spanned by $(1, 1, 1, 1)$. Therefore, there is one 2-invariant given by the linear combination $L_1 + L_2 + L_3 + L_4$, i.e.,

$$\begin{array}{c} \text{---} \bullet \\ \diagup \quad \diagdown \\ \bullet \quad \bullet \\ \text{---} \bullet \end{array} + \begin{array}{c} \bullet \quad \bullet \\ \text{---} \quad \text{---} \\ \bullet \quad \bullet \end{array} + \begin{array}{c} \bullet \quad \bullet \\ \text{---} \quad \text{---} \\ \bullet \quad \bullet \end{array} + \begin{array}{c} \bullet \quad \bullet \\ \text{---} \quad \text{---} \\ \bullet \quad \bullet \end{array} \quad (4.7)$$

Therefore, (4.7) gives the only independent minimal 2-invariant for $N = 4$.

4.3.2. The Minimal Invariant: $(P, N, \Delta) = (3, 4, 6)$

Next, let us consider $P = 3$, $N = 4$, for which each vertex degree must be at least $\frac{1}{2}(P + 1) = 2$. Again we would like to find the minimal invariant in this case. By counting alone, it is possible to write down Medusas with $\Delta = 5$. In fact, a 3-invariant with $N = 4$ and $\Delta = 5$ would also be 2-invariant. The only possible 2-invariant with $(N, \Delta) = (4, 5)$ is (4.7). However, this is not a 3-invariant because it is impossible for some graphs contained in it to appear in a 3-invariant. For example, by replacing a degree-2 vertex in L_2 in (4.7) with a \times -vertex, a \times -graph Γ^\times is produced; Γ^\times and the only $P = 3$ Medusa M that generates Γ^\times are given below:

$$\Gamma^\times = \begin{array}{c} \otimes \quad \bullet \\ \text{---} \quad \text{---} \\ \bullet \quad \bullet \end{array} \quad M = \begin{array}{c} \star \quad \star \\ \diagdown \quad \diagup \\ \otimes \quad \bullet \\ \text{---} \quad \text{---} \\ \bullet \quad \bullet \end{array}$$

But M contains a \bullet -vertex of degree lower than 2, and therefore (4.7) cannot be 3-invariant. This sets a lower bound for Δ : $\Delta \geq 6$. For $\Delta = 6$, the Medusas are:

$$\begin{array}{cccc} M_1 = \begin{array}{c} \otimes \quad \star \\ \diagdown \quad \diagup \\ \bullet \quad \bullet \\ \text{---} \quad \text{---} \\ \bullet \quad \bullet \end{array} & M_2 = \begin{array}{c} \otimes \quad \star \\ \diagdown \quad \diagup \\ \bullet \quad \bullet \\ \text{---} \quad \text{---} \\ \bullet \quad \bullet \end{array} & M_3 = \begin{array}{c} \otimes \quad \star \\ \text{---} \quad \text{---} \\ \bullet \quad \bullet \end{array} & M_4 = \begin{array}{c} \otimes \quad \star \\ \diagdown \quad \diagup \\ \bullet \quad \bullet \\ \text{---} \quad \text{---} \\ \bullet \quad \bullet \end{array} \\ M_5 = \begin{array}{c} \otimes \quad \star \\ \diagdown \quad \diagup \\ \bullet \quad \bullet \\ \text{---} \quad \text{---} \\ \bullet \quad \bullet \end{array} & M_6 = \begin{array}{c} \otimes \quad \star \\ \diagdown \quad \diagup \\ \bullet \quad \bullet \\ \text{---} \quad \text{---} \\ \bullet \quad \bullet \end{array} & M_7 = \begin{array}{c} \star \quad \star \\ \diagdown \quad \diagup \\ \otimes \quad \bullet \\ \text{---} \quad \text{---} \\ \bullet \quad \bullet \end{array} & M_8 = \begin{array}{c} \star \quad \star \\ \diagdown \quad \diagup \\ \otimes \quad \bullet \\ \text{---} \quad \text{---} \\ \bullet \quad \bullet \end{array} \end{array}$$

These give the following total derivative relations:

$$\begin{aligned} \rho^{(0)}(M_1) &= \begin{array}{c} \otimes \quad \bullet \\ \text{---} \quad \text{---} \\ \bullet \quad \bullet \end{array} + \begin{array}{c} \otimes \quad \bullet \\ \diagdown \quad \diagup \\ \bullet \quad \bullet \end{array} + \begin{array}{c} \otimes \quad \bullet \\ \text{---} \quad \text{---} \\ \bullet \quad \bullet \end{array} \equiv L_a^\times + L_b^\times + L_c^\times \\ \rho^{(0)}(M_2) &= \begin{array}{c} \otimes \quad \bullet \\ \diagdown \quad \diagup \\ \bullet \quad \bullet \end{array} + 2 \begin{array}{c} \otimes \quad \bullet \\ \text{---} \quad \text{---} \\ \bullet \quad \bullet \end{array} \equiv L_d^\times + 2L_e^\times \\ \rho^{(0)}(M_3) &= \begin{array}{c} \otimes \quad \bullet \\ \text{---} \quad \text{---} \\ \bullet \quad \bullet \end{array} + 2 \begin{array}{c} \otimes \quad \bullet \\ \text{---} \quad \text{---} \\ \bullet \quad \bullet \end{array} \equiv L_f^\times + 2L_g^\times \\ \rho^{(0)}(M_4) &= \begin{array}{c} \otimes \quad \bullet \\ \text{---} \quad \text{---} \\ \bullet \quad \bullet \end{array} + \begin{array}{c} \otimes \quad \bullet \\ \diagdown \quad \diagup \\ \bullet \quad \bullet \end{array} + \begin{array}{c} \otimes \quad \bullet \\ \text{---} \quad \text{---} \\ \bullet \quad \bullet \end{array} \equiv L_a^\times + L_h^\times + L_i^\times \\ \rho^{(0)}(M_5) &= 2 \begin{array}{c} \otimes \quad \bullet \\ \text{---} \quad \text{---} \\ \bullet \quad \bullet \end{array} + \begin{array}{c} \otimes \quad \bullet \\ \text{---} \quad \text{---} \\ \bullet \quad \bullet \end{array} \equiv 2L_e^\times + L_j^\times \end{aligned}$$

$$\begin{aligned}
\rho^{(0)}(M_6) &= \begin{array}{c} \circlearrowleft \\ \text{---} \\ \bullet \\ \text{---} \\ \bullet \end{array} + \begin{array}{c} \circlearrowleft \\ \text{---} \\ \bullet \\ \text{---} \\ \bullet \end{array} + \begin{array}{c} \circlearrowleft \\ \text{---} \\ \bullet \\ \text{---} \\ \bullet \end{array} \equiv L_b^\times + L_k^\times + L_h^\times \\
\rho^{(0)}(M_7) &= 2 \begin{array}{c} \circlearrowleft \\ \text{---} \\ \bullet \\ \text{---} \\ \bullet \end{array} + \begin{array}{c} \circlearrowleft \\ \text{---} \\ \bullet \\ \text{---} \\ \bullet \end{array} + 4 \begin{array}{c} \circlearrowleft \\ \text{---} \\ \bullet \\ \text{---} \\ \bullet \end{array} + 2 \begin{array}{c} \circlearrowleft \\ \text{---} \\ \bullet \\ \text{---} \\ \bullet \end{array} \equiv 2L_\ell^\times + L_m^\times + 4L_n^\times + 2L_o^\times \\
\rho^{(0)}(M_8) &= 2 \begin{array}{c} \circlearrowleft \\ \text{---} \\ \bullet \\ \text{---} \\ \bullet \end{array} + \begin{array}{c} \circlearrowleft \\ \text{---} \\ \bullet \\ \text{---} \\ \bullet \end{array} + 2 \begin{array}{c} \circlearrowleft \\ \text{---} \\ \bullet \\ \text{---} \\ \bullet \end{array} + 4 \begin{array}{c} \circlearrowleft \\ \text{---} \\ \bullet \\ \text{---} \\ \bullet \end{array} \equiv 2L_p^\times + L_q^\times + 2L_r^\times + 4L_s^\times
\end{aligned}$$

Then the invariants must be made up of plain-graphs whose variations are contained in the total derivative relations above. In other words, the invariants are made from:

$$\begin{array}{ccccc}
L_1 = \begin{array}{c} \bullet \\ \text{---} \\ \bullet \\ \text{---} \\ \bullet \end{array} &
L_2 = \begin{array}{c} \bullet \\ \text{---} \\ \bullet \\ \text{---} \\ \bullet \end{array} &
L_3 = \begin{array}{c} \bullet \\ \text{---} \\ \bullet \\ \text{---} \\ \bullet \end{array} &
L_4 = \begin{array}{c} \bullet \\ \text{---} \\ \bullet \\ \text{---} \\ \bullet \end{array} &
L_5 = \begin{array}{c} \bullet \\ \text{---} \\ \bullet \\ \text{---} \\ \bullet \end{array} \\
L_6 = \begin{array}{c} \bullet \\ \text{---} \\ \bullet \\ \text{---} \\ \bullet \end{array} &
L_7 = \begin{array}{c} \bullet \\ \text{---} \\ \bullet \\ \text{---} \\ \bullet \end{array} &
L_8 = \begin{array}{c} \bullet \\ \text{---} \\ \bullet \\ \text{---} \\ \bullet \end{array} &
L_9 = \begin{array}{c} \bullet \\ \text{---} \\ \bullet \\ \text{---} \\ \bullet \end{array} &
L_{10} = \begin{array}{c} \bullet \\ \text{---} \\ \bullet \\ \text{---} \\ \bullet \end{array}
\end{array}$$

We can now determine the 3-invariants:

$$\delta_3 \begin{pmatrix} L_1 \\ L_2 \\ L_3 \\ L_4 \\ L_5 \\ L_6 \\ L_7 \\ L_8 \\ L_9 \\ L_{10} \end{pmatrix} = \begin{pmatrix} 4 & 0 & 0 & 0 & 0 & 0 & 0 & 0 & 0 & 0 & 0 & 0 & 0 & 0 & 0 & 0 & 0 & 0 & 0 & 0 \\ 0 & 2 & 0 & 0 & 0 & 0 & 0 & 0 & 0 & 0 & 0 & 1 & 0 & 0 & 0 & 0 & 0 & 0 & 0 & 0 \\ 0 & 0 & 0 & 0 & 1 & 0 & 0 & 1 & 0 & 0 & 0 & 0 & 0 & 1 & 0 & 0 & 0 & 0 & 0 & 0 \\ 0 & 0 & 0 & 0 & 0 & 4 & 0 & 0 & 0 & 0 & 0 & 0 & 0 & 0 & 0 & 0 & 0 & 0 & 0 & 0 \\ 0 & 0 & 0 & 0 & 0 & 0 & 0 & 0 & 2 & 0 & 0 & 0 & 0 & 0 & 0 & 0 & 0 & 0 & 1 & 0 \\ 0 & 0 & 0 & 0 & 0 & 0 & 0 & 0 & 0 & 4 & 0 & 0 & 0 & 0 & 0 & 0 & 0 & 0 & 0 & 0 \\ 0 & 0 & 0 & 0 & 0 & 0 & 0 & 0 & 0 & 0 & 0 & 1 & 1 & 0 & 0 & 0 & 0 & 0 & 0 & 1 \\ 0 & 0 & 0 & 0 & 0 & 0 & 0 & 0 & 0 & 0 & 0 & 0 & 0 & 0 & 0 & 2 & 0 & 0 & 0 & 0 \\ 0 & 0 & 0 & 0 & 0 & 0 & 0 & 0 & 0 & 0 & 0 & 0 & 0 & 0 & 0 & 0 & 2 & 0 & 0 & 0 \\ 0 & 0 & 0 & 0 & 0 & 0 & 0 & 0 & 0 & 0 & 0 & 0 & 0 & 0 & 0 & 0 & 0 & 0 & 3 & 0 & 0 \end{pmatrix} \begin{pmatrix} L_a^\times \\ L_b^\times \\ L_c^\times \\ L_d^\times \\ L_e^\times \\ L_f^\times \\ L_g^\times \\ L_h^\times \\ L_i^\times \\ L_j^\times \\ L_k^\times \\ L_\ell^\times \\ L_m^\times \\ L_n^\times \\ L_o^\times \\ L_p^\times \\ L_q^\times \\ L_r^\times \\ L_s^\times \end{pmatrix}$$

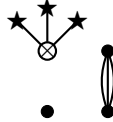
$$\sim \begin{pmatrix} 4 & 0 & 0 & 0 & 0 & 0 & 0 & 0 & 0 & 0 & 0 \\ 0 & 2 & 0 & 0 & 0 & -2 & -4 & -2 & 0 & 0 & 0 \\ 0 & 0 & 1 & 0 & 1 & 0 & 1 & 0 & 0 & 0 & 0 \\ 0 & 0 & 0 & 4 & 0 & 0 & 0 & 0 & 0 & 0 & 0 \\ -2 & 0 & 0 & 0 & -2 & 0 & 0 & 0 & 0 & 1 & 0 \\ 0 & 0 & -8 & 0 & 0 & 0 & 0 & 0 & 0 & 0 & 0 \\ 0 & -1 & 0 & 0 & -1 & 1 & 0 & 0 & 0 & 0 & 1 \\ 0 & 0 & 0 & 0 & 0 & 0 & 0 & 2 & 0 & 0 & 0 \\ 0 & 0 & 0 & 0 & 0 & 0 & 0 & 0 & 2 & 0 & 0 \\ 0 & 0 & 0 & 0 & 0 & 0 & 0 & 0 & -6 & -6 & -12 \end{pmatrix} \begin{pmatrix} L_a^\times \\ L_b^\times \\ L_e^\times \\ L_f^\times \\ L_h^\times \\ L_l^\times \\ L_n^\times \\ L_o^\times \\ L_p^\times \\ L_r^\times \\ L_s^\times \end{pmatrix}$$

The nullspace of the transpose of this matrix is spanned by $(3, 6, 24, 0, 6, 3, 12, 6, 3, 1)$, giving the only invariant linear combination,

$$\begin{aligned} & 3 \begin{array}{c} \bullet \quad \bullet \\ | \quad | \\ \bullet \quad \bullet \end{array} + 6 \begin{array}{c} \bullet \quad \bullet \\ / \quad \backslash \\ \bullet \quad \bullet \end{array} + 24 \begin{array}{c} \bullet \quad \bullet \\ / \quad \backslash \\ \bullet \quad \bullet \end{array} \\ & + 6 \begin{array}{c} \bullet \quad \bullet \\ \backslash \quad / \\ \bullet \quad \bullet \end{array} + 3 \begin{array}{c} \bullet \quad \bullet \\ / \quad \backslash \\ \bullet \quad \bullet \end{array} + 12 \begin{array}{c} \bullet \quad \bullet \\ / \quad \backslash \\ \bullet \quad \bullet \end{array} \\ & + 6 \begin{array}{c} \bullet \quad \bullet \\ / \quad \backslash \\ \bullet \quad \bullet \end{array} + 3 \begin{array}{c} \bullet \quad \bullet \\ | \quad | \\ \bullet \quad \bullet \end{array} + \begin{array}{c} \bullet \quad \bullet \\ / \quad \backslash \\ \bullet \quad \bullet \end{array} \end{aligned} \quad (4.8)$$

This gives the only independent minimal 3-invariant for $N = 4$.

Note that L_4 does not appear in the invariant. Indeed, it can be discarded immediately, since the unique Medusa associated with L_4 is



This Medusa has an empty vertex, which violates the lower bound on vertex degree.

4.3.3. Medusas and Total Derivative Relations

We have seen that Medusas play a central role in the search for P -invariants. It is thus worthwhile to discuss the key features of Medusas and to demonstrate how a total derivative relation consisting of loopless \times -graphs is constructed from a Medusa. Given any Medusa, $\rho^{(0)}(M)$ is in fact a total derivative relation, as can be seen from the following construction.

For fixed P and N , consider a Medusa M that contains $N(\star)$ \star -vertices. Then, by definition, it has a \times -vertex of degree $\deg(\times) = P + 1 - N(\star)$. Since the maximal degree of a \times -vertex is P , graphs in $\rho(M)$ contain at most $N(\star) - 1$ loops. Form a \star -graph $\Gamma^{(\ell)}$ from M by deleting $\ell \leq N(\star) - 1$ \star -vertices in M and then adding ℓ loops to the \times -vertex. By this definition, $M = \Gamma^{(0)}$. In the algebraic expression represented by $\Gamma^{(\ell)}$, the $N(\star) - \ell$ \star -vertices stand for $N(\star) - \ell$ partial derivatives acting on the whole term. Distributing $N(\star) - \ell - 1$ ∂ 's over all ϕ 's in this algebraic expression will result in a linear combination

of total derivative terms. In the graphical representation, this is equivalent to acting ρ on $\Gamma^{(\ell)}$ but keeping fixed exactly one \star -vertex and its incident edge. Setting to zero all coefficients of graphs in the resulting linear combination, except for the ones containing exactly ℓ loops, generates a linear combination $L^{(\ell)}$ of \star -graphs, each containing exactly one \star -vertex. By construction,

$$\rho^{(0)}(M) = \rho \left(\sum_{\alpha=0}^{N(\star)-1} (-1)^\alpha L^{(\alpha)} \right). \quad (4.9)$$

The algebraic form of the RHS of (4.9) is explicitly a total derivative relation. For a rigorous treatment of the above discussion, refer to Proposition 4 in Appendix B.2.3.

As a simple example, we consider the Medusa M_7 referred to in §4.3.2. We have

$$M_7 = \begin{array}{c} \star \\ \diagup \\ \circ \\ \diagdown \\ \star \\ \bullet \quad \bullet \\ \diagup \quad \diagdown \\ \bullet \quad \bullet \end{array} \Rightarrow \rho^{(0)}(M_7) = \rho \left(\begin{array}{c} \star \\ \diagup \\ \circ \\ \diagdown \\ \star \\ \bullet \quad \bullet \\ \diagup \quad \diagdown \\ \bullet \quad \bullet \end{array} + 2 \begin{array}{c} \star \\ \diagup \\ \circ \\ \diagdown \\ \star \\ \bullet \quad \bullet \\ \diagup \quad \diagdown \\ \bullet \quad \bullet \end{array} - \begin{array}{c} \star \\ \diagup \\ \circ \\ \diagdown \\ \star \\ \bullet \quad \bullet \\ \diagup \quad \diagdown \\ \bullet \quad \bullet \end{array} \right)$$

For a second example, we consider $(P, N, \Delta) = (5, 3, 6)$ and the Medusa

$$M = \begin{array}{c} \star \\ \diagup \\ \circ \\ \diagdown \\ \star \\ \bullet \quad \bullet \\ \diagup \quad \diagdown \\ \bullet \quad \bullet \end{array}$$

By (4.9), we obtain

$$\rho^{(0)}(M) = \rho \left(2 \begin{array}{c} \star \\ \diagup \\ \circ \\ \diagdown \\ \star \\ \bullet \quad \bullet \\ \diagup \quad \diagdown \\ \bullet \quad \bullet \end{array} + 2 \begin{array}{c} \star \\ \diagup \\ \circ \\ \diagdown \\ \star \\ \bullet \quad \bullet \\ \diagup \quad \diagdown \\ \bullet \quad \bullet \end{array} - 2 \begin{array}{c} \star \\ \diagup \\ \circ \\ \diagdown \\ \star \\ \bullet \quad \bullet \\ \diagup \quad \diagdown \\ \bullet \quad \bullet \end{array} + \begin{array}{c} \star \\ \diagup \\ \circ \\ \diagdown \\ \star \\ \bullet \quad \bullet \\ \diagup \quad \diagdown \\ \bullet \quad \bullet \end{array} \right).$$

This Medusa is involved in a 5-invariant that we will construct in §4.4.

4.4. Superposition of Graphs

In §3, we discovered an intriguing construction of the minimal 1-invariant for given N , which is a sum with equal coefficients of all possible trees with N vertices. A close study of the P -invariants with $P > 1$ in §4 also reveals an elegant structure in these invariants: They can all be decomposed as a *superposition* of equal-weight tree summations and *exact* invariants. Recall that an exact invariant is a linear combination that is invariant exactly, instead of up to a total derivative. In the graphical representation, a linear combination of graphs is an exact P_E -invariant if and only if all vertices are of degree larger than P_E (Corollary 4). Each graph in an exact invariant is itself exactly invariant.

Next we illustrate “the superposition of linear combinations” by explicit examples. When appropriate, we will consider labeled graphs and only remove the labels at the end. Consider two labeled graphs,

$$\Gamma_1 = \begin{array}{c} \bullet \\ \diagup \\ \bullet \quad \bullet \\ \diagdown \\ \bullet \end{array} \quad \Gamma_2 = \begin{array}{c} \bullet \\ \diagup \\ \bullet \quad \bullet \\ \diagdown \\ \bullet \end{array}$$

The superposition of Γ_1 and Γ_2 is defined to be the graph formed by taking all edges in Γ_2 and adding them to Γ_1 , i.e.,

$$\Gamma_1 \cup \Gamma_2 = \begin{array}{c} \bullet \\ \diagup \quad \diagdown \\ \bullet \quad \bullet \\ \hline \bullet \end{array}$$

The superposition of two linear combinations, $L_A = \sum_{i=1}^{k_A} a_i \Gamma_i^A$ and $L_B = \sum_{i=1}^{k_B} b_i \Gamma_i^B$, of plain graphs Γ_i^A, Γ_j^B with the same N , is defined as

$$L_A \cup L_B \equiv \sum_{i=1}^{k_A} \sum_{j=1}^{k_B} a_i b_j \Gamma_i^A \cup \Gamma_j^B.$$

In the following we present numerous examples of invariants constructed by superposing equal-weight tree summations and exact invariants for various P 's. In fact, Theorem 7 of Appendix B.4 states:

For fixed N , the superposition of an exact P_E -invariant with the superposition of Q minimal loopless 1-invariants results in a P -invariant, provided $P_E + 2Q \geq P$.⁶

We conjecture that the above result captures all P -invariants, up to total derivatives. Since we have classified all exact invariants and all 1-invariants (Theorem 4), it is straightforward to construct the P -invariants in the above statement for any specific case. We now proceed to construct the minimal P -invariants for some important cases.

4.4.1. Quadratic Shift ($P=2$)

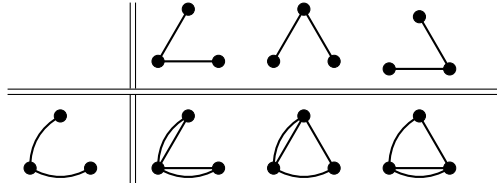
$N = 3$ Case: A 2-invariant can be constructed by superposing an equal-weight tree summation with an exact 0-invariant. In the labeled representation, all possible trees for $N = 3$ are given by (3.3),



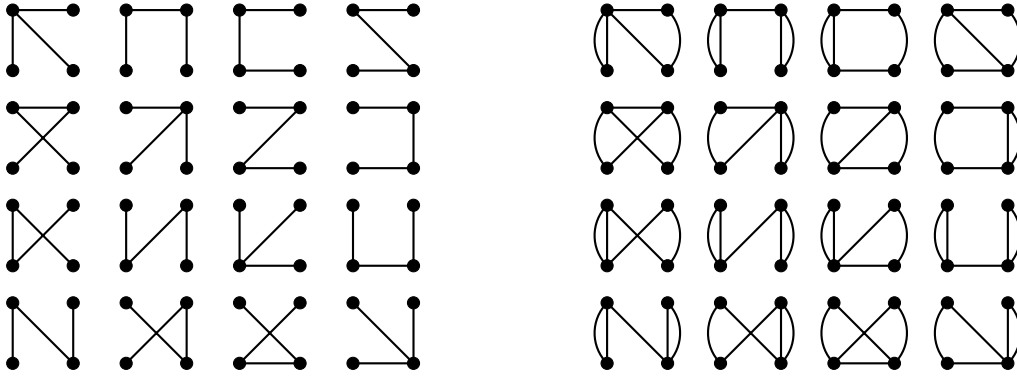
The sum of all three $N = 3$ trees with unit coefficients gives a 1-invariant, $L_{3\text{-pt}}$. On the other hand, up to total derivatives, an exact 0-invariant with $\Delta = 2$ is isomorphic to

$$\Gamma_0 = \begin{array}{c} \bullet \\ \diagup \quad \diagdown \\ \bullet \quad \bullet \\ \hline \bullet \end{array}$$

Then $\Gamma_0 \cup L_{3\text{-pt}}$ contains the three superposed graphs as follows:



⁶Note that this theorem also applies when $P_E < 0$, where we take an exact P_E -invariant for $P_E < 0$ to mean any linear combination of plain-graphs. In particular, the plain-graph consisting only of empty vertices is a P_E -invariant for any $P_E < 0$, and superposing this graph on any other is equivalent to not superposing anything at all.



(a) All 16 trees for $N = 4$.⁷

(b) Superposition of (4.11) and the 16 trees.

Figure 1: The most relevant 2-invariant for $N = 4$ from superposition of graphs.

Summing over all superposed graphs with unit coefficients gives a 2-invariant for $N = 3$ (after identifying isomorphic graphs),

$$\delta_2 \left(\begin{array}{c} \bullet \\ \diagup \quad \diagdown \\ \bullet \end{array} + 2 \begin{array}{c} \bullet \\ \diagup \quad \diagdown \\ \bullet \end{array} \right) = \rho^{(0)} \left(2 \begin{array}{c} \otimes \quad \star \\ \diagdown \quad \diagup \\ \bullet \end{array} \right). \quad (4.10)$$

Note that for $P = 2$ and $N = 3$, we need only consider Medusas with at least four edges, since that the \times -vertex and \bullet -vertices have degree no less than 2. The Medusa in (4.10) is the only such Medusa with $\Delta = 4$. Therefore, this is the only independent minimal 2-invariant. Note that the 2-invariant given in (4.10) and the 3-invariant in (4.3) happen to be the same.

In fact, we can prove a general minimality statement for $N = 3$. Consider a Medusa with $\Delta = P + 1$ for odd P , and $\Delta = P + 2$ for even P . The \bullet -vertices of this Medusa have degree at least $\frac{1}{2}\Delta$. For odd P this already saturates the lower bound for the degree of a \bullet -vertex; no edge joining the two \bullet -vertices can be removed and thus Δ cannot be lowered further. For even P , one \bullet -vertex saturates the lower bound on vertex degree and the other \bullet -vertex has an excess of exactly one edge. Nevertheless, the same conclusion holds.

$N = 4$ Case: In §4.3.1 we found that (4.7) gives the only independent minimal 2-invariant for $N = 4$. It has the structure of a superposition of the sum with unit coefficients of all $N = 4$ trees (Figure 1a) and an exact 0-invariant:

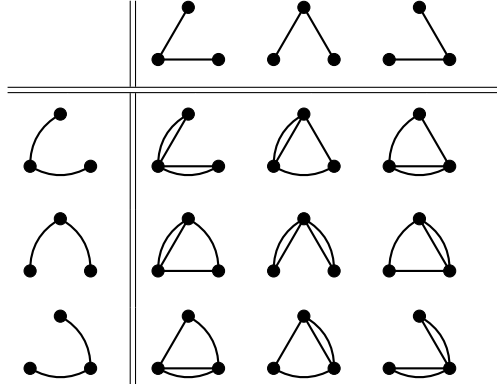
$$\left(\begin{array}{c} \bullet \\ \diagup \quad \diagdown \\ \bullet \end{array} \right) \quad (4.11)$$

The superposition of this 0-invariant with the trees in Figure 1a is given in Figure 1b. The sum of all graphs in Figure 1b with unit coefficients gives the 2-invariant in (4.7) (with an overall prefactor of 4).

⁷The trees are arranged in order of their Prüfer sequences [23].

4.4.2. Cubic Shift ($P=3$)

$N = 3$ Case: For $P = 3$, the only independent minimal invariant for $N = 3$ is given in (4.3), which can be written as a superposition of two equal-weight tree summations:



As we already pointed out, this 3-invariant happens to be the minimal 2-invariant as well.

We can produce more 3-invariants by superposing an exact 1-invariant on the equal-weight sum of $N = 3$ trees. This would have two more derivatives compared to the minimal term above. For example, there are two independent exact 1-invariants for $N = 3$ with 3 edges:



which yield the following two 3-invariants:

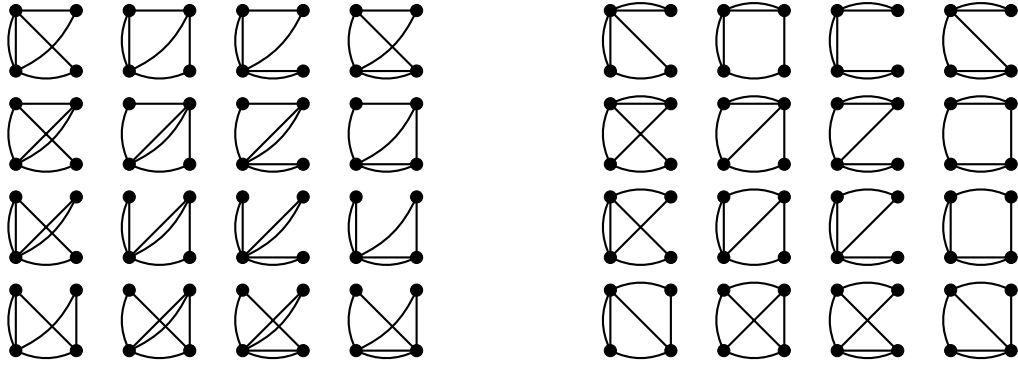


$N = 4$ Case: In §4.3.2 we found that (4.8) gives the only independent minimal 3-invariant for $N = 4$. It has the structure of a superposition of two sums with unit coefficients of all trees in Figure 1a. As mentioned in §3, there are two isomorphism classes of $N = 4$ trees:

$$T_A = \begin{array}{c} \bullet \\ \diagdown \quad \diagup \\ \bullet \quad \bullet \\ \diagup \quad \diagdown \\ \bullet \end{array} \quad T_B = \begin{array}{c} \bullet \\ \diagdown \quad \diagup \\ \bullet \quad \bullet \\ \diagup \quad \diagdown \\ \bullet \end{array} \quad (4.12)$$

Superposing these graphs on the $N = 4$ trees produces the graphs in Figure 2. If T and T' are isomorphic trees, then superposing T on the trees in Figure 1a produces 16 graphs which are isomorphic to the 16 graphs formed by superposing T' on the same trees. There are four trees in the isomorphism class of T_A and twelve for T_B . Therefore, we just have to give the 16 graphs in Figure 2a weight 4 and the 16 graphs in Figure 2b weight 12 and then add them all up. The result is (4.8) with an overall prefactor of 4. Again, we have already shown that this is the unique minimal 3-invariant for $N = 4$.

As in the $N = 3$ case, we can produce non-minimal 3-invariants by superposing an exact 1-invariant on the equal-weight sum of $N = 4$ trees. For example, there are four



(a) Superposition of T_A and Figure 1a.

(b) Superposition of T_B and Figure 1a.

Figure 2: Superposition of graphs in (4.12) on trees in Figure 1a.

independent exact 1-invariants for $N = 4$ with the lowest number of edges:



4.4.3. Quartic Shift ($P=4$)

$N = 3$ Case: As argued earlier, $\Delta_{\min} = 6$ in this case. There are two Medusas with the fewest edges such that the \times -vertex and the \bullet -vertices have degree no less than 3 (note that $\frac{1}{2}(P+1) = \frac{5}{2}$ in this case):



There is exactly one minimal 4-invariant in this case, which is constructed by superposing two equal-weight sums of trees with an exact 0-invariant:



Note that the sum of the coefficients is 9, as it should be, since there are three $N = 3$ trees, and thus there are nine superpositions of two $N = 3$ trees.

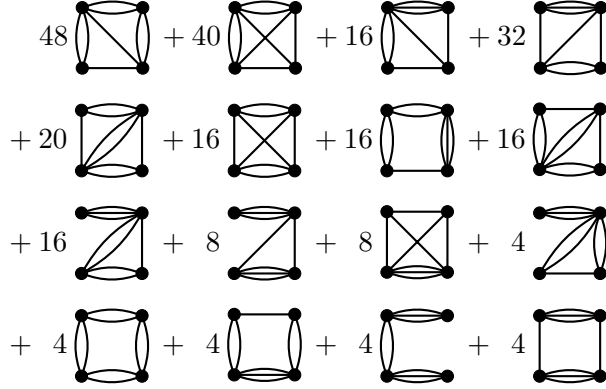
Examples of non-minimal invariants can be constructed by superposing an equal-weight sum of trees with an exact 2-invariant, or two equal-weight sums of trees with an exact 1-invariant.

The proofs of uniqueness and minimality for the remaining $N = 4$ examples are lengthy and involve many more Medusas than the previous examples, but the process is the same. Therefore, we will simply write the invariants and state that they are unique and minimal.

$N=4$ Case: We construct the minimal 4-invariant by superposing two copies of equal-weight sums of trees with an exact 0-invariant. There is one independent exact 0-invariant:



Superposing this on the superposition of two copies of equal-weight sums of trees yields



Note that the sum of the coefficients is $256 = 16^2$.

4.4.4. Quintic Shift ($P=5$)

$N = 3$ Case: In this case, $\Delta_{\min} = 6$. There are three Medusas with the fewest edges such that the \times -vertex and the \bullet -vertices have degree no less than 3 (note that $\frac{1}{2}(P+1) = 3$):



There is exactly one minimal 5-invariant in this case, which is constructed by superposing three equal-weight sums of trees:



Note that the sum of the coefficients is $27 = 3^3$. Also, note that this is proportional to the unique independent minimal 4-invariant found in the previous section, which was the superposition of two equal-weight sums of trees and an exact 0-invariant.

$N = 4$ Case: The superposition of three equal-weight sums of $N = 4$ trees yields

$$\begin{aligned}
& 4 \begin{array}{c} \bullet \\ \diagup \diagdown \\ \bullet \end{array} + 12 \begin{array}{c} \bullet \\ \text{---} \text{---} \\ \bullet \end{array} + 108 \begin{array}{c} \bullet \\ \diagup \diagdown \\ \bullet \end{array} + 432 \begin{array}{c} \bullet \\ \diagup \diagdown \\ \bullet \end{array} + 288 \begin{array}{c} \bullet \\ \diagup \diagdown \\ \bullet \end{array} \\
& + 72 \begin{array}{c} \bullet \\ \diagup \diagdown \\ \bullet \end{array} + 216 \begin{array}{c} \bullet \\ \diagup \diagdown \\ \bullet \end{array} + 216 \begin{array}{c} \bullet \\ \diagup \diagdown \\ \bullet \end{array} + 36 \begin{array}{c} \bullet \\ \text{---} \text{---} \\ \bullet \end{array} + 72 \begin{array}{c} \bullet \\ \text{---} \text{---} \\ \bullet \end{array} \\
& + 72 \begin{array}{c} \bullet \\ \diagup \diagdown \\ \bullet \end{array} + 144 \begin{array}{c} \bullet \\ \diagup \diagdown \\ \bullet \end{array} + 144 \begin{array}{c} \bullet \\ \diagup \diagdown \\ \bullet \end{array} + 612 \begin{array}{c} \bullet \\ \diagup \diagdown \\ \bullet \end{array} + 144 \begin{array}{c} \bullet \\ \diagup \diagdown \\ \bullet \end{array} \\
& + 216 \begin{array}{c} \bullet \\ \diagup \diagdown \\ \bullet \end{array} + 72 \begin{array}{c} \bullet \\ \text{---} \text{---} \\ \bullet \end{array} + 72 \begin{array}{c} \bullet \\ \diagup \diagdown \\ \bullet \end{array} + 432 \begin{array}{c} \bullet \\ \diagup \diagdown \\ \bullet \end{array} + 72 \begin{array}{c} \bullet \\ \text{---} \text{---} \\ \bullet \end{array} \\
& + 72 \begin{array}{c} \bullet \\ \diagup \diagdown \\ \bullet \end{array} + 72 \begin{array}{c} \bullet \\ \diagup \diagdown \\ \bullet \end{array} + 216 \begin{array}{c} \bullet \\ \diagup \diagdown \\ \bullet \end{array} + 192 \begin{array}{c} \bullet \\ \diagup \diagdown \\ \bullet \end{array} + 108 \begin{array}{c} \bullet \\ \diagup \diagdown \\ \bullet \end{array}
\end{aligned}$$

Note that the sum of the coefficients is $4096 = 16^3$.

To facilitate the check of the invariance of the above linear combination, denoted as L , we provide the linear combination of Medusas L_M such that $\delta_5(L) = \rho^{(0)}(L_M)$:

$$\begin{aligned}
& 12 \begin{array}{c} \star \\ \diagup \diagdown \\ \otimes \end{array} + 72 \begin{array}{c} \star \\ \diagup \diagdown \\ \otimes \end{array} + 24 \begin{array}{c} \star \\ \diagup \diagdown \\ \otimes \end{array} + 72 \begin{array}{c} \star \\ \diagup \diagdown \\ \otimes \end{array} + 72 \begin{array}{c} \star \\ \text{---} \text{---} \\ \otimes \end{array} + 144 \begin{array}{c} \star \\ \diagup \diagdown \\ \otimes \end{array} \\
& + 144 \begin{array}{c} \star \\ \diagup \diagdown \\ \otimes \end{array} + 216 \begin{array}{c} \star \\ \diagup \diagdown \\ \otimes \end{array} + 72 \begin{array}{c} \star \\ \text{---} \text{---} \\ \otimes \end{array} + 72 \begin{array}{c} \star \\ \text{---} \text{---} \\ \otimes \end{array} + 72 \begin{array}{c} \star \\ \diagup \diagdown \\ \otimes \end{array} + 288 \begin{array}{c} \star \\ \diagup \diagdown \\ \otimes \end{array} \\
& + 432 \begin{array}{c} \star \\ \diagup \diagdown \\ \otimes \end{array} + 108 \begin{array}{c} \star \\ \diagup \diagdown \\ \otimes \end{array} + 216 \begin{array}{c} \star \\ \diagup \diagdown \\ \otimes \end{array} + 144 \begin{array}{c} \star \\ \text{---} \text{---} \\ \otimes \end{array} + 216 \begin{array}{c} \star \\ \diagup \diagdown \\ \otimes \end{array}
\end{aligned}$$

5. Conclusions and Outlook

In this paper, we studied nonrelativistic scalar field theories with polynomial shift symmetries. In the free-field limit, such field theories arise in the context of Goldstone’s theorem, where they lead to the hierarchies of possible universality classes of Nambu-Goldstone modes, as reviewed in §2. Our main focus in §3 and §4 has been on *interacting* effective field theories which respect the polynomial shift symmetries of degree $P = 1, 2, \dots$. In order to find such theories, one needs to identify possible Lagrangian terms invariant under the polynomial shift up to total derivatives, and organize them by their scaling dimension, starting from the most relevant. As we showed in §3, §4 and Appendix B, this essentially cohomological classification problem can be usefully translated into the language of graph theory. This graphical technique is important for two reasons. First, it is quite powerful: The translation of the classification problem into a graph-theory problem allows us to generate sequences of invariants for various values of P , number N of fields, the number 2Δ

of spatial derivatives, and as a function of the spatial dimension D , in a way that is much more efficient than any “brute force” technique. Secondly, and perhaps more importantly, the graphical technique reveals some previously hidden structure even in those invariants already known in the literature. For example, the known Galileon N -point invariants are given by the equal-weight sums of all labeled trees with N vertices! This hidden simplicity of the Galileon invariants is a feature previously unsuspected in the literature, and its mathematical explanation deserves further study. In addition, we also discovered patterns that allow the construction of higher polynomials from the superposition of graphs representing a collection of invariants of a lower degree – again a surprising result, revealing glimpses of intriguing connections among the *a priori* unrelated spaces of invariants across the various values of P , N and Δ .

Throughout this paper, we focused for simplicity on the unrestricted polynomial shift symmetries of degree P , whose coefficients $a_{i_1\dots i_\ell}$ are general real symmetric tensors of rank $\ell = 0, \dots, P$. As we pointed out in §2.4, at $P \geq 2$, this maximal polynomial shift symmetry algebra allows various subalgebras, obtained by imposing additional conditions on the structure of $a_{i_1\dots i_\ell}$ ’s. While this refinement does not significantly impact the classification of Gaussian fixed points, reducing the symmetry to one of the subalgebras inside the maximal polynomial shift symmetry can lead to new N -point invariants, beyond the ones presented in this paper. It is possible to extend our graphical technique to the various reduced polynomial shift symmetries, and to study the refinement of the structure of polynomial shift invariants associated with the reduced symmetries.

Our main motivation for the study of scalar field theories with polynomial shift symmetries has originated from our desire to map out phenomena in which technical naturalness plays a crucial role, in general classes of field theories with or without relativistic symmetries. The refined classification of the universality classes of NG modes and the nonrelativistic refinement of Goldstone’s theorem have provided an example of scenarios where our naive relativistic intuition about technical naturalness may be misleading, and new interesting phenomena can emerge. We anticipate that other surprises of naturalness are still hidden not only in the landscape of quantum field theories, but also in the landscape of nonrelativistic theories of quantum gravity.

Acknowledgments

We wish to thank Hitoshi Murayama and Haruki Watanabe for useful discussions. This work has been supported by NSF Grant PHY-1214644 and by Berkeley Center for Theoretical Physics.

A. Glossary of Graph Theory

In this section, we list the standard terminologies in graph theory to which we will refer. (These essentially coincide with the ones in [23].)

Graph A *graph* Γ is an ordered pair $(V(\Gamma), E(\Gamma))$ consisting of a set $V(\Gamma)$ of *vertices* and a set $E(\Gamma)$, disjoint from $V(\Gamma)$, of *edges*, together with an *incident function* Ψ_Γ that

associates with each edge of Γ an ordered pair of (not necessarily distinct) vertices of Γ . If e is an edge and u and v are vertices such that $\Psi_\Gamma(e) = \{u, v\}$, then e is said to *join* u and v .

Isomorphism Two graphs Γ_A and Γ_B are *isomorphic* if there exist a pair of bijections $f : V(\Gamma_A) \rightarrow V(\Gamma_B)$ and $\phi : E(\Gamma_A) \rightarrow E(\Gamma_B)$ such that $\Psi_{\Gamma_A}(e) = \{u, v\}$ if and only if $\Psi_{\Gamma_B}(\phi(e)) = \{f(u), f(v)\}$.

Identical Graphs Two graphs are *identical*, written $\Gamma_A = \Gamma_B$, if $V(G) = V(H)$, $E(G) = E(H)$ and $\Psi_G = \Psi_H$.

Labeled Graph A graph in which the vertices are labeled but the edges are not, is called a *labeled graph*. This will be the notion of graphs that we will refer to most frequently.

Unlabeled Graph An *unlabeled graph* is a representative of an equivalence class of isomorphic graphs.

Finite Graph A graph is *finite* if both of its vertex set and edge set are finite.

Null Graph The graph with no vertices (and hence no edges) is the *null graph*.

Incident The ends of an edge are said to be *incident* to the edge, and *vice versa*.

Adjacent Two vertices which are incident to a common edge are *adjacent*.

Loop A *loop* is an edge that joins a vertex to itself.

Cycle A *cycle* on two or more vertices is a graph in which the vertices can be arranged in a cyclic sequence such that two vertices are joined by exactly one edge if they are consecutive in the sequence, and are nonadjacent otherwise. A *cycle* on one vertex is a graph consisting of a single vertex with a loop.

Loopless Graph A *loopless* graph contains no loops. Note that a loopless graph may still contain cycles on two or more vertices.

Vertex Degree The *degree* of a vertex v , denoted by $\deg(v)$, in a graph Γ is the number of edges of Γ incident to v , with each loop counting as two edges.

Empty Vertex A vertex of degree 0 is called an *empty vertex*.

Leaf A vertex of degree 1 is called a *leaf*.

Edge Deletion The *edge deletion* of an edge e in a graph Γ is defined by deleting from Γ the edge e but leaving the vertices and the remaining edges intact.

Vertex Deletion The *vertex deletion* of a vertex v in a graph Γ is defined by deleting from Γ the vertex v together with all the edges incident to v . The resulting graph is denoted by $\Gamma - v$.

Connected Graph A graph is *connected* if, for every partition of its vertex set into two nonempty sets X and Y , there is an edge with one end in X and one end in Y .

Connected Component A *connected component* of a graph Γ is a connected subgraph Γ' of Γ such that any vertex v in Γ' satisfies the following condition: all edges incident to v in Γ are also contained in Γ' .

Tree A *tree* is a connected graph that contains no cycles. In particular, note that a tree has no empty vertices if it contains more than one vertex.

Cayley's Formula The number of labeled trees on N vertices is N^{N-2} .

B. Theorems and Proofs

B.1. The Graphical Representation

Consider the polynomial shift symmetry applied to a real scalar field ϕ ,

$$\phi(t, x^i) \rightarrow \phi(t, x^i) + \delta_P \phi, \quad \delta_P \phi = a_{i_1 \dots i_P} x^{i_1} \dots x^{i_P} + \dots + a_i x^i + a. \quad (\text{B.1})$$

The polynomial ends at P^{th} order in the spatial coordinate x^i with $P = 0, 1, 2, \dots$, respectively corresponding to constant shift, linear shift, quadratic shift, and so on. The a 's are arbitrary real coefficients that parametrize the symmetry transformation, and are symmetric in any pair of indices. In the algebraic language, for a specific P , we are searching for a Lagrangian that is invariant under the polynomial shift up to a total derivative. Let L be a term in the Lagrangian with N ϕ 's and 2Δ spatial derivatives. Then,

$$\delta_P(L) = \partial_i(L_i), \quad (\text{B.2})$$

where L_i is an expression containing $N - 1$ ϕ 's and an index i , which is not contracted. Such L 's are called *P-invariants*. We will mainly focus on interaction terms, i.e., $N \geq 3$.

We want to express these P -invariants using a graphical representation. The ingredients of the graphical representation are:

1. \bullet -vertices, denoted in a graph by \bullet .
2. \times -vertices, denoted in a graph by \otimes .
3. \star -vertices, denoted in a graph by \star .
4. Edges, denoted in a graph by a line, that join the above vertices.

In this context, a graph contains up to three types of vertices. This means that these graphs carry an additional structure regarding vertex type, compared to the conventional definition of a graph in Appendix A.

We construct graphs using the following rules:

1. The maximal degree of a \times -vertex is P . Any graph containing a \times -vertex of degree greater than P is identified with the null graph.



Figure 3: Examples for the graphical representation of algebraic expressions.

2. There is at most one \times -vertex in a graph.
3. A \star -vertex is always a leaf (i.e., it has degree one).
4. Two \star -vertices are not allowed to be adjacent to each other.

We now describe what these graph ingredients represent. A \bullet -vertex represents a ϕ and a \times -vertex represents $\delta_P\phi$. A pair of derivatives with contracted indices, each one acting on a certain ϕ or $\delta_P\phi$, is represented by an edge joining the relevant \bullet - and \times -vertices. Note that Rule 1, which requires that there be at most P edges incident to the \times -vertex, is justified since $P + 1$ derivatives acting on $\delta_P\phi$ gives zero.

A graph with \star -vertices will represent terms which are total derivatives. By Rules 3 and 4, a \star -vertex must always have exactly one edge incident to it, and this edge is incident to a \bullet -vertex or \times -vertex. This edge represents a derivative acting on the entire term as a whole, and the index of that derivative is contracted with the index of another derivative acting on the ϕ or $\delta_P\phi$ of the \bullet - or \times -vertex, respectively, to which the \star -vertex is adjacent. Therefore, any graph with a \star -vertex represents a total derivative term.

Since the Lagrangian terms that these graphs represent have a finite number of ϕ 's and ∂ 's, we will consider only finite graphs. In addition, by the definition of graphs, all vertices and edges are automatically labeled, due to the fact that all elements in a set are distinct from each other. Therefore, a graph represents an algebraic expression in which each ϕ and ∂ carries a label. It will be convenient to keep the labels on ϕ , but it is unnecessary to label the derivatives. This motivates the definition given in Appendix A for “labeled” graphs. In the rest of Appendix B, unless otherwise stated, a graph is understood to be a labeled graph.

The desired algebraic expressions in which all ϕ 's are identical can be recovered by identifying all isomorphic graphs (for examples, refer to §3). In fact, the labeled P -invariants already capture all of the unlabeled ones (Appendix B.5).

Note that not all algebraic expressions are captured in the graphical representation described above. For example, $\partial^2(\partial_j\phi\partial_j\phi)$ cannot be represented by a graph, since two \star -vertices are forbidden to be adjacent to each other by Rule 4. However, this algebraic expression can be written as $2\partial_i(\partial_i\partial_j\phi\partial_j\phi)$, which is graphically represented in Figure 3a, disregarding the coefficient 2. Another peculiar example is $\partial_i(\partial_j\phi\partial_j\phi)\partial_i\partial^2\phi$, which is equal to $4(\partial_i\partial_j\phi)(\partial_j\phi)(\partial_i\partial^2\phi)$. Although the graphical representation for the former expression is beyond the current framework, the graphical representation for the latter one is given in Figure 3b. One could generalize the graphical representation to include all possible algebraic expressions. However, for our purposes, the present framework will suffice.

B.1.1. Types of Graphs and Vector Spaces

We classify graphs by different combinations of vertices:

Definition 1.

1. A plain-graph is a graph in which all vertices are \bullet 's.
2. A \star -ed plain-graph is a graph with vertex set consisting of only \bullet -vertices and at least one \star -vertex.
3. A \times -graph is a plain-graph with one \bullet -vertex replaced with a \times -vertex.
4. A \star -graph is a graph with one \times -vertex and at least one \star -vertex.

We define sets of graphs and the real vector spaces that they generate:

Definition 2.

1. $\mathcal{G}_{N,\Delta}$ is the set of plain-graphs with N \bullet -vertices and Δ edges.
2. $\mathcal{G}_{N,\Delta}^\times$ is the set of \times -graphs with $N - 1$ \bullet -vertices, one \times -vertex and Δ edges.
3. $\mathcal{G}_{N,\Delta}^\star$ is the set of \star -graphs with $N - 1$ \bullet -vertices, one \times -vertex, at least one \star -vertex and Δ edges.

In the above graphs, we choose the labels of the \bullet - and \times -vertices to go from v_1 to v_N and the labels of the \star -vertices to go from v_1^\star to $v_{N(\star)}^\star$, where $N(\star)$ is the number of \star -vertices. Let $\mathcal{L}_{N,\Delta}$, $\mathcal{L}_{N,\Delta}^\times$ and $\mathcal{L}_{N,\Delta}^\star$ be the real vector spaces of formal linear combinations generated by $\mathcal{G}_{N,\Delta}$, $\mathcal{G}_{N,\Delta}^\times$ and $\mathcal{G}_{N,\Delta}^\star$, respectively. The zero vector in any of these vector spaces is the null graph.

Note that $N = N(\bullet) + N(\times)$, where $N(\bullet)$ is the number of \bullet -vertices and $N(\times)$ is the number of \times -vertices. N does not include $N(\star)$ since \star -vertices represent neither ϕ nor $\delta_P\phi$. These sets of graphs are finite and therefore the vector spaces of formal linear combinations are finite-dimensional.

By Definition 2, graphs in a linear combination $L \in \mathcal{L}_{N,\Delta}$ ($\mathcal{L}_{N,\Delta}^\times$ or $\mathcal{L}_{N,\Delta}^\star$) share the same number of N and Δ . In most of the following discussion, N and Δ are fixed. We will therefore omit these subscripts as long as no confusion arises. However, the number of \star -vertices $N(\star)$ is not fixed in a generic linear combination of \star -graphs.

B.1.2. Maps

We now define some maps between the sets and vector spaces in Definition 2. This will model the operations that act on the algebraic expressions represented by the graphs.

Firstly, the variation under the polynomial shift δ_P of an algebraic term, expressed by a graph Γ , is represented graphically by summing over all graphs that have one \bullet -vertex in Γ replaced with a \times -vertex.

Definition 3 (Variation Map). *Given a plain-graph $\Gamma \in \mathcal{G}$, with $V(\Gamma) = (v_1, \dots, v_N)$, the map $\delta_P : \mathcal{G} \rightarrow \mathcal{L}^\times$ is defined by $\delta_P(\Gamma) = \sum_{i=1}^N \Gamma_i^\times$, where Γ_i^\times is a graph given by replacing v_i with a \times -vertex. This map extends to $\mathcal{L} \rightarrow \mathcal{L}^\times$ by distributing δ_P over the formal sum.*

Note that Γ_i^\times is the null graph if v_i has degree greater than P . We will omit the subscript P in δ_P as long as no confusion arises. It is also necessary to define a map that operates in the reverse direction:

Definition 4. *The map $v : \mathcal{G}^\times \rightarrow \mathcal{G}$ is defined by replacing the \times -vertex with a \bullet -vertex.*

In the algebraic expressions, a total derivative term looks like $\partial_i L_i$, and the ∂_i can be distributed over L_i as usual, by applying the Leibniz rule. This feature will be captured by the graphical representation in the following definition.

Definition 5 (Derivative Map). *For a given \star -graph $\Gamma^\star \in \mathcal{G}^\star$, the derivative map $\rho : \mathcal{G}^\star \rightarrow \mathcal{L}^\times$ is defined using the following construction:*

1. *For the \star -graph Γ^\star , denote the \bullet -vertices by v_1, \dots, v_{N-1} , the \times -vertex by v_N and the \star -vertices by $v_1^\star, \dots, v_k^\star$, $k = N(\star)$. Take any \star -vertex v_i^\star in Γ^\star . For each $j_1 \in \{1, \dots, N\}$, form a graph Γ_{j_1} by deleting v_i^\star in Γ^\star and then adding an edge joining v_{j_1} and the vertex that was adjacent to v_i^\star in Γ^\star .*
2. *Apply the above procedure to each of the Γ_{j_1} to form $\Gamma_{j_1 j_2}$ by removing the next v_i^\star . Iterate this procedure until all \star -vertices have been removed, forming the \times -graph $\Gamma_{j_1 \dots j_k}$.*
3. *Define $\rho(\Gamma^\star) \equiv \sum_{j_1, \dots, j_k=1}^N \Gamma_{j_1 \dots j_k}^\times$.*

The domain of this map can be extended to \mathcal{L}^\star by distributing ρ over the formal sum. The derivative map ρ can be similarly defined on \star -ed plain-graphs. Furthermore, we take ρ to be the identity map when it acts on \times -graphs.

Note that the above definition is well-defined since ρ is independent of the order in which the \star -vertices are deleted.

B.1.3. Relations

There are many linear combinations of plain- and \times -graphs representing terms that can be written as a total derivative. To take this feature into account, we define two notions of relations for plain- and \times -graphs, respectively.

Definition 6 (Relations). *If a linear combination of plain-graphs $L \in \mathcal{L}$ can be written as $\rho(L')$, where L' is a sum of \star -ed plain-graphs, then L is called a plain-relation. If a linear combination of \times -graphs $L^\times \in \mathcal{L}^\times$ can be written as $\rho(L^\star)$, with L^\star a sum of \star -graphs, then L^\times is called a \times -relation.*

We shall denote the set of all plain-relations by \mathcal{R} and the set of all \times -relations by \mathcal{R}^\times . \mathcal{R} and \mathcal{R}^\times have a natural vector space structure and are subspaces of \mathcal{L} and \mathcal{L}^\times , respectively.

B.1.4. The Consistency Equation and Associations

Recall that P -invariants are defined algebraically by equation (B.2), $\delta_P(L) = \partial_i(L_i)$. This equation is written in the graphical representation as

$$\delta_P(L) = \rho(L^*), \quad (\text{B.3})$$

for $L \in \mathcal{L}$ and $L^* \in \mathcal{L}^*$. We call (B.3) the *consistency equation*. Searching for P -invariants is equivalent to constructing all consistency equations. Note that, by Definition 6, the consistency equation implies that $\delta_P(L)$ is a \times -relation and so we make the following definition:

Definition 7 (*P-Invariant*). $L \in \mathcal{L}$ is a P -invariant if $\delta_P(L) \in \mathcal{R}^\times$.

Furthermore, there is a simple class of P -invariants, which we call *exact P-invariants*. These represent terms which are *exactly* invariant under the polynomial shift symmetry (B.1), not just up to a total derivative.

Definition 8 (*Exact P-Invariant*). $L \in \mathcal{L}$ is an exact P -invariant if $\delta_P(L) = 0$.

The following notion, called “association between graphs”, will turn out to be indispensable in constructing consistency equations.

Definition 9 (*Associations*). The associations between pairs of plain- and \times -graphs, plain- and plain-graphs, \star - and \times -graphs, \star - and \star -graphs and plain- and \star -graphs are defined as follows:

1. $\Gamma \in \mathcal{G}$ and $\Gamma^\times \in \mathcal{G}^\times$ are associated with each other if Γ^\times is contained in $\delta_P(\Gamma)$, or, equivalently, $v(\Gamma^\times) = \Gamma$.
2. Any two graphs $\Gamma_1, \Gamma_2 \in \mathcal{G}$ are associated with each other if either they are associated with the same $\Gamma^\times \in \mathcal{G}^\times$, or Γ_1 is identical to Γ_2 .
3. $\Gamma^* \in \mathcal{G}^*$ and $\Gamma^\times \in \mathcal{G}^\times$ are associated with each other if Γ^\times is contained in $\rho(\Gamma^*)$.
4. Any two graphs $\Gamma_1^*, \Gamma_2^* \in \mathcal{G}^*$ are associated with each other if either they are associated with the same $\Gamma^\times \in \mathcal{G}^\times$, or Γ_1^* and Γ_2^* are identical to each other.
5. Any two graphs $\Gamma \in \mathcal{G}$ and $\Gamma^* \in \mathcal{G}^*$ are associated with each other if they are associated with the same $\Gamma^\times \in \mathcal{G}^\times$.

It turns out that the associations between only plain-graphs and \times -graphs have a simple structure. Note that for any \times -graph $\Gamma^\times \in \mathcal{G}^\times$, $v(\Gamma^\times)$ uniquely defines the associated plain-graph. Hence,

Proposition 1. A \times -graph is associated with exactly one plain-graph.

The corollaries below directly follow:

Corollary 1. For $L \in \mathcal{L}$ and Γ^\times a \times -graph in $\delta(L)$, L contains the plain-graph $v(\Gamma^\times)$.

Corollary 2. *Any two associated plain-graphs are identical to each other.*

Proof. If two distinct plain-graphs are associated with each other, then they are associated with a common \times -graph, which violates Proposition 1. Therefore, only identical plain-graphs are associated with each other. \square

Corollary 3. *For $L \in \mathcal{L}$ and a plain-graph Γ in L , $\delta(L)$ contains all \times -graphs in $\delta(\Gamma)$.*

Proof. Without loss of generality, suppose Γ appears in L with unit coefficient (otherwise, simply divide L by the coefficient of Γ). Let Γ^\times be a \times -graph in $\delta(\Gamma)$. By Proposition 1, Γ is the only plain-graph associated with Γ^\times . Therefore, Γ^\times cannot drop out of $\delta(\Gamma + L')$ for any $L' \in \mathcal{L}$ that does not contain Γ . Applying this statement to $L' = L - \Gamma$ proves that Γ^\times must appear in $\delta(L)$. \square

This now allows us to find all *exact* P -invariants in a simple manner:

Corollary 4. *$L \in \mathcal{L}$ is an exact P -invariant if and only if all vertices in all graphs contained in L have degree at least $P + 1$.*

Proof. If there is a vertex v in some plain-graph Γ in L of degree lower than $P + 1$, then $\delta_P(\Gamma)$ contains the \times -graph where v is replaced with a \times -vertex. But by Corollary 3, this means that $\delta_P(L)$ also contains this \times -graph, which contradicts $\delta_P(L) = 0$. \square

All of the above definitions and conclusions make sense when extended to $P < 0$. Even though $P < 0$ no longer corresponds to any polynomial shift symmetry, it will occasionally be useful to consider graphs with $P < 0$. Since any vertex has a non-negative degree, Corollary 4 implies:

Corollary 5. *If $P < 0$, any $L \in \mathcal{L}$ is an exact P -invariant.*

Associations between \star -graphs and \times -graphs also have a simple and useful property:

Lemma 1. *Suppose that a \times -graph $\Gamma^\times \in \mathcal{G}^\times$ is associated with a \star -graph $\Gamma^\star \in \mathcal{G}^\star$ that contains a single \star -vertex. Then Γ^\times appears in $\rho(\Gamma^\star)$ with coefficient 1.*

In general, a \times -graph can be associated with more than one \star -graph. Figure 4 presents a simple example with $(P, N, \Delta) = (2, 3, 2)$. Consequently, there can exist multiple consistency equations for the same P -invariant. In the next section we will develop techniques to deal with this difficulty.

B.2. Building Blocks for Consistency Equations

In this section, we introduce the building blocks with which we will construct the consistency equation (B.3), $\delta_P(L) = \rho(L^\star)$. Any polynomial shift-invariant can be generated using these building blocks. We show that we can constrain L to contain only loopless plain-graphs, and all other invariants are equal to these ones up to total derivatives. Consequently, $\delta_P(L)$, and thus $\rho(L^\star)$, contains only loopless \times -graphs. Therefore, $\rho(L^\star) = \rho^{(0)}(L^\star)$, where $\rho^{(0)}$ acts in the same way as ρ but omits any looped graphs (Definition 13). In fact, we can restrict L^\star to be a linear combination L_M of a particular type of

$$\rho \left(\begin{array}{c} \circledast \\ \bullet \end{array} \begin{array}{c} \star \\ \bullet \end{array} \right) = 2 \begin{array}{c} \circledast \\ \bullet \end{array} \begin{array}{c} \star \\ \bullet \end{array} + \begin{array}{c} \circledast \\ \bullet \end{array} \begin{array}{c} \bullet \\ \bullet \end{array} + \begin{array}{c} \circledast \\ \bullet \end{array} \begin{array}{c} \bullet \\ \bullet \end{array} = \rho \left(\begin{array}{c} \circledast \\ \bullet \end{array} \begin{array}{c} \star \\ \bullet \end{array} + \begin{array}{c} \circledast \\ \bullet \end{array} \begin{array}{c} \bullet \\ \bullet \end{array} \right)$$

Figure 4: Two different linear combinations of \star -graphs result in an identical \times -relation for $P = 2$. In particular, the \times -graph with a coefficient 2 is associated with all three \star -graphs in the figure.

\star -graph, such that $\rho^{(0)}(L^\star) = \rho^{(0)}(L_M)$. These \star -graphs will be called Medusas (Definition 10). In Appendix B.2.5 we determine a lower bound on the degree of a vertex in any graph that appears in the consistency equation.

B.2.1. The Loopless Realization of \mathcal{L}/\mathcal{R}

There are usually many alternative expressions for a single P -invariant algebraic term, which are equal to each other up to total derivatives. In the graphical language, the graphs representing these equivalent expressions are related by plain-relations. Therefore, we are interested in the space of linear combinations of plain-graphs modding out plain-relations, i.e., the quotient space \mathcal{L}/\mathcal{R} . We need to find subset of graphs, $\mathcal{B} \subset \mathcal{G}$, whose span is isomorphic to \mathcal{L}/\mathcal{R} . In other words, every element of \mathcal{L} can be written as a linear combination of graphs in \mathcal{B} and plain-relations. Furthermore, this means that there are no plain-relations between elements in the set \mathcal{B} . The following proposition shows that the set of loopless plain-graphs realizes the set \mathcal{B} .

Proposition 2 (Loopless Basis). *The span of loopless plain-graphs is isomorphic to \mathcal{L}/\mathcal{R} .*

Proof. Denote the span of all loopless plain-graphs by $\mathcal{L}_{\text{loopless}}$. If $\partial_i \partial_i$ acts on a single ϕ , then one can always integrate by parts to move one of the ∂_i 's to act on the remaining ϕ 's. In the graphical language, this means that any graph with loops can always be written as a linear combination of loopless graphs up to a plain-relation. This proves $\mathcal{L}/\mathcal{R} \subset \mathcal{L}_{\text{loopless}}$.

Now, we show that there are no plain-relations between the loopless plain-graphs. Suppose there exists a linear combination of loopless plain-graphs L that is a plain-relation. That is, there exists a linear combination L' of \star -ed plain-graphs such that $L = \rho(L')$. Let Γ' be a \star -ed plain-graph in L' . Then, $\rho(\Gamma')$ is a linear combination of plain-graphs each of which has a number of loops no greater than the number of \star -vertices in Γ' . There will be exactly one graph, $\Gamma_{\text{f.l.}}$, which is fully-looped (with the number of loops equal to the number of \star -vertices in Γ'), produced when all the original \star -vertices (and the edges incident to them) are replaced with loops. Furthermore, $\Gamma_{\text{f.l.}}$ uniquely determines Γ' by replacing each loop in $\Gamma_{\text{f.l.}}$ with an edge incident to an extra \star -vertex. Choose the \star -ed plain-graph appearing in L' with the largest number of \star -vertices (the maximally \star -ed plain-graphs). This maximum exists since the number of the edges incident to the \star -vertices is bounded above by the number of edges Δ . The fully-looped graphs formed from these maximally \star -ed plain-graphs cannot cancel each other (by uniqueness) and cannot be canceled by

any other graphs that are not fully-looped (by maximality). Therefore $\rho(L')$ is a linear combination containing looped graphs, which contradicts the initial assumption that L only consists of loopless graphs. This proves $\mathcal{L}_{\text{loopless}} \subset \mathcal{L}/\mathcal{R}$.

Therefore, $\mathcal{L}_{\text{loopless}} \cong \mathcal{L}/\mathcal{R}$. \square

Henceforth, we can restrict our search for P -invariants to $\mathcal{L}_{\text{loopless}}$. Note that if $L \in \mathcal{L}_{\text{loopless}}$, then all the graphs in $\delta(L)$ are also loopless, so it is sufficient to consider only loopless \times -graphs. We can also restrict to loopless \times -relations, $\mathcal{R}_{\text{loopless}}^\times \subset \mathcal{R}^\times$, which is the vector space consisting of \times -relations that are linear combinations of loopless graphs. We summarize this discussion in the following corollary:

Corollary 6. *The P -invariants that are independent up to total derivatives are represented by $L \in \mathcal{L}_{\text{loopless}}$ with $\delta(L) \in \mathcal{R}_{\text{loopless}}^\times$. Equivalently, they span the kernel of the map:*

$$q \circ \delta : \mathcal{L}_{\text{loopless}} \rightarrow \mathcal{L}_{\text{loopless}}^\times / \mathcal{R}_{\text{loopless}}^\times,$$

where q is the quotient map $q : \mathcal{L}_{\text{loopless}}^\times \rightarrow \mathcal{L}_{\text{loopless}}^\times / \mathcal{R}_{\text{loopless}}^\times$.

B.2.2. Medusas and Spiders

Corollary 6 motivates us to look for a basis of $\mathcal{R}_{\text{loopless}}^\times$, the \times -relations that are linear combinations of loopless graphs. To classify all such loopless \times -relations, we are led to study the linear combinations of \star -graphs that give rise to these relations under the derivative map ρ . We will realize a convenient choice for the basis of $\mathcal{R}_{\text{loopless}}^\times$, which will tremendously simplify our calculations: It turns out that the basis of $\mathcal{R}_{\text{loopless}}^\times$ is in one-to-one correspondence with a particular subset of loopless \star -graphs, which we now define.

Definition 10 (Medusa). *A Medusa is a loopless \star -graph with all \star -vertices adjacent to the \times -vertex, such that the degree of the \times -vertex $\deg(\times)$ and the number of \star -vertices $N(\star)$ satisfy $\deg(\times) = P + 1 - N(\star)$. We denote the set of Medusas by $\mathcal{M}_{N,\Delta}$.*

We should point out that applying ρ to a Medusa does not necessarily generate a \times -relation in $\mathcal{R}_{\text{loopless}}^\times$; it will sometimes produce \times -graphs with loops. In order to form a loopless \times -relation, these looped \times -graphs must be canceled by contributions from other \star -graphs.

In the proof of the one-to-one correspondence between the basis of $\mathcal{R}_{\text{loopless}}^\times$ and the subset of Medusas, we will frequently refer to the following definitions.

Definition 11 (Primary \star -Graphs). *A primary \star -graph is a \star -graph that contains exactly one \star -vertex.*

Definition 12 (Spider). *A spider is a primary \star -graph with the \star -vertex adjacent to the \times -vertex and $\deg(\times) = P$.*

Since $\deg(\times) \geq N(\star)$ for a Medusa, we have $\frac{1}{2}(P + 1) \leq \deg(\times) \leq P$. In particular, if $P = 1$ or 2 , then $\deg(\times) = P$ and $N(\star) = 1$ (i.e., a Medusa is a loopless spider for $P = 1$ or 2). Spiders will play an important role in sorting out all independent loopless \times -relations in Appendix B.2.4, and loopless spiders will lead us to the classification of 1-invariants in Appendix B.3.

In B.2.3 and B.2.4 we will construct $\mathcal{R}_{\text{loopless}}^\times$ by spiders and Medusas. We will need to keep track of graphs containing specific numbers of loops, and the following refinement of the derivative map ρ (Definition 5) will allow us to formulate the graphical operations algebraically.

Definition 13. *The map $\rho^{(\ell)} : \mathcal{L}^\star \rightarrow \mathcal{L}^\times$ is defined such that, for $L^\star \in \mathcal{L}^\star$, $\rho^{(\ell)}(L^\star)$ is equal to $\rho(L^\star)$, with the coefficient of any graph that does not contain ℓ loops set to zero.*

Note that $\rho = \sum_{i=0}^{\infty} \rho^{(i)}$. If $\Gamma^\star \in \mathcal{G}^\star$ contains a loop, then $\rho^{(0)}(\Gamma^\star)$ is identically zero. In Theorem 1 we will show that the map $\rho^{(0)}$ defines the one-to-one correspondence between \mathcal{M} and the preferred basis of $\mathcal{R}_{\text{loopless}}^\times$.

It is also useful to introduce the operation of “undoing” loops.

Definition 14. *Given a $\Gamma \in \mathcal{G}^\times \cup \mathcal{G}^\star$ which contains ℓ loops, labeled from 1 to ℓ , the map $\theta_i : \mathcal{G}^\times \cup \mathcal{G}^\star \rightarrow \mathcal{G}^\star$ is defined such that $\theta_i(\Gamma)$ is a \star -graph constructed by deleting the i^{th} loop from Γ , adding an extra \star -vertex v^\star and adding an edge joining v^\star to the vertex at which the i^{th} deleted loop ended. Define $\theta : \mathcal{G}^\times \cup \mathcal{G}^\star \rightarrow \mathcal{G}^\star$ by $\theta(\Gamma) \equiv \theta_1 \circ \dots \circ \theta_\ell(\Gamma)$. This map extends to $\mathcal{L}^\times \cup \mathcal{L}^\star \rightarrow \mathcal{L}^\star$ by distributing θ over the formal sum. The map θ can be similarly defined on \star -ed plain-graphs.*

We will need to distinguish different types of loops:

Definition 15. *A loop at the \times -vertex is called a \times -loop, and a loop at a \bullet -vertex is a \bullet -loop. A graph that contains ℓ loops is called ℓ -looped.*

We can now prove a key formula:

Proposition 3. *If an ℓ -looped \star -graph Γ^\star contains a loop at vertex v_A , then*

$$\rho^{(\ell-1)} \circ \theta_A(\Gamma^\star) = \rho^{(\ell-1)} \circ \theta_A \circ \rho^{(\ell)}(\Gamma^\star) + \rho^{(\ell-1)} \left(\mathbf{L}_{\text{spider}}^{(\ell-1)} \right), \quad (\text{B.4})$$

where θ_A undoes a loop at v_A , and $\mathbf{L}_{\text{spider}}^{(\ell-1)}$ is a linear combination of $(\ell-1)$ -looped spiders. Every graph in a nonzero $\mathbf{L}_{\text{spider}}^{(\ell-1)}$ has one fewer \times -loop than Γ^\star . $\mathbf{L}_{\text{spider}}^{(\ell-1)}$ is nonzero if and only if the following three conditions are satisfied:

- (a) v_A is the \times -vertex;
- (b) There is a \star -vertex that is not adjacent to the \times -vertex;
- (c) $\deg(\times) \geq P+1 - N^\bullet(\star)$, where $N^\bullet(\star)$ is the number of \star -vertices in Γ^\star that are adjacent to \bullet -vertices.

Proof. Denote the vertices in Γ^\star adjacent to \star -vertices by v_i , $i = 1, \dots, k$, and the \times -vertex by v^\times . Note that v^\times and v_A may coincide with each other and with some of the v_i 's. Form an $(\ell-1)$ -looped graph Γ from Γ^\star by deleting all \star -vertices and deleting a loop at v_A . We now show that all graphs in $\rho^{(\ell-1)} \circ \theta_A(\Gamma^\star)$ and $\rho^{(\ell-1)} \circ \theta_A \circ \rho^{(\ell)}(\Gamma^\star)$ in (B.4) contain Γ as a subgraph:

- $\rho^{(\ell-1)} \circ \theta_A(\Gamma^*)$: Define $\Gamma_{v_{\beta_1} \dots v_{\beta_k}}$ to be a graph formed from Γ by adding k edges joining v_i and v_{β_i} , respectively. Then

$$\rho^{(\ell-1)} \circ \theta_A(\Gamma^*) = \sum_{v_\alpha \neq v_A} \sum_{v_{\beta_1} \neq v_1} \dots \sum_{v_{\beta_k} \neq v_k} \Gamma_{v_{\beta_1} \dots v_{\beta_k}}^{v_\alpha}, \quad (\text{B.5})$$

where $\Gamma_{v_{\beta_1} \dots v_{\beta_k}}^{v_\alpha}$ is the graph $\Gamma_{v_{\beta_1} \dots v_{\beta_k}}$ with an extra edge joining v_A and v_α . Note that the graphs formed from Γ by adding edges joining v_A (or v_i) to itself are not included in this sum, because these graphs are not $(\ell - 1)$ -looped.

- $\rho^{(\ell-1)} \circ \theta_A \circ \rho^{(\ell)}(\Gamma^*)$: Define Γ_A to be the graph Γ with a loop added at v_A . Then $\rho^{(\ell)}(\Gamma^*) = \sum_{v_{\beta_i} \neq v_i} \tilde{\Gamma}_{v_{\beta_1} \dots v_{\beta_k}}$, where $\tilde{\Gamma}_{v_{\beta_1} \dots v_{\beta_k}}$ is the graph formed from Γ_A by adding k edges joining v_i and v_{β_i} , respectively. $v_{\beta_i} \neq v_i$ in the sum because only ℓ -looped graphs are included. Applying $\rho^{(\ell-1)} \circ \theta_A$ gives:

$$\rho^{(\ell-1)} \circ \theta_A \circ \rho^{(\ell)}(\Gamma^*) = \sum_{v_\alpha \neq v_A} \sum_{v_{\beta_1} \neq v_1} \dots \sum_{v_{\beta_k} \neq v_k} \tilde{\Gamma}_{v_{\beta_1} \dots v_{\beta_k}}^{v_\alpha}, \quad (\text{B.6})$$

where $\tilde{\Gamma}_{v_{\beta_1} \dots v_{\beta_k}}^{v_\alpha}$ is formed from $\tilde{\Gamma}_{v_{\beta_1} \dots v_{\beta_k}}$ by deleting a loop at v_A and adding an edge joining v_A and v_α . $v_\alpha \neq v_A$ in the sum because only $(\ell - 1)$ -looped graphs are included.

We now want to compare $\Gamma_{v_{\beta_1} \dots v_{\beta_k}}^{v_\alpha}$ and $\tilde{\Gamma}_{v_{\beta_1} \dots v_{\beta_k}}^{v_\alpha}$ for $v_\alpha \neq v_A$ and $v_{\beta_i} \neq v_i$. At first it might seem that $\Gamma_{v_{\beta_1} \dots v_{\beta_k}}^{v_\alpha} = \tilde{\Gamma}_{v_{\beta_1} \dots v_{\beta_k}}^{v_\alpha}$, since both ultimately involve taking Γ and adding an edge joining v_A and v_α , and edges joining v_i and v_{β_i} . However, there is a subtlety involved: Recall that graphs containing a \times -vertex of degree larger than P are identified with the null graph. Therefore, $\Gamma_{v_{\beta_1} \dots v_{\beta_k}}^{v_\alpha} = \tilde{\Gamma}_{v_{\beta_1} \dots v_{\beta_k}}^{v_\alpha}$, provided neither side is null or both sides are null; when one side of this equation represents the null graph and the other does not, then this equation will not hold. This violation happens only if there is a difference in $\deg(\times)$ of the graphs formed during the construction of $\Gamma_{v_{\beta_1} \dots v_{\beta_k}}^{v_\alpha}$ and $\tilde{\Gamma}_{v_{\beta_1} \dots v_{\beta_k}}^{v_\alpha}$. Note that we add the same k edges (joining v_i and v_{β_i}) to both Γ and Γ_A to form the intermediate graphs, $\Gamma_{v_{\beta_1} \dots v_{\beta_k}}$ and $\tilde{\Gamma}_{v_{\beta_1} \dots v_{\beta_k}}$, respectively. Thus the difference between the latter two graphs is the same as the difference between Γ and Γ_A : There is an extra loop at v_A in Γ_A compared to Γ , which will only be deleted after the edges have been added. Hence, the violation of the equality, $\Gamma_{v_{\beta_1} \dots v_{\beta_k}}^{v_\alpha} = \tilde{\Gamma}_{v_{\beta_1} \dots v_{\beta_k}}^{v_\alpha}$, happens only if $v_A = v^\times$. This is condition (a).

From now on, we assume $v_A = v^\times$. In addition, there must exist at least one $v_{\beta_i} = v^\times$ in order for the violation to occur, since otherwise $\deg(\times)$ in any graph we are considering never exceeds the one in Γ^* , and thus no graph in (B.5) and (B.6) is null. Hence for at least one v_{β_i} , $v^\times = v_{\beta_i} \neq v_i$, which implies condition (b). From now on we assume $v^\times = v_{\beta_i} \neq v_i$, for at least one v_{β_i} , and denote the number of v_{β_i} equal to v^\times by b , where $1 \leq b \leq N^\bullet(\star)$.

We know that $\deg(\times)$ in $\tilde{\Gamma}_{v_{\beta_1} \dots v_{\beta_k}}$ is 2 higher than $\deg(\times)$ in $\Gamma_{v_{\beta_1} \dots v_{\beta_k}}$, due to the one extra loop at v_A in Γ_A .

Therefore, if $\Gamma_{v_{\beta_1} \dots v_{\beta_k}}^{v_\alpha}$ vanishes, then $\tilde{\Gamma}_{v_{\beta_1} \dots v_{\beta_k}}^{v_\alpha}$ should also vanish, since $\tilde{\Gamma}_{v_{\beta_1} \dots v_{\beta_k}}$ already has a higher $\deg(\times)$. Furthermore, $\deg(\times)$ in $\tilde{\Gamma}_{v_{\beta_1} \dots v_{\beta_k}}$ is 1 higher than $\deg(\times)$ in

$\Gamma_{v_{\beta_1} \dots v_{\beta_k}}^{v_\alpha}$, and thus $\Gamma_{v_{\beta_1} \dots v_{\beta_k}}^{v_\alpha} \neq \tilde{\Gamma}_{v_{\beta_1} \dots v_{\beta_k}}^{v_\alpha}$ if and only if $\deg(\times) = P$ in $\Gamma_{v_{\beta_1} \dots v_{\beta_k}}^{v_\alpha}$. In this case, $\Gamma_{v_{\beta_1} \dots v_{\beta_k}}^{v_\alpha}$ does not vanish, but $\tilde{\Gamma}_{v_{\beta_1} \dots v_{\beta_k}}^{v_\alpha}$ contains a \times -vertex of degree $P+1$ and is identified with the null graph, which means $\tilde{\Gamma}_{v_{\beta_1} \dots v_{\beta_k}}^{v_\alpha}$ is also null. So the equality is violated if and only if $\deg(\times) = P+1$ in $\tilde{\Gamma}_{v_{\beta_1} \dots v_{\beta_k}}^{v_\alpha}$. We want to write this condition in terms of $\deg(\times)$ in Γ^* . Note that $\deg(\times) = P+1$ in $\tilde{\Gamma}_{v_{\beta_1} \dots v_{\beta_k}}^{v_\alpha}$ if and only if $\deg(\times) = P+1-b-(k-N^\bullet(\star))$ in Γ_A , and $\deg(\times) = P-1-b-(k-N^\bullet(\star))$ in Γ . Finally this implies $\deg(\times) = P+1-b$ in Γ^* . Since $1 \leq b \leq N^\bullet(\star)$, we have that $P \geq \deg(\times) \geq P+1-N^\bullet(\star)$, which is condition (c). Moreover,

$$\sum_{v_\alpha \neq v_A} \Gamma_{v_{\beta_1} \dots v_{\beta_k}}^{v_\alpha} = \rho(\Gamma_{\text{spider}}),$$

where Γ_{spider} is an $(\ell-1)$ -looped spider formed from $\Gamma_{v_{\beta_1} \dots v_{\beta_k}}$ by adding a \star -vertex and then adding an edge that joins this \star -vertex and the \times -vertex. By construction, Γ_{spider} has one fewer \times -loop than Γ^* . Such spiders form the desired $L_{\text{spider}}^{(\ell-1)}$ in (B.4). \square

B.2.3. Constructing Loopless \times -Relations

Constructing a basis for $\mathcal{R}_{\text{loopless}}^\times$ requires a thorough examination of \star -graphs. The next lemma shows that any \times -relation can be written as a derivative map acting on a linear combination of primary \star -graphs, which allows us to restrict to primary \star -graphs in classifying all loopless \times -relations.

Lemma 2. *For any $L^\times \in \mathcal{R}^\times$, there exists $L^\star \in \mathcal{L}^\star$ that contains only primary \star -graphs, satisfying $L^\times = \rho(L^\star)$.*

Proof. Since L^\times is a \times -relation, there exists $\tilde{L}^\star = \sum_i b_i \Gamma_i^\star \in \mathcal{L}^\star$ such that $\rho(\tilde{L}^\star) = L^\times$. Starting with Γ_i^\star , one can follow steps 1 and 2 in Definition 5 to construct a series of \star -graphs, $(\Gamma_i^\star)_{j_1}, (\Gamma_i^\star)_{j_1 j_2}, \dots, (\Gamma_i^\star)_{j_1 \dots j_{k-1}}$, with $j_\alpha = 0, \dots, n-1$ and $\alpha = 1, \dots, k$. By construction, $(\Gamma_i^\star)_{j_1 \dots j_{k-1}}$ contains exactly one \star -vertex (which makes it a primary \star -graph), and $\rho(\Gamma_i^\star) = \rho\left(\sum_{j_1, \dots, j_{k-1}=0}^{n-1} (\Gamma_i^\star)_{j_1 \dots j_{k-1}}\right)$. Therefore,

$$L^\times = \sum_i b_i \cdot \rho(\Gamma_i^\star) = \rho\left(\sum_i \sum_{j_1, \dots, j_{k-1}=0}^{N-1} b_i (\Gamma_i^\star)_{j_1 \dots j_{k-1}}\right).$$

This linear combination of primary \star -graphs $(\Gamma_i^\star)_{j_1 \dots j_{k-1}}$ defines the desired L^\star . Operationally, such L^\star is constructed from \tilde{L}^\star by removing the \star -vertices one by one, as per the steps in the definition of ρ , until only one \star -vertex remains. \square

The following proposition presents a general construction for loopless \times -relations. In the next section we will prove that this procedure generates all elements in $\mathcal{R}_{\text{loopless}}^\times$.

Proposition 4. *Let $L^\star \in \mathcal{L}^\star$ be a linear combination of ℓ -looped primary \star -graphs such that all \times -graphs in $\rho(L^\star)$ are ℓ -looped. There exists an $L_\ell^\star \in \mathcal{L}^\star$, such that*

(a) $L_\ell^\star - L^\star$ contains no graph with more than $\ell-1$ loops;

(b) $\rho(L_\ell^\star) = (-1)^\ell \rho^{(0)} \circ \theta(L^\star + L_{\text{spider}}) \in \mathcal{R}_{\text{loopless}}^\times$. L_{spider} is a linear combination of spiders.

Proof. Since each graph in $\rho(L^\star)$ is ℓ -looped, $\rho(L^\star) = \rho^{(\ell)}(L^\star)$. Let $\rho^{(\ell)}(L^\star) \equiv \sum_{i=1}^k b_i \Gamma_i^\times$, where each Γ_i^\times contains ℓ loops. For each Γ_i^\times , label the loops from 1 to ℓ . By Definition 14, θ_1 undoes the 1st loop, and $\theta_1(\Gamma_i^\times)$ defines a primary \star -graph with $\ell - 1$ loops that is associated with Γ_i^\times . By Lemma 1, Γ_i^\times drops out of $\rho(L^\star - b_i \cdot \theta_1(\Gamma_i^\times))$. Moreover, all \times -graphs in $\rho \circ \theta_1(\Gamma_i^\times)$, except for Γ_i^\times , are $(\ell - 1)$ -looped. Then

$$L_1^\star \equiv L^\star - \sum_{i=1}^k b_i \cdot \theta_1(\Gamma_i^\times) = L^\star - \theta_1 \circ \rho^{(\ell)}(L^\star)$$

defines an L_1^\star that satisfies $\rho(L_1^\star) = \rho^{(\ell-1)}(L_1^\star)$. Repeat this procedure for L_1^\star and the 2nd loop, in place of L^\star and the 1st loop, obtaining

$$L_2^\star \equiv L_1^\star - \theta_2 \circ \rho^{(\ell-1)}(L_1^\star) = L^\star - \theta_1 \circ \rho^{(\ell)}(L^\star) + \theta_2 \circ \rho^{(\ell-1)} \circ \theta_1 \circ \rho^{(\ell)}(L^\star).$$

The second equality holds because $\rho^{(\ell-1)}(L^\star) = 0$. Furthermore, $\rho(L_2^\star) = \rho^{(\ell-2)}(L_2^\star)$. Iterating this ℓ times, we will reach a linear combination of primary \star -graphs

$$L_\ell^\star \equiv L^\star + \sum_{i=1}^{\ell} (-1)^i X_i^\star, \quad X_i^\star \equiv \theta_i \circ \rho^{(\ell-i+1)} \circ \dots \circ \theta_2 \circ \rho^{(\ell-1)} \circ \theta_1 \circ \rho^{(\ell)}(L^\star). \quad (\text{B.7})$$

Here $\rho(L_\ell^\star) = \rho^{(0)}(L_\ell^\star) \in \mathcal{R}_{\text{loopless}}^\times$. Moreover, X_i^\star only contains $(\ell - i)$ -looped graphs. This means that graphs in $L_\ell^\star - L^\star = \sum_{i=1}^{\ell} (-1)^i X_i^\star$ contain at most $\ell - 1$ loops. Therefore, L_ℓ^\star satisfies condition (a) of the proposition.

To prove that L_ℓ^\star also satisfies condition (b), take $L_{\text{spider}}^{(i)}$ to stand for “any linear combination of i -looped spiders” and, for $0 < k \leq \ell$, define

$$Z_{\ell-k}^\star \equiv \theta_k \circ \dots \circ \theta_1(L^\star) - \sum_{\alpha=2}^k \theta_k \circ \dots \circ \theta_\alpha \left(L_{\text{spider}}^{(\ell-\alpha+1)} \right) - L_{\text{spider}}^{(\ell-k)}$$

which contains only $(\ell - k)$ -looped graphs. Define $Z_\ell^\star \equiv L^\star$. Therefore, for $0 \leq k \leq \ell$, applying Proposition 3,

$$\begin{aligned} & \rho^{(\ell-k-1)} \circ \theta_{k+1} \circ \rho^{(\ell-k)}(Z_{\ell-k}^\star) = \rho^{(\ell-k-1)} \left[\theta_{k+1}(Z_{\ell-k}^\star) - L_{\text{spider}}^{(\ell-k-1)} \right] \\ & = \rho^{(\ell-k-1)} \left[\theta_{k+1} \circ \dots \circ \theta_1(L^\star) - \sum_{\alpha=2}^{k+1} \theta_{k+1} \circ \dots \circ \theta_\alpha \left(L_{\text{spider}}^{(\ell-\alpha+1)} \right) - L_{\text{spider}}^{(\ell-k-1)} \right], \end{aligned}$$

i.e.,

$$\rho^{(\ell-k-1)} \circ \theta_{k+1} \circ \rho^{(\ell-k)}(Z_{\ell-k}^\star) = \rho^{(\ell-k-1)}(Z_{\ell-k-1}^\star). \quad (\text{B.8})$$

Note that $\rho^{(0)}(L^\star) = 0$ and $\rho^{(0)}(X_i^\star) = 0$ for $i = 1, \dots, \ell - 1$. Then, by (B.7) and (B.8),

$$\begin{aligned}
\rho^{(0)}(L_\ell^\star) &= (-1)^\ell \rho^{(0)}(X_\ell^\star) \\
&= (-1)^\ell \rho^{(0)} \circ \theta_\ell \circ \rho^{(1)} \circ \dots \circ \theta_2 \circ \rho^{(\ell-1)} \circ \theta_1 \circ \rho^{(\ell)}(Z_\ell^\star) \\
&= (-1)^\ell \rho^{(0)} \circ \theta_\ell \circ \rho^{(1)} \circ \dots \circ \theta_2 \circ \rho^{(\ell-1)}(Z_{\ell-1}^\star) = \dots = (-1)^\ell \rho^{(0)}(Z_0^\star) \\
&= (-1)^\ell \rho^{(0)} \left(\theta_\ell \circ \dots \circ \theta_1(L^\star) - \sum_{\alpha=2}^{\ell} \theta_\ell \circ \dots \circ \theta_\alpha \left(L_{\text{spider}}^{(\ell-\alpha+1)} \right) - L_{\text{spider}}^{(0)} \right) \\
&= (-1)^\ell \rho^{(0)} \circ \theta \left(L^\star - \sum_{\alpha=2}^{\ell+1} L_{\text{spider}}^{(\ell-\alpha+1)} \right).
\end{aligned}$$

Hence,

$$\rho(L_\ell^\star) = \rho^{(0)}(L_\ell^\star) = (-1)^\ell \rho^{(0)} \circ \theta(L^\star + L_{\text{spider}}) \in \mathcal{R}_{\text{loopless}}^\times.$$

This gives condition (b), with $L_{\text{spider}} = -\sum_{\alpha=2}^{\ell+1} L_{\text{spider}}^{(\ell-\alpha+1)}$. \square

Corollary 7. *Given L_s , a linear combination of spiders, $\rho^{(0)} \circ \theta(L_s) \in \mathcal{R}_{\text{loopless}}^\times$.*

Proof. It is enough to show that this corollary is true for one spider S . We claim that Proposition 4 holds for $L^\star = S$ and where L_{spider} is null if we order the loops such that loops 1 to ℓ^\times are \times -loops and $\ell^\times + 1$ to ℓ are \bullet -loops and the loops are removed in this order. Define $Z_{\ell-k}^\star \equiv \theta_k \circ \dots \circ \theta_1(S)$ and $Z_\ell^\star \equiv S$. As in the proof of Proposition 4, we are done if we can prove (B.8), but with this new definition of $Z_{\ell-k}^\star$ (i.e., when L_{spider} is always taken to be zero).

For $k = 0$, $Z_\ell^\star = S$, a spider, which has no \star -vertex adjacent to a \bullet -vertex in violation of Proposition 3(b). Thus, $\rho^{(\ell-1)} \circ \theta_1 \circ \rho^{(\ell)}(Z_\ell^\star) = \rho^{(\ell-1)} \circ \theta_1(Z_\ell^\star) = \rho^{(\ell-1)}(Z_{\ell-1}^\star)$. This holds regardless of which loop is chosen to be undone first. However, if the first loop is a \times -loop, then $Z_{\ell-1}^\star = \theta_1(S)$ will continue to violate Proposition 3(b). Therefore, if all of the \times -loops are undone first, then $\rho^{(\ell-k-1)} \circ \theta_{k+1} \circ \rho^{\ell-k}(Z_{\ell-k}^\star) = \rho^{(\ell-k-1)}(Z_{\ell-k-1}^\star)$ holds for $0 \leq k \leq \ell^\times$.

Now, there are no longer any \times -loops. Whenever there are \bullet -loops, $Z_{\ell-\ell^\times}^\star$ will violate Proposition 3(a). Thus, $\rho^{(\ell-k-1)} \circ \theta_{k+1} \circ \rho^{\ell-k}(Z_{\ell-k}^\star) = \rho^{(\ell-k-1)}(Z_{\ell-k-1}^\star)$ continues to hold all the way until $k = \ell$. \square

B.2.4. A Basis for $\mathcal{R}_{\text{loopless}}^\times$

To find a basis for $\mathcal{R}_{\text{loopless}}^\times$, we first show that any loopless \times -relation can be written as $\rho^{(0)} \circ \theta$ acting on a linear combination of spiders. We start with the following lemmas:

Lemma 3. *Let $L^\times \in \mathcal{R}_{\text{loopless}}^\times$ satisfy $L^\times = \rho(L^\star)$, with L^\star a linear combination of primary \star -graphs. For any Γ_A^\star in L^\star that is associated with a looped \times -graph Γ^\times , there exists another \star -graph $\Gamma_B^\star \neq \Gamma_A^\star$ in L^\star , such that Γ^\times is not contained in $\rho(\Gamma_A^\star - \Gamma_B^\star)$.*

Proof. Suppose Γ_A^\star is the only \star -graph in L^\star that is associated with Γ_A^\star . Assume that the coefficient of Γ_A^\star in L^\star is $b_A \neq 0$. Therefore, none of the \star -graphs in $L^\star - b_A \Gamma_A^\star$ is associated with Γ^\times , and thus Γ^\times is not contained in $\rho(L^\star - b_A \Gamma_A^\star)$. Hence, the looped \times -graph Γ^\times

appears in $\rho(L^\star) = \rho(L^\star - b_A \Gamma_A^\star) + b_A \cdot \rho(\Gamma_A^\star)$ with coefficient $b_A \neq 0$, which contradicts the fact that $\rho(L^\star) \in \mathcal{R}_{\text{loopless}}^\times$.

The above argument shows that there exists a $\Gamma_B^\star \neq \Gamma_A^\star$ in L^\star that is associated with Γ^\times . By Lemma 1, Γ^\times appears in both $\rho(\Gamma_A^\star)$ and $\rho(\Gamma_B^\star)$ with coefficient 1. Then, $\rho(\Gamma_A^\star - \Gamma_B^\star)$ does not contain Γ^\times . \square

Specifically, if Γ_A^\star is ℓ -looped and Γ^\times is $(\ell + 1)$ -looped, then Γ_B^\star is also ℓ -looped.

Lemma 4. *If $\Gamma_A^\star, \Gamma_B^\star \in \mathcal{G}^\star$ are ℓ -looped primary \star -graphs that are associated with the same $(\ell + 1)$ -looped \times -graph, then $\theta(\Gamma_A^\star - \Gamma_B^\star) = 0$.*

Proof. Since Γ_A^\star and Γ_B^\star are both associated with the same $(\ell + 1)$ -looped \times -graph, Γ^\times , $\theta(\Gamma_A^\star) = \theta(\Gamma_B^\star) = \theta(\Gamma^\times)$. Therefore, $\theta(\Gamma_A^\star - \Gamma_B^\star) = 0$. \square

Proposition 5. *For any loopless \times -relation $L^\times \in \mathcal{R}_{\text{loopless}}^\times$, there exists a linear combination of spiders L_s , such that $L^\times = \rho^{(0)} \circ \theta(L_s)$.*

Proof. In the following, we take L_{spider} to stand for “any linear combination of spiders”. Since L^\times is a \times -relation, there exists $L^\star \in \mathcal{L}^\star$, consisting of primary \star -graphs, such that $L^\times = \rho(L^\star)$. Take the set, $\mathcal{H}_\ell = \{\Gamma_1^\star, \dots, \Gamma_{H_\ell}^\star\}$, of \star -graphs in L^\star that contain the highest number, ℓ , of loops. Let b_ℓ^i be the coefficient of Γ_i^\star in L^\star . Therefore, $L^\star - \sum_{i=1}^{H_\ell} b_\ell^i \Gamma_i^\star$ contains no graphs with more than $\ell - 1$ loops. We implement the following procedure for all graphs in \mathcal{H}_ℓ in order from Γ_1^\star to $\Gamma_{H_\ell}^\star$:

1. Define $\beta_\ell^{(1)} \equiv b_\ell^{(1)}$. Apply to Γ_1^\star the construction outlined in Proposition 4:
 - (a) If Γ_1^\star is a spider: By Corollary 7, Proposition 4(b) becomes that there exists a linear combination of primary \star -graphs $L_\ell^{(1)}$, such that

$$\rho(L_\ell^{(1)}) = \rho^{(0)} \circ \theta(\Gamma_1^\star) = \rho^{(0)} \circ \theta(L_{\text{spider}}) \in \mathcal{R}_{\text{loopless}}^\times.$$

By Proposition 4(a), graphs in $L_\ell^{(1)} - \Gamma_1^\star$ contain at most $\ell - 1$ loops.

- (b) If Γ_1^\star is not a spider: $\rho(\Gamma_1^\star)$ contains an $(\ell + 1)$ -looped \times -graph Γ^\times . By Lemma 3, there exists an ℓ -looped \star -graph $\Gamma_j^\star \in \mathcal{H}$, $\Gamma_j^\star \neq \Gamma_1^\star$, that is associated with Γ^\times and Γ^\times is not in $\rho(\Gamma_1^\star - \Gamma_j^\star)$. By Lemma 4, $\theta(\Gamma_1^\star - \Gamma_j^\star) = 0$. By Proposition 4,

$$\rho(L_\ell^{(1)}) = \rho^{(0)} \circ \theta(L_{\text{spider}}) \in \mathcal{R}_{\text{loopless}}^\times,$$

where graphs in $L_\ell^{(1)} - (\Gamma_1^\star - \Gamma_j^\star)$ contain at most $\ell - 1$ loops.

2. Define $\beta_\ell^{(i)}$, for $i > 1$, as the coefficient (which may be zero) of Γ_i^\star in $L^\star - \beta_\ell^{(1)} L_\ell^{(1)}$.
3. If $\beta_\ell^{(2)} = 0$, skip this step; if not, repeat step 1 for Γ_2^\star , resulting in an $L_\ell^{(2)}$ with

$$\rho(L_\ell^{(2)}) = \rho^{(0)} \circ \theta(L_{\text{spider}}) \in \mathcal{R}_{\text{loopless}}^\times.$$

Redefine $\beta_\ell^{(i)}$, for $i > 2$, to be the coefficient of Γ_i^\star in $(L^\star - \beta_\ell^{(1)} L_\ell^{(1)}) - \beta_\ell^{(2)} L_\ell^{(2)}$.

4. Repeat step 3 for $\Gamma_\ell^{(3)}, \dots, \Gamma_\ell^{(H_\ell)}$ in sequence. This will eventually generate a linear combination of \star -graphs, $L^\star - \sum_{i=1}^{H_\ell} \beta_\ell^{(i)} L_\ell^{(i)}$, where

$$\rho \left(\sum_{i=1}^{H_\ell} \beta_\ell^{(i)} L_\ell^{(i)} \right) = \rho^{(0)} \circ \theta(L_{\text{spider}}) \in \mathcal{R}_{\text{loopless}}^\times,$$

and all graphs in $L^\star - \sum_{i=1}^{H_\ell} \beta_\ell^{(i)} L_\ell^{(i)}$ contain at most $\ell - 1$ loops.

We can now repeat this procedure for $L^\star - \sum_{i=1}^{H_\ell} \beta_\ell^{(i)} L_\ell^{(i)}$. We will obtain

$$L^\star - \sum_{i=1}^{H_\ell} \beta_\ell^{(i)} L_\ell^{(i)} - \sum_{i=1}^{H_{\ell-1}} \beta_{\ell-1}^{(i)} L_{\ell-1}^{(i)}, \quad \rho \left(\sum_{i=1}^{H_{\ell-1}} \beta_{\ell-1}^{(i)} L_{\ell-1}^{(i)} \right) = \rho^{(0)} \circ \theta(L_{\text{spider}}) \in \mathcal{R}_{\text{loopless}}^\times.$$

In the first expression graphs contain at most $\ell - 2$ loops. Iterate ℓ times to get

$$\tilde{L}^\star \equiv L^\star - \sum_{\alpha=1}^{\ell} \sum_{i=1}^{H_\alpha} \beta_\alpha^i L_\alpha^{(i)},$$

which contains only loopless primary \star -graphs. In addition,

$$\rho \left(\sum_{\alpha=1}^{\ell} \sum_{i=1}^{H_\alpha} \beta_\alpha^i L_\alpha^{(i)} \right) = \rho^{(0)} \circ \theta(L_{\text{spider}}) \in \mathcal{R}_{\text{loopless}}^\times.$$

Therefore,

$$\rho(\tilde{L}^\star) = L^\times - \rho \left(\sum_{\alpha=1}^{\ell} \sum_{i=1}^{H_\alpha} \beta_\alpha^i L_\alpha^{(i)} \right) \in \mathcal{R}_{\text{loopless}}^\times.$$

Next we show that \tilde{L}^\star is a linear combination of spiders. Suppose there exists a \star -graph Γ_A^\star in \tilde{L}^\star that is not a spider. Then, by Lemma 3, there should exist another \star -graph $\Gamma_B^\star \neq \Gamma_A^\star$ in \tilde{L}^\star that is associated with the 1-looped \times -graph Γ^\times in $\rho(\Gamma_A^\star)$. But since Γ^\times is associated with a unique loopless \star -graph (resulting from undoing the loop), this is impossible. Therefore, graphs in \tilde{L}^\star are loopless spiders, and thus $\rho(\tilde{L}^\star) = \rho^{(0)} \circ \theta(\tilde{L}^\star)$. Hence,

$$L^\times = \rho \left(\tilde{L}^\star + \sum_{\alpha=1}^{\ell} \sum_{i=1}^{H_\alpha} \beta_\alpha^i L_\alpha^{(i)} \right) = \rho^{(0)} \circ \theta(L_{\text{spider}}).$$

The L_{spider} within the last pair of parentheses is the desired L_s . \square

Thus we have shown that any loopless \times -relation can be written as $\rho^{(0)} \circ \theta(L_s)$. In fact, we can go further and show that it is equal to $\rho^{(0)}(L_M)$, where L_M is a linear combination of Medusas. We start with the following Lemma:

Lemma 5. *Given a spider S that contains ℓ^\times \times -loops, there exist two linear combinations of spiders Y^\star , with graphs containing ℓ^\times \times -loops but no \bullet -loop, and W^\star , with graphs containing fewer than ℓ^\times \times -loops, such that $\rho^{(0)} \circ \theta(Y^\star) = \rho^{(0)} \circ \theta(S + W^\star)$.*

Proof. Suppose S contains ℓ^\bullet \bullet -loops, labeled from 1 to ℓ^\bullet . Denote the total number of loops in S to be $\ell = \ell^\times + \ell^\bullet$. Label the \times -loops in S from $\ell^\bullet + 1$ to ℓ . We will follow the proof of Proposition 4 to undo these \bullet -loops. However, we want to keep the \star -vertex in S untouched. Therefore, define ρ_s to be the usual derivative map except that it keeps the original \star -vertex in S untouched; we can grade ρ_s by number of loops in analogy with ρ .

Apply θ_1 to S to undo the 1st \bullet -loop. Define $Y_1^\star \equiv S - \rho_s \circ \theta_1(S)$ and note that S drops out of Y_1^\star . Furthermore, since S is the only ℓ -looped graph in $\rho_s \circ \theta(S)$,

$$Y_1^\star = S - \rho_s \circ \theta_1(S) = -\rho_s^{(\ell-1)} \circ \theta_1(S).$$

Repeat this procedure for all graphs in Y_1^\star and the 2nd \bullet -loop, in place of S and the 1st \bullet -loop, obtaining $Y_2^\star \equiv Y_1^\star - \rho_s \circ \theta_2(Y_1^\star)$, which is a linear combination of $(\ell - 2)$ -looped graphs. However, since all graphs in Y_1^\star are $(\ell - 1)$ -looped, we have

$$Y_2^\star = (-1)^2 \rho_s^{(\ell-2)} \circ \theta_2 \circ \rho_s^{(\ell-1)} \circ \theta_1(S).$$

Iterate this ℓ^\bullet times, resulting in

$$Y_{\ell^\bullet}^\star = (-1)^{\ell^\bullet} \rho_s^{(\ell-\ell^\bullet)} \circ \theta_{\ell^\bullet} \circ \dots \circ \rho_s^{(\ell-2)} \circ \theta_2 \circ \rho_s^{(\ell-1)} \circ \theta_1(S).$$

Graphs in $Y_{\ell^\bullet}^\star$ contain no \bullet -loops. As in the derivation of (B.2.3) in Proposition 4,

$$Y_{\ell^\bullet}^\star = (-1)^{\ell^\bullet} \rho_s^{(\ell-\ell^\bullet)} \left(\theta_{\ell^\bullet} \circ \dots \circ \theta_1(S) - \sum_{\alpha=2}^{\ell^\bullet} \theta_{\ell^\bullet} \circ \dots \circ \theta_\alpha \left(L_{\text{spider}}^{(\ell-\alpha+1)} \right) - L_{\text{spider}}^{(\ell-\ell^\bullet)} \right) \quad (\text{B.9})$$

By Proposition 3, each graph in $L_{\text{spider}}^{(\ell-\alpha+1)}$ and $L_{\text{spider}}^{(\ell-\ell^\bullet)}$ contains fewer than ℓ^\times \times -loops.

Take $Y^\star = (-1)^{\ell^\bullet} Y_{\ell^\bullet}^\star$. Then, by Proposition 3,

$$\rho^{(0)} \circ \theta(Y^\star) = \rho^{(0)} \circ \theta_{\ell^\bullet} \circ \dots \circ \theta_{\ell^\bullet+1}(Y^\star) = \rho^{(0)} \circ \theta(S + W^\star),$$

where W^\star is a linear combination of spiders containing fewer than ℓ^\times \times -loops. \square

The next proposition finally allows us to relate spiders and Medusas.

Proposition 6. *For any linear combination of spiders $L_s \in \mathcal{L}^\star$, there exists a linear combination of Medusas L_M , such that $\rho^{(0)} \circ \theta(L_s) = \rho^{(0)}(L_M)$.*

Proof. Take the set,

$$\mathcal{H}_{\ell^\times} = \left\{ S_1^{(\ell^\times)}, \dots, S_{H_{\ell^\times}}^{(\ell^\times)} \right\},$$

of spiders in L_s that contain the highest number, ℓ^\times , of \times -loops. Denote the coefficient of $S_i^{(\ell^\times)}$ in L_s as $b_i^{(\ell^\times)}$. Therefore, graphs in $L_s - \sum_{i=1}^{H_{\ell^\times}} b_i^{(\ell^\times)} S_i^{(\ell^\times)}$ contain at most $\ell^\times - 1$ \times -loops. Applying Lemma 5 to each $S_i^{(\ell^\times)}$ yields two linear combinations of spiders $Y^{(\ell^\times)}$, comprised of graphs containing ℓ^\times \times -loops but no \bullet -loop, and $W^{(\ell^\times)}$, comprised of graphs containing fewer than ℓ^\times \times -loops, such that

$$\sum_{i=1}^{H_{\ell^\times}} \rho^{(0)} \circ \theta \left(b_i^{(\ell^\times)} S_i^{(\ell^\times)} \right) = \rho^{(0)} \circ \theta \left(Y^{(\ell^\times)} - W^{(\ell^\times)} \right). \quad (\text{B.10})$$

Furthermore,

$$L_s = \left(\sum_{i=1}^{H_{\ell^\times}} b_i^{(\ell^\times)} S_i^{(\ell^\times)} + W^{(\ell^\times)} \right) \quad (\text{B.11})$$

is a linear combination of spiders that contain at most $\ell^\times - 1$ \times -loops. Replace L_s with (B.11), and the above procedure applies, resulting in a linear combination of spiders that contain at most $\ell^\times - 2$ \times -loops. Iterating ℓ^\times times, we will obtain

$$L_s^{(0)} \equiv L_s - \sum_{\alpha=1}^{\ell^\times} \left(\sum_{i=1}^{H_\alpha} b_i^{(\alpha)} S_i^{(\alpha)} + W^{(\alpha)} \right), \quad (\text{B.12})$$

By construction, $L_s^{(0)}$ is a linear combination of spiders containing no \times -loop. Moreover,

$$\rho^{(0)} \circ \theta \left(Y^{(\alpha)} \right) = \rho^{(0)} \circ \theta \left(\sum_{i=1}^{H_\alpha} b_i^{(\alpha)} S_i^{(\alpha)} + W^{(\alpha)} \right), \quad (\text{B.13})$$

in analogy with (B.10). Finally, repeat the same procedure one last time with $L_s^{(0)}$ in (B.12) in place of L_s . Since there are no longer any \times -loops in $L_s^{(0)}$, no $W^{(\alpha)}$'s will arise. We obtain

$$L_s^{(0)} = \sum_{i=1}^{H_0} b_i^{(0)} S_i^{(0)}, \quad \rho^{(0)} \circ \theta \left(Y^{(0)} \right) = \rho^{(0)} \circ \theta \left(\sum_{i=1}^{H_0} b_i^{(0)} S_i^{(0)} \right). \quad (\text{B.14})$$

Combining (B.12), (B.13) and (B.14), we obtain

$$\rho^{(0)} \circ \theta \left(L_s \right) = \rho^{(0)} \circ \theta \left(\sum_{\alpha=0}^{\ell^\times} Y^{(\alpha)} \right).$$

Since the $Y^{(\alpha)}$'s are linear combinations of spiders with no \bullet -loops and α \times -loops, $\theta(Y^{(\alpha)})$, is a linear combination of loopless \star -graphs with $\deg(\times) = P - \alpha$ and $N(\star) = \alpha + 1$. This means $\deg(\times) + N(\star) = P + 1$ in these loopless \star -graphs. By Definition 10, such graphs are Medusas. Therefore,

$$L_M = \theta \left(\sum_{\alpha=0}^{\ell^\times} Y^{(\alpha)} \right)$$

gives the desired linear combination of Medusas in $\rho^{(0)} \circ \theta \left(L_s \right) = \rho^{(0)} \left(L_M \right)$. \square

Theorem 1. $\rho^{(0)} \left(\mathcal{M} \right)$ forms a basis of $\mathcal{R}_{\text{loopless}}^\times$.

Proof. Proposition 5 states that any $L^\times \in \mathcal{R}_{\text{loopless}}^\times$ can be written as $\rho^{(0)} \circ \theta(L_s)$, with L_s a linear combination of spiders. Proposition 6 states that there exists a linear combination of Medusas L_M , such that $\rho^{(0)} \circ \theta(L_s) = \rho^{(0)}(L_M)$. Therefore, $L^\times = \rho^{(0)}(L_M)$. This proves the completeness.

Suppose that there exists a linear combination of Medusas $L_M = \sum_{i=1}^k \alpha_i M_i \neq 0$, such that $\rho^{(0)}(L_M) = 0$. Note that if two Medusas M_A and M_B have \times -vertices of different

degrees, then $\rho^{(0)}(M_A)$ and $\rho^{(0)}(M_B)$ do not have \times -graphs in common. Therefore, without loss of generality, we can assume that the \times -vertices in all M_i have the same degree. By the definition of Medusas, $P = \deg(\times) + N(\star) - 1$, and this implies that they also have the same number of \star -vertices. Furthermore, we can assume that, after deleting the \times -vertex, all M_i 's are identical since this must be the case in order for the $\rho^{(0)}(M_i)$ to cancel each other. Therefore, the only differences between the M_i are in the edges incident to the \times -vertex.

For any \bullet -vertex, v , take the set $\mathcal{H} = \{\widetilde{M}_1, \dots, \widetilde{M}_H\}$ of distinct Medusas in L_M , such that each \widetilde{M}_i contains the highest number, E , of edges that join v and the \times -vertex among all Medusas in L_M . For each \widetilde{M}_i , form a specific graph, Γ_i^\times , in $\rho^{(0)}(\widetilde{M}_i)$ by deleting all $N(\star)$ \star -vertices and adding $N(\star)$ edges joining the \times -vertex and v . Now, Γ_i^\times contains $E + N(\star)$ edges joining v and the \times -vertex. By construction, the Γ_i^\times contain the highest number of edges joining v and the \times -vertex, among all \times -graphs in $\rho^{(0)}(L_M)$. Therefore, the Γ_i^\times can only be canceled among $\rho^{(0)}(\widetilde{M}_i)$'s. Thus in order for Γ_i^\times to be canceled, we need $\Gamma_i^\times = \Gamma_j^\times$ for some $i \neq j$ (note that this Γ_i^\times appears in $\rho^{(0)}(\widetilde{M}_i)$ with unit coefficient). But this means $\widetilde{M}_i = \widetilde{M}_j$ which is a contradiction since the \widetilde{M}_i are distinct. This proves independence. \square

We can use this result to systematically find any P -invariant. When $P = 0$ or $P = 1$, a simple classification is possible for any N . The case $P = 1$ is studied in detail in Appendix B.3 and $P = 0$ is dealt with in the following corollary.

Corollary 8. *Any loopless 0-invariant is an exact 0-invariant.*

Proof. There are no Medusas in $P = 0$ (since Medusas require $N(\star) \geq 1$ and $N(\star) \leq \deg(\times) = P + 1 - N(\star) \leq P$). Therefore $\mathcal{R}_{\text{loopless}}^\times = \{0\}$. \square

Since we have already identified all exact invariants in Corollary 4, this classifies all loopless 0-invariants.

B.2.5. Lower Bound on Vertex Degree

Within the loopless basis, we will set a lower bound on the degree of any \bullet - or \times -vertex in any graph appearing in a consistency equation for a P -invariant.

Proposition 7. *The vertices of a plain-graph Γ in a P -invariant $L \in \mathcal{L}_{\text{loopless}}$ are of degree no less than $\frac{1}{2}(P + 1)$.*

Proof. Let v be a vertex in Γ of degree less than $\frac{1}{2}(P + 1)$. Let Γ^\times in $\delta(\Gamma)$ be the term given by replacing v with a \times -vertex. By Corollary 3, Γ^\times is in $\delta(L)$. Since L is P -invariant, by Theorem 1, $\delta(L) = \rho^{(0)}(\sum_i \alpha_i M_i)$ for $M_i \in \mathcal{M}$ and thus, Γ^\times is in $\rho^{(0)}(M_j)$ for some j . Since M_j is a Medusa, the \times -vertex in M_j is of degree no less than $\frac{1}{2}(P + 1)$. This contradicts the fact that the \times -vertex in Γ^\times is of degree less than $\frac{1}{2}(P + 1)$. \square

Proposition 8. *If $L \in \mathcal{L}_{\text{loopless}}$ is a P -invariant and L_M is a linear combination of Medusas, such that $\delta L = \rho^{(0)}(L_M)$, then the vertices of any Medusa in L_M are of degree no less than $\frac{1}{2}(P + 1)$.*

Proof. Suppose that a Medusa M_0 in L_M has a vertex, v , of degree lower than $\frac{1}{2}(P+1)$. For an interaction term, there exists at least one other vertex v_0 in M_0 to which the \star -vertices can be joined such that v_0 is neither v nor the \times -vertex. The resulting graph in $\rho^{(0)}(M_0)$ is a \times -graph Γ_0^\times with vertex v of degree lower than $\frac{1}{2}(P+1)$, and thus, by Proposition 7, does not appear in $\delta(L)$. Therefore, there must exist another Medusa M_1 in L_M such that $M_0 \neq M_1$ and Γ_0^\times is absent from $\rho^{(0)}(M_0 - M_1)$. Therefore, M_1 must produce Γ_0^\times after deleting the \star -vertices and adding the same number, $N(\star)$, of edges joining the \times -vertex and the other vertices. Since $M_0 \neq M_1$ at least one of these other vertices is not v_0 , so the degree of v_0 is larger in M_1 than in M_0 . Now, form another \times -graph, Γ_1^\times , in $\rho^{(0)}(M_1)$ by deleting the \star -vertices in M_1 and adding the same number of edges joining the \times -vertex and v_0 . Γ_1^\times again contains v with degree lower than $\frac{1}{2}(P+1)$. This \times -graph must be canceled by introducing a third Medusa M_2 . This procedure can be iterated to obtain an infinite sequence of Medusas M_0, M_1, M_2, \dots in L_M , with the number of edges incident to v_0 in M_i monotonically increasing with i . But this is impossible since the Medusas have a fixed finite number of edges and thus we have a contradiction. \square

B.3. Linear Shift Symmetry, Trees and Galileons

For $P = 1$, Medusas have a very limited configuration: A Medusa M has two subgraphs, which are disconnected from each other, one of which is $\star \text{---} \otimes$, and the other of which is a loopless plain-graph. This strongly restricts the possible associations between graphs. In addition, for $P = 1$, $\rho(M) = \rho^{(0)}(M)$ for any Medusa M .

Proposition 9. *For $P = 1$, a loopless \times -graph is associated with at most one Medusa.*

Proof. If the \times -vertex in the loopless \times -graph has degree zero, then it cannot be associated with a Medusa. If the \times -vertex in the loopless \times -graph has degree one, then the loopless \times -graph takes the form of a \times -vertex and an edge joining this \times -vertex to a vertex in a loopless plain-graph, Γ . The unique Medusa associated with this \times -graph is given by deleting the edge incident to the \times -vertex and adding a \star -vertex together with an edge joining the \star -vertex and the \times -vertex. \square

Following the same logic as in the proofs of Corollary 2 and 3, we obtain:

Corollary 9. *For $P = 1$, any two associated Medusas are identical to each other.*

Corollary 10. *For $P = 1$, if M is a Medusa in a sum of Medusas L_M , then $\rho(L_M)$ contains all graphs in $\rho(M)$.*

Corollary 11. *For $P = 1$, if a Medusa M is associated with a plain-graph in a 1-invariant, $L \in \mathcal{L}_{\text{loopless}}$, then $\delta(L)$ contains all graphs in $\rho(M)$.*

Proof. If M is associated with Γ in the 1-invariant L , then there exists Γ^\times shared by $\delta(\Gamma)$ and $\rho(M)$. Corollary 3 implies Γ^\times is in $\delta(L)$. Theorem 1 implies $\delta(L) = \rho(L_M)$ where L_M is a sum of Medusas. Therefore, Γ^\times is in $\rho(L_M)$. Proposition 9 implies M is in L_M . Corollary 10 implies $\rho(L_M)$ contains $\rho(M)$ and thus $\delta(L)$ contains $\rho(M)$. \square

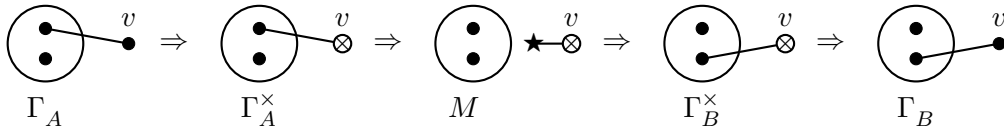
B.3.1. Minimal Invariants

Definition 16. A nonzero P -invariant $L_{N,\Delta}$ is minimal if there is no nonzero P -invariant $L'_{N,\Delta'}$ for any $\Delta' < \Delta$. For a given P and N , let Δ_{\min} denote the minimum Δ for which a P -invariant exists.

Now, we prove that a minimal 1-invariant is a sum of trees. We start with the following lemma.

Lemma 6 (Leaf Shuffling). *If a graph Γ_A that contains a leaf v appears in a 1-invariant L , then any graph Γ_B that contains v as a leaf and satisfies $\Gamma_B - v = \Gamma_A - v$ is also contained in L .*

Proof. Depicted below is a series of graphs, which are all associated with each other:



where the circles denote subgraphs. In particular, both Γ_A and Γ_B are associated with the Medusa M . By Corollary 11, δL contains all graphs in $\rho(M)$. Furthermore, by Corollary 1, L contains both Γ_A and Γ_B . \square

We call the procedure that relates Γ_B to Γ_A described in the above lemma *leaf shuffling*. The corollaries below follow immediately.

Corollary 12. *If a plain-graph Γ_A is contained in a 1-invariant L , and Γ_B is formed from Γ_A by shuffling leaves, then Γ_B is also contained in L .*

Corollary 13. *If a plain-graph Γ in a loopless 1-invariant L contains more than one connected component, then none of these connected components is a tree.*

Proof. Note that there are at least two leaves in a tree, if the tree is not an empty vertex. If in Γ there is a connected component T that is a tree, then we can shuffle all leaves in T to be joined to other connected components, while turning T into another tree with at least one fewer vertex. This procedure can be iterated until all but one vertex in T are shuffled to be joined to other connected components, which turns Γ into a graph $\tilde{\Gamma}$ containing an empty vertex. By Corollary 12, since L contains Γ , it also contains $\tilde{\Gamma}$, which violates the lower bound on vertex degree. Therefore, such Γ cannot appear in loopless 1-invariants. \square

Proposition 10. *If L is a nonzero minimal N -point loopless 1-invariant, then it contains all trees with N vertices.*

Proof. If L contains no plain-graphs with leaves, then the vertices in L have degree at least 2 (note that an empty vertex is disallowed by Proposition 7). Then the number of edges Δ satisfies

$$\Delta \geq N. \tag{B.15}$$

Otherwise, consider a plain-graph Γ contains a leaf v and appears in L . If there exist any other leaves in Γ , shuffle them to be adjacent to v . Iterate for the resulting graphs until reaching a plain-graph Γ_0 in which all leaves are adjacent to v . By Corollary 12, Γ_0 is also contained in L . Denote the subgraph of Γ_0 consisting of all leaves in Γ_0 and v by T , which is a particular type of tree usually called a *star*. Define Γ' as a subgraph of Γ_0 that is formed by deleting from Γ_0 all vertices in T .

If Γ' is not null, by Corollary 13, T cannot be disconnected from Γ' , since otherwise T would be a tree disconnected from at least one other connected component in Γ_0 . Moreover, since v is a leaf in Γ , Γ' is joined to T by exactly one edge incident to v . Define N_T as the number of vertices in T and N' as the number of vertices in Γ' , then $N = N_T + N'$. Note that there is no leaf in Γ' , and thus the vertices in Γ' have degree at least 2. Therefore,

$$\Delta \geq (N_T - 1) + N' + 1 = N. \quad (\text{B.16})$$

If Γ' is null, then $\Gamma_0 = T$ and the original graph Γ is a tree. In this case, $\Delta = N - 1$, which is lower than the bounds ((B.15) and (B.16)) for the other cases. By Corollary 12, L contains T . The Galileon invariants presented in §3 realize this bound $\Delta_{\min} = N - 1$. In fact, any tree with N vertices can be turned into a star by shuffling leaves. Since L contains the star with N vertices, it contains all trees with N vertices. \square

Next, we prove the uniqueness of the minimal term.

Proposition 11. *The minimal N -point loopless 1-invariant with $\Delta = N - 1$ is unique up to proportionality.*

Proof. Let L_1 and L_2 be minimal N -point loopless 1-invariants with $\Delta = N - 1$. Let T be a tree in L_1 and L_2 , which exists by Proposition 10. Rescale L_1 and L_2 so that T appears in each with unit coefficient. Then, T is not in $L_1 - L_2$. However, $L_1 - L_2$ is a minimal N -point loopless 1-invariant. Therefore, Proposition 10 implies that $L_1 - L_2$ vanishes. \square

Finally, we prove the existence of the minimal N -point loopless 1-invariant with $\Delta = N - 1$:

Theorem 2. *Any minimal N -point loopless 1-invariant is proportional to the sum with unit coefficients of all trees with N vertices.*

Proof. Let T_N be a general tree with N \bullet -vertices. Let T_N^\times be a general tree with $(N - 1)$ \bullet -vertices and one \times vertex. Let T_N^* have two connected components, one of which is $\star \text{---} \otimes$ and the other is a tree T_{N-1} . Let L , L^\times and L^* be the sum with unit coefficients of all T_N , T_N^\times and T_N^* , respectively. Replacing a \bullet -vertex in T_N with a \times produces a unique T_N^\times , since vertices are labeled. Therefore, $\delta(L)$ is simply L^\times . Similarly, $\rho(L^*) = L^\times$. Therefore, $\delta(L) = \rho(L^*)$ and L is 1-invariant, which is unique by virtue of Proposition 11. \square

It is shown in [13] that the Galileon-like term in spacetime dimension $d = D + 1 \geq N$:

$$\epsilon^{i_1 \dots i_{N-1} k_N \dots k_D} \epsilon^{j_1 \dots j_{N-1}}{}_{k_N \dots k_D} \partial_{i_1} \phi \partial_{j_1} \phi \partial_{i_2} \partial_{j_2} \phi \dots \partial_{i_{N-1}} \partial_{j_{N-1}} \phi, \quad (\text{B.17})$$

is invariant up to a total derivative. By Theorem 2, the sum with unit coefficients of all trees with N vertices is proportional to (B.17), up to a total derivative. In fact, the constant of proportionality is 1.

B.3.2. Non-minimal Invariants

So far we have found the unique minimal 1-invariant for each N , that is with $\Delta = N - 1$. In what follows we argue that any non-minimal 1-invariant ($\Delta > N - 1$) is equal to an exact 1-invariant up to a plain-relation (a total derivative). We begin with the following definition:

Definition 17 (Frame). *For $\Gamma \in \mathcal{G}_{N,\Delta}$, delete all edges incident to leaves; iterate this procedure until reaching a graph Γ_f that contains no leaves. We call Γ_f the frame of Γ .*

Note that, by definition, after deleting from Γ all edges that appear in Γ_f , each of the connected components in the resulting graph is a tree. We also define:

Definition 18 (Frame Invariant). *A loopless 1-invariant $L = \sum_{i=1}^k \alpha_i \Gamma_i$ is a frame invariant if the frames of Γ_i for all $i = 1, \dots, k$ are identical.*

For convenience, we define a map f on frame invariants, such that $f(L)$ is the frame which is common to all of the graphs contained in L .

By definition, the nonempty vertices in any frame have degree greater than 1. No such vertex can be turned into a \times -vertex or be adjacent to a \star -vertex in a \star -graph associated with Γ . This means that terms with different frames cannot lead to cancellations in the consistency equation. Therefore, a consistency equation naturally splits into multiple consistency equations, each one a frame invariant. This is summarized in the lemma below:

Lemma 7. *Any loopless 1-invariant is a linear combination of frame invariants.*

The proofs presented in Proposition 10 and 11 and Theorem 2 are directly applicable to frame invariants, from which we conclude:

Proposition 12. *Up to proportionality, any loopless frame invariant L is equal to the sum with unit coefficients of all plain-graphs that satisfy the following conditions:*

- (a) *The plain-graph has a frame $f(L)$.*
- (b) *If there is more than one connected component in the plain graph, then none of them is a tree.*

Note that condition (b) follows directly from Corollary 13. Proposition 12 effectively provides an equivalent definition for frame invariants. Classifying all non-minimal 1-invariants is thus reduced to classifying all non-minimal frame invariants. Furthermore, by Proposition 2, we can restrict our search to loopless frame invariants. In the following we will show that any loopless frame invariant is equal to an exact invariant up to total derivatives. We start with a useful lemma:

Lemma 8. *Let $\Gamma^{(\ell)} \in \mathcal{G}$ be an ℓ -looped exact 1-invariant, such that all vertices with loops have degree 2. Then $\rho^{(0)} \circ \theta(\Gamma^{(\ell)})$ is a loopless 1-invariant and is equal to $\Gamma^{(\ell)}$ up to a plain-relation.*

Proof. Label the loops in $\Gamma^{(\ell)}$ from 1 to ℓ . Note that $\rho \circ \theta_1(\Gamma^{(\ell)}) = \Gamma^{(\ell)} + \rho^{(\ell-1)} \circ \theta_1(\Gamma^{(\ell)})$. Since $\theta_1(\Gamma^{(\ell)})$ is a \star -ed plain graph, $\rho \circ \theta_1(\Gamma^{(\ell)})$ is a plain-relation. Hence $\rho^{(\ell-1)} \circ \theta_1(\Gamma^{(\ell)})$ is 1-invariant. Define

$$L_1 \equiv \rho^{(\ell-1)} \circ \theta_1(\Gamma^{(\ell)}) = \rho \circ \theta_1(\Gamma^{(\ell)}) - \Gamma^{(\ell)},$$

L_1 is by definition an exact 1-invariant up to a plain-relation $\rho \circ \theta_1(\Gamma^{(\ell)})$. Furthermore, all graphs in L_1 are $(\ell - 1)$ -looped. Therefore, $\rho \circ \theta_2(L_1) = L_1 + \rho^{(\ell-2)} \circ \theta_2(L_1)$. Define

$$L_2 \equiv \rho^{(\ell-2)} \circ \theta_2(L_1) = \rho \circ \theta_2(L_1) - L_1,$$

which is also an exact 1-invariant up to plain-relations and consists of graphs that are $(\ell - 2)$ -looped. Iterating ℓ times, we obtain

$$L_\ell = \rho^{(0)} \circ \theta_{\ell-1} \circ \dots \circ \rho^{(\ell-2)} \circ \theta_2 \circ \rho^{(\ell-1)} \circ \theta_1(\Gamma^{(\ell)}) = \rho^{(0)} \circ \theta(\Gamma^{(\ell)}),$$

which is an exact 1-invariant up to plain-relations. \square

Theorem 3. *A non-minimal frame invariant is an exact invariant up to a plain-relation.*

Proof. It is sufficient to consider any loopless non-minimal frame invariant $L^{(k)} \in \mathcal{L}_{N,\Delta}$, with k the number of empty vertices in $f(L^{(k)})$. Note that since $L^{(k)}$ is non-minimal, it is not a tree and therefore $k < N$. We prove the theorem by induction on k .

1. $k = 0$: In this case, $f(L^{(0)}) = L^{(0)}$. By construction, a vertex in a graph in $L^{(0)}$ is of degree no less than 2, and thus $L^{(0)}$ is already exactly invariant.
2. If any $L^{(k)}$ with $k < \alpha$ is an exact invariant plus a plain-relation: Consider any loopless non-minimal frame invariant $L^{(\alpha)}$. Form an ℓ -looped exact 1-invariant $\Gamma^{(\alpha)}$ from $f(L^{(\alpha)})$ by adding a loop to each empty vertex. By Lemma 8, $\rho^{(0)} \circ \theta(\Gamma^{(\alpha)})$ is a loopless 1-invariant, equal to $\Gamma^{(\alpha)}$ up to plain-relations. Using Lemma 7, $\rho^{(0)} \circ \theta(\Gamma^{(\alpha)}) = \sum_i F_i$, where each F_i is a frame invariant with a distinct frame. Provided $\alpha < n$, there is exactly one F_i , say \tilde{F} , with $f(\tilde{F}) = f(L^{(\alpha)})$, and all other F_i have fewer than α empty vertices in $f(F_i)$. Since all other F_i 's have fewer than α empty vertices in $f(F_i)$, they are exact 1-invariants up to a plain-relation, by the induction hypothesis. But this means that \tilde{F} is also an exact 1-invariant up to plain-relations. By Proposition 12, since \tilde{F} and $L^{(\alpha)}$ share the same frame, \tilde{F} is proportional to $L^{(\alpha)}$ and thus $L^{(\alpha)}$ is also an exact 1-invariant up to plain-relations.

By induction, $L^{(k)}$ is exactly 1-invariant up to plain-relations for any $0 \leq k < N$. \square

From the above discussion, we can conclude: The set of all exact 1-invariants with all looped vertices of degree 2 generates all non-minimal 1-invariants, up to plain-relations. An example of these graphs for $N = 3$ and $\Delta = 4$ is shown in Figure 5.

We end our discussion of the linear shift symmetry with a summary of the full classification of 1-invariants:



Figure 5: All 1-invariant terms up to total derivatives, with $N = 3$, $\Delta = 4$ and $P = 1$.

Theorem 4 (Classification of 1-invariants). *The sum with unit coefficients of all trees with n vertices is the unique 1-invariant with $\Delta = N - 1$ (up to proportionality and plain-relations). The set of all graphs consisting of N vertices, with all vertices of degree higher than 1 and any looped vertex of degree 2, generate all 1-invariants with $\Delta > N - 1$ (up to plain-relations). There are no invariants with $\Delta < N - 1$.*

B.4. Invariants from Superpositions

In this section, we describe a method of combining invariants to form other invariants. Therefore, we will need to keep track of the degree of the polynomial shifts under which the variation of various terms are taken. It is important to recall at this point that the variation map δ_P depends crucially on P . Therefore, all the different types of graphs depend on P as well. Until now, this dependence on P has been kept implicit. We will now make it explicit by referring to graphs as P -graphs.

The method of combining invariants involves the notion of superposition, defined below, which combines graphs with different values of P .

Definition 19 (Superposition of Graphs). *Given a P_A -graph Γ_A and a P_B -graph Γ_B , which each have the same value of N , the superposition of Γ_A and Γ_B is a P -graph formed by applying the the following procedure:*

1. *If there is a \times -vertex in Γ_B , replace the vertex in Γ_A that has the same label as the \times -vertex in Γ_B with a \times -vertex.*
2. *Add any \star -vertices in Γ_B to Γ_A .*
3. *Take all edges in Γ_B and add them to Γ_A , joining the same vertices as they do in Γ_B .*
4. *Identify the resulting graph as a null graph if $\deg(\times)$ is higher than P or there are two \times -vertices.*

The resulting graph is denoted by $\Gamma_A \cup \Gamma_B$.

Note that $\Gamma_A \cup \Gamma_B = \Gamma_B \cup \Gamma_A$. Note that the above definition of superposition depends on P . We will refer to such a superposition as a P -superposition.

Definition 20 (Superposition of Linear Combinations). *Given the linear combinations $L_A = \sum_{i=1}^{k_A} a_i \Gamma_i^A$ and $L_B = \sum_{i=1}^{k_B} b_i \Gamma_i^B$, where Γ_i^A, Γ_j^B are graphs with the same n , the superposition of L_A and L_B is defined as*

$$L_A \cup L_B \equiv \sum_{i=1}^{k_A} \sum_{j=1}^{k_B} a_i b_j \Gamma_i^A \cup \Gamma_j^B.$$

B.4.1. Superposition of a P -invariant and an Exact Invariant

This section involves the construction of new invariants by taking the superposition of a P -invariant with an exact invariant.

Lemma 9.

1. Given a P -graph $\Gamma \in \mathcal{L}_{N,\Delta}$ and a P_E -graph $\Gamma_E \in \mathcal{L}_{N,\Delta_E}$, where Γ_E is an exact P_E -invariant,

$$\Gamma_E \cup \delta_P(\Gamma) = \delta_{P+P_E+1}(\Gamma_E \cup \Gamma), \quad (\text{B.18})$$

where \cup denotes $(P + P_E + 1)$ -superposition.

2. Given a P -graph $\Gamma^* \in \mathcal{L}_{N,\Delta}^*$ and a P_E -graph $\Gamma_E \in \mathcal{L}_{N,\Delta_E}$, where Γ_E is an exact P_E -invariant,

$$\Gamma_E \cup \rho(\Gamma^*) = \rho(\Gamma_E \cup \Gamma^*), \quad (\text{B.19})$$

where \cup denotes $(P + P_E + 1)$ -superposition.

Proof.

1. Operationally, a graph in the LHS of (B.18) is given by substituting one \bullet -vertex, v , in Γ with a \times -vertex and then adding the edges in Γ_E to the result. Meanwhile, the RHS is given by adding the edges in Γ_E to Γ first before substituting v by a \times -vertex. Thus, (B.18) is violated only when a graph vanishes from one side and not the other. A graph vanishes from the RHS if and only if the degree of the vertex v in $\Gamma_E \cup \Gamma$ is greater than $P + P_E + 1$. If this condition holds, then the graph also vanishes from the LHS by the rules of $(P + P_E + 1)$ -superposition. A graph could also possibly vanish from the LHS if $\deg(v) > P$ in Γ . However, if $\deg(v) > P$ in Γ , then $\deg(v) > P + P_E + 1$ in $\Gamma_E \cup \Gamma$ since the degree of a vertex in Γ_E is at least $P_E + 1$ (by Corollary 4). Therefore, the conditions for the vanishing of a graph from either side of (B.18) are identical and thus the equation holds.
2. Once again, (B.19) is violated only when a graph vanishes from one side and not the other. A graph vanishes from the RHS if and only if the degree of the \times -vertex in $\rho(\Gamma_E \cup \Gamma^*)$ is greater than $P + P_E + 1$. If this condition holds, then the graph also vanishes from the LHS by the rules of $(P + P_E + 1)$ -superposition. A graph on the LHS could also possibly vanish if $\deg(\times) > P$ for a graph Γ^\times in $\rho(\Gamma^*)$. However, then $\deg(\times) > P + P_E + 1$ in $\Gamma_E \cup \Gamma^\times$, since the degree of a vertex in Γ_E is at least $P_E + 1$ (by Corollary 4). Therefore, the conditions for the vanishing of a graph from either side of (B.19) are identical and thus the equation holds. □

Now we apply Lemma 9 to prove the main result:

Theorem 5. For fixed N , the superposition of a P -invariant and an exact P_E -invariant is a $(P + P_E + 1)$ -invariant.

Proof. Denote the P -invariant by $L = \sum_{i=1}^k b_i \Gamma_i$ and the exact P_E -invariant by $L_E = \sum_{i=1}^{k_E} a_i \Gamma_i^E$. By Corollary 4, all vertices in Γ_i^E have degree greater than P_E . Since L is a P -invariant, there exists a linear combination of \star -graphs, $L^\star = \sum_{i=1}^{k^\star} c_i \Gamma_i^\star$, such that the following consistency equation holds:

$$\delta_P(L) = \rho(L^\star). \quad (\text{B.20})$$

Define $\tilde{L} \equiv L_E \cup L = \sum_{i,j} a_i b_j \Gamma_i^E \cup \Gamma_j$. Then, using Statement 1 of Lemma 9:

$$\begin{aligned} \delta_{P+P_E+1}(\tilde{L}) &= \sum_{i,j} a_i b_j \delta_{P+P_E+1}(\Gamma_i^E \cup \Gamma_j) \\ &= \sum_{i,j} a_i b_j \Gamma_i^E \cup \delta_P(\Gamma_j) = \sum_i a_i \Gamma_i^E \cup \delta_P(L) \end{aligned} \quad (\text{B.21})$$

Furthermore, define $\tilde{L}^\star \equiv \sum_{i,j} a_i c_j \Gamma_i^E \cup \Gamma_j^\star$ using $(P + P_E + 1)$ -superposition. Using Statement 2 of Lemma 9:

$$\rho(\tilde{L}^\star) = \sum_{i,j} a_i c_j \rho(\Gamma_i^E \cup \Gamma_j^\star) = \sum_{i,j} a_i c_j \Gamma_i^E \cup \rho(\Gamma_j^\star) = \sum_i a_i \Gamma_i^E \cup \rho(L^\star) \quad (\text{B.22})$$

Combining (B.20), (B.21) and (B.22) we have that $\delta_{P+P_E+1}(\tilde{L}) = \rho(\tilde{L}^\star)$ and therefore $\tilde{L} \equiv L_E \cup L$ is a $(P + P_E + 1)$ -invariant. \square

B.4.2. Superposition of Minimal Loopless 1-invariants

In this section we show that the superposition of Q minimal loopless 1-invariants results in a $(2Q - 1)$ -invariant. To prove this statement, we need to construct a linear combination of Medusas in order to write down a valid consistency equation. This construction requires intermediate \star -graphs called ‘‘hyper-Medusas’’, which we now define:

Definition 21 (Hyper-Medusa). *A hyper-Medusa is a loopless \star -graph with all \star -vertices adjacent to the \times -vertex, such that the degree of the \times -vertex $\deg(\times)$ and the number of \star -vertices $N(\star)$ satisfy $\deg(\times) \geq P + 1 - N(\star)$.*

Lemma 10. *Given M_h a hyper-Medusa, there exists a linear combination of Medusas L_M that satisfies $\rho^{(0)}(M_h) = \rho^{(0)}(L_M)$.*

Proof. Within the action of $\rho^{(0)}$, we can delete $\deg(\times) + N(\star) - P + 1 \geq 0$ \star -vertices and then add the same number of edges in M_h , yielding a linear combination of \star -graphs with exactly $P + 1 - \deg(\times)$ \star -vertices. These resulting graphs are Medusas. \square

The following definition will allow us to construct the desired hyper-Medusas:

Definition 22. *Take Γ_1 to be any \times -graph or \star -graph and for each $i = 2, \dots, Q$, take T_i to be any tree, such that Γ and T_i have the same value of n . Label the \times -vertex in Γ_1 by v^\times and define T_i^\times to be the graph formed from T_i by replacing the vertex that is labeled by v^\times with a \times -vertex. If v^\times is a leaf in T_i , then define \tilde{T}_i to be the unique $P = 1$ Medusa that is associated with T_i^\times , otherwise $\tilde{T}_i = T_i^\times$. Then we define:*

$$\chi(\Gamma_1 \cup T_2 \cup \dots \cup T_Q) \equiv \Gamma_1 \cup \tilde{T}_1 \cup \dots \cup \tilde{T}_Q.$$

Theorem 6. For fixed N , the superposition of Q minimal loopless 1-invariants is a $(2Q - 1)$ -invariant.

Proof. By Theorem 2, any minimal N -point loopless 1-invariant is equal to the sum with unit coefficients of all trees with N vertices, up to proportionality. Therefore, denote the Q copies of the minimal loopless 1-invariants by $L_N^{(c)} = \sum_{\alpha_c=1}^{N^{N-2}} T_{\alpha_c}^{(c)}$, for $c = 1, \dots, Q$. We add an additional structure to all graphs in this proof: We color all edges in all graphs in $L_N^{(c)}$ by a distinct color (c). Throughout this proof, two graphs are equal if and only if they are the same graph and, in addition, their edges are the same colors. Taking into account this coloring, all of the plain-graphs in $L \equiv \bigcup_{c=1}^Q L_N^{(c)}$ now have unit coefficients, and the number of these plain-graphs is $(N^{N-2})^Q$. Moreover, L is the sum over $\alpha_1, \dots, \alpha_Q$ of all such $T_{\alpha_1}^{(1)} \cup T_{\alpha_2}^{(2)} \cup \dots \cup T_{\alpha_Q}^{(Q)}$'s with unit coefficients. By Theorem 2, there is a unique linear combination of Medusas $\sum_{\beta_c} M_{\beta_c}^{(c)}$ satisfying

$$\delta_1 \left(L_N^{(c)} \right) = \delta_1 \left(\sum_{\alpha_c=1}^{N^{N-2}} T_{\alpha_c}^{(c)} \right) = \rho^{(0)} \left(\sum_{\beta_c=1}^{N(N-1)^{N-3}} M_{\beta_c}^{(c)} \right),$$

where each $T_{\alpha_c}^{(c)}$ is a distinct tree and each $M_{\beta_c}^{(c)}$ is a distinct $P = 1$ Medusa, consisting of a subgraph tree and a disconnected subgraph $\star \text{---} \otimes$. In the following, we take the limit $P \rightarrow \infty$, so that no graph vanishes. Note that we have

$$\begin{aligned} \sum_{\alpha_1} \delta_\infty \left(T_{\alpha_1}^{(1)} \cup T_{\alpha_2}^{(2)} \cup \dots \cup T_{\alpha_Q}^{(Q)} \right) &= \sum_{\alpha_1} \left(\delta_\infty(T_{\alpha_1}^{(1)}) \right) \cup T_{\alpha_2}^{(2)} \cup \dots \cup T_{\alpha_Q}^{(Q)} \\ &= \sum_{\beta_1} \rho^{(0)} \left(M_{\beta_1}^{(1)} \right) \cup T_{\alpha_2}^{(2)} \cup \dots \cup T_{\alpha_Q}^{(Q)} + \sum_{\alpha_1} (\delta_\infty - \delta_1)(T_{\alpha_1}^{(1)}) \cup T_{\alpha_2}^{(2)} \cup \dots \cup T_{\alpha_Q}^{(Q)}. \end{aligned} \quad (\text{B.23})$$

Define $X_L \equiv \sum_{\beta_1, \alpha_2, \dots, \alpha_Q} M_{\beta_1}^{(1)} \cup T_{\alpha_2}^{(2)} \cup \dots \cup T_{\alpha_Q}^{(Q)}$ and X_R to be the sum with unit coefficients of all distinct graphs contained in $\sum_{\beta_1, \alpha_2, \dots, \alpha_Q} \chi(M_{\beta_1}^{(1)} \cup T_{\alpha_2}^{(2)} \cup \dots \cup T_{\alpha_Q}^{(Q)})$. In the following, we show that

$$\rho^{(0)}(X_L) = \rho^{(0)}(X_R). \quad (\text{B.24})$$

Since $T_{\alpha_c}^{(c)}$, $\alpha_c = 1, \dots, N^{N-2}$, and $M_{\beta_c}^{(c)}$, $\beta_c = 1, \dots, N(N-1)^{N-3}$, are all distinct from each other, all elements in X_L and X_R have unit coefficient. Therefore, it will suffice to show that any graph in $\rho^{(0)}(X_R)$ is also in $\rho^{(0)}(X_L)$, and vice versa.

RHS contains LHS: Let Γ^\times be a \times -graph in $\rho^{(0)}(X_L)$. Then, Γ^\times is contained in $\rho^{(0)}(M_{\beta_1}^{(1)} \cup T_{\alpha_2}^{(2)} \cup \dots \cup T_{\alpha_Q}^{(Q)})$ for some $\beta_1, \alpha_2, \dots, \alpha_Q$. The \star -graph, $M_{\beta_1}^{(1)} \cup T_{\alpha_2}^{(2)} \cup \dots \cup T_{\alpha_Q}^{(Q)}$ induces a unique $\chi(M_{\beta_1}^{(1)} \cup T_{\alpha_2}^{(2)} \cup \dots \cup T_{\alpha_Q}^{(Q)})$, such that all \times -graphs in $\rho^{(0)}(M_{\beta_1}^{(1)} \cup T_{\alpha_2}^{(2)} \cup \dots \cup T_{\alpha_Q}^{(Q)})$ (including Γ^\times) are contained in $\rho^{(0)} \circ \chi(M_{\beta_1}^{(1)} \cup T_{\alpha_2}^{(2)} \cup \dots \cup T_{\alpha_Q}^{(Q)})$. Therefore, Γ^\times is in $\rho^{(0)}(X_R)$ and $\rho^{(0)}(X_R)$ contains $\rho^{(0)}(X_L)$.

LHS contains RHS: Let Γ^\times be a \times -graph in $\rho^{(0)}(X_R)$. Then, Γ^\times is contained in $\rho^{(0)} \circ \chi(M_{\beta_1}^{(1)} \cup T_{\alpha_2}^{(2)} \cup \dots \cup T_{\alpha_Q}^{(Q)})$ for some $\beta_1, \alpha_2, \dots, \alpha_Q$. In particular, Γ^\times is contained in some

$\rho^{(0)}(M_{\beta'_1}^{(1)} \cup T_{\alpha'_2}^{(2)} \cup \dots \cup T_{\alpha'_Q}^{(Q)})$ with $T_{\alpha'_2}^{(2)} \cup \dots \cup T_{\alpha'_Q}^{(Q)}$ in $\rho^{(0)} \circ \chi(T_{\alpha'_2}^{(2)} \cup \dots \cup T_{\alpha'_Q}^{(Q)})$. Since $M_{\beta'_1}^{(1)} \cup T_{\alpha'_2}^{(2)} \cup \dots \cup T_{\alpha'_Q}^{(Q)}$ is in X_L , Γ^\times is in $\rho^{(0)}(X_L)$ and $\rho^{(0)}(X_L)$ contains $\rho^{(0)}(X_R)$.

From (B.24) we obtain

$$\sum_{\beta_1, \dots, \alpha_Q} \rho^{(0)} \left(M_{\beta_1}^{(1)} \right) \cup T_{\alpha_2}^{(2)} \cup \dots \cup T_{\alpha_Q}^{(Q)} = \rho^{(0)}(X_R). \quad (\text{B.25})$$

Similarly,

$$\sum_{\alpha_1, \dots, \alpha_Q} (\delta_\infty - \delta_1) T_{\alpha_1}^{(1)} \cup T_{\alpha_2}^{(2)} \cup \dots \cup T_{\alpha_Q}^{(Q)} = \rho^{(0)}(\tilde{X}_R), \quad (\text{B.26})$$

with \tilde{X}_R given by the sum with unit coefficients of all graphs contained in

$$\sum_{\alpha_1, \dots, \alpha_Q} \chi \left((\delta_\infty - \delta_1) T_{\alpha_1}^{(1)} \cup T_{\alpha_2}^{(2)} \cup \dots \cup T_{\alpha_Q}^{(Q)} \right).$$

Therefore, by (B.23), (B.25) and (B.26), we conclude that

$$\delta_\infty(L) = \sum_{\alpha_1, \dots, \alpha_Q} \delta_\infty \left(T_{\alpha_1}^{(1)} \cup T_{\alpha_2}^{(2)} \cup \dots \cup T_{\alpha_Q}^{(Q)} \right) = \rho^{(0)}(X_R + \tilde{X}_R). \quad (\text{B.27})$$

Finally, switch back to $P = 2Q - 1$. Then graphs with $\deg(\times) > 2Q - 1$ will vanish simultaneously on both sides of (B.27), and thus, in $P = 2Q - 1$:

$$\delta_{2Q-1}(L) = \rho^{(0)}(X_R + \tilde{X}_R). \quad (\text{B.28})$$

Next we show that any graph, Γ , in $X_R + \tilde{X}_R$ is a hyper-Medusa. By construction, Γ results from the superposition of graphs with either a \times -vertex of degree 1 joined to a \star -vertex or a \times -vertex of degree larger than 1. Therefore, $\deg(\times)$ in Γ satisfies $\deg(\times) \geq N(\star) + 2(Q - N(\star))$. So, with $P = 2Q - 1$, $\deg(\times) \geq P + 1 - N(\star)$ and Γ is a hyper-Medusa. Hence, by Lemma 10, there exists a linear combination, L_M , of Medusas, such that $\rho^{(0)}(X_R + \tilde{X}_R) = \rho^{(0)}(L_M)$. Therefore, combined with (B.28), we obtain $\delta_{2Q-1}(L) = \rho^{(0)}(L_M)$, which proves that L is a $(2Q - 1)$ -invariant. \square

We end our search for P -invariants with a summary of all invariants that we found:

Theorem 7. *For fixed N , the superposition of any exact P_E -invariant with the superposition of Q minimal loopless 1-invariants results in a P -invariant, provided $P_E + 2Q \geq P$.⁸*

We conjecture that the above theorem captures all P -invariants, up to total derivatives. Since we have classified all exact invariants and all 1-invariants, it is straightforward to construct the P -invariants in the above theorem for any specific case.

⁸This theorem applies even for $P_E < 0$. Recall that, by Corollary 5, an exact P -invariant for $P < 0$ is just any possible linear combination of plain-graphs. For example, the plain-graph consisting only of empty vertices is an exact P -invariant for any $P < 0$.

Note that we have classified exact invariants and 1-invariants using the two parameters, N (number of vertices) and Δ (number of edges). Finite connected graphs can always be embedded on a Riemann surface of some genus, in which case Euler's theorem relates N , Δ and the number of faces F of the embedding to the genus g of the surface. Therefore, one could also use the parameters N and F instead to classify invariants⁹. Any finite graph that can be embedded into a 2-sphere can also be embedded into a plane, and is known as a planar graph. In particular, this is true for any graph with $N \leq 4$ and also for any tree. Furthermore, any superposition of planar graphs is again a planar graph. The number of faces of these planar graphs is exactly the number of "loops" when the graph is interpreted as a Feynman diagram¹⁰. One can check this statement for all of the examples in §4.4 since they were all generated by superposition of planar graphs. Note that, in §4.4, except for $P = 0$ (which is a trivial case), all superpositions involve trees, so that all superposed graphs are connected. For example, all of the graphs in Figure 2 have three faces when embedded into a plane. Indeed, when interpreted as Feynman diagrams, these graphs have three "loops". In general, the superposition of Q minimal loopless 1-invariants yields graphs have F "loops" as Feynman diagrams, where F is given by $F = (Q - 1)(N - 1)$. Theorem 7 says that these superpositions will be P -invariant for $P \leq 2Q - 1$. For example, the superposition of three minimal loopless 1-invariants with $N = 4$ produces a 5-invariant with 6 faces.

B.5. Unlabeled Invariants

So far we have been dealing entirely with labeled graphs, which represent algebraic terms where each ϕ is given a distinct label. But we are primarily interested in invariants where all ϕ 's are the same. These are represented by *unlabeled* graphs, that is, where isomorphic graphs are identified with each other. One may wonder whether or not the labeled P -invariants capture all of the unlabeled ones. The following proposition addresses this question, and shows that our restriction to labeled P -invariants still allows us to find all unlabeled P -invariants.

Proposition 13. *Given an unlabeled P -invariant L_{unlab} , there exists a labeled P -invariant L_{lab} , such that L_{lab} reduces to an integer multiple of L_{unlab} once the labels are removed.*

Proof. Define $L_{\text{unlab}}^\times = \delta(L_{\text{unlab}})$, where $\delta(L_{\text{unlab}})$ contains $\delta(\Gamma_{\text{unlab}})$ for all Γ_{unlab} in L_{unlab} . Label L_{unlab} (i.e., label the vertices from 1 to N) to form L_{lab} . This labeling is fiducial since we will eventually sum over all possible labelings. Do the same for L_{unlab}^\times to form L_{lab}^\times . Define $L_{\text{lab}'}^\times = \delta(L_{\text{lab}})$, which is a labeling of L_{unlab}^\times , possibly distinct from L_{lab}^\times . However, if $\Gamma_{\text{lab}}^\times$ in L_{lab}^\times and $\Gamma_{\text{lab}'}^\times$ in $L_{\text{lab}'}^\times$ reduce to the same $\Gamma_{\text{unlab}}^\times$ in L_{unlab}^\times once the labels are removed, then $\Gamma_{\text{lab}}^\times$ and $\Gamma_{\text{lab}'}^\times$ are simply related by a permutation. Therefore,

$$\sum_{\sigma \in S_N} \sigma \circ \delta(L_{\text{lab}}) = \sum_{\sigma \in S_N} \sigma(L_{\text{lab}}^\times) = \sum_{\sigma \in S_N} \sigma(L_{\text{lab}'}^\times), \quad (\text{B.29})$$

where S_N is the group of permutations on the N vertices.

⁹In principle, Δ and F could also be used, but this seems less natural.

¹⁰Thanks to Kurt Hinterbichler for bringing this issue to our attention at the 2014 BCTP Tahoe Summit.

Since L_{unlab} is P -invariant, there exists L_{unlab}^* such that $\delta(L_{\text{unlab}}) = \rho(L_{\text{unlab}}^*)$. Label L_{unlab}^* to form L_{lab}^* and define $L_{\text{lab}''}^\times = \rho(L_{\text{lab}}^*)$. Generically, there can be cancellations between isomorphic graphs in $L_{\text{lab}''}^\times$, once the labels are removed, since one \times -graph can be associated with more than one \star -graph. Therefore, $L_{\text{lab}''}^\times$ is not necessarily a labeling of L_{unlab}^\times . Nevertheless, if $\alpha \Gamma_{\text{unlab}}^\times$ appears in L_{unlab}^\times with $\alpha \neq 0$, then all of the graphs, $\Gamma_1^\times, \dots, \Gamma_k^\times$ in $L_{\text{lab}''}^\times$ which are isomorphic to $\Gamma_{\text{unlab}}^\times$ appear in $L_{\text{lab}''}^\times$ as a linear combination $\sum_{i=1}^k \alpha_i \Gamma_i^\times$ with $\sum_{i=1}^k \alpha_i = \alpha$. Conversely, if $\sum_{i=1}^k \alpha_i \Gamma_i^\times$ appears in $L_{\text{lab}''}^\times$, but the graph, $\Gamma_{\text{unlab}}^\times$, to which Γ_i^\times reduces once the labels are removed, does not appear in L_{unlab}^\times , then $\sum_{i=1}^k \alpha_i = 0$. Therefore,

$$\sum_{\sigma \in S_N} \sum_{i=1}^k \alpha_i \cdot \sigma(\Gamma_i^\times) = \sum_{i=1}^k \alpha_k \sum_{\sigma \in S_N} \sigma(\Gamma_{\text{lab}}^\times) = \alpha \sum_{\sigma \in S_N} \sigma(\Gamma_{\text{lab}}^\times),$$

which implies

$$\sum_{\sigma \in S_N} \sigma \circ \rho(L_{\text{lab}}^*) = \sum_{\sigma \in S_N} \sigma(L_{\text{lab}''}^\times) = \sum_{\sigma \in S_N} \sigma(L_{\text{lab}}^\times). \quad (\text{B.30})$$

Combining Eqs. (B.29) and (B.30) with the facts that $\sigma \circ \delta = \delta \circ \sigma$ and $\sigma \circ \rho = \rho \circ \sigma$ for each $\sigma \in S_N$, yields the desired labeled consistency equation:

$$\delta \left(\sum_{\sigma \in S_N} \sigma(L_{\text{lab}}) \right) = \rho \left(\sum_{\sigma \in S_N} \sigma(L_{\text{lab}}^*) \right).$$

$\sum_{\sigma \in S_N} \sigma(L_{\text{lab}})$ is P -invariant and reduces to $N! L_{\text{unlab}}$ once the labels are removed. \square

C. Coset Construction

The standard technique for finding terms which are invariant under a nonlinear realization of a symmetry is to use a coset construction [24–27]. In this appendix we explore the connection between our invariant Lagrangians and this construction. Although we find that the coset construction can reproduce some of the invariants that we have discovered, using this method is computationally difficult when compared to the graphical method introduced in this paper.

We first review the coset construction applied to the polynomial shift symmetry as presented in [18, 28]. In dimension D , consider the polynomial shift transformations of the Goldstone fields defined in (B.1), accompanied with space-time translations and spatial rotations. Denote the corresponding generators by $Z, Z^i, \dots, Z^{i_1 \dots i_P}$ for polynomial shifts, \mathcal{P}_i for spacial translations, \mathcal{P}_0 for temporal translations, and J^{ij} for spatial rotations. Note that there are no boost symmetries. For the nonlinear realization of space-time symmetry, the translation generators are treated as the broken generators [26, 27]. The Goldstone fields transform as

$$\delta_{\mathcal{P}_i} \phi = \partial_i \phi, \quad \delta_Z \phi = 1, \quad \delta_{Z^{i_1 \dots i_k}} \phi = \frac{1}{k!} x^{i_1} \dots x^{i_k}, \quad k = 1, \dots, P.$$

The commutators between the operators can be readily calculated,

$$[\mathcal{P}_i, Z] = 0, \quad [\mathcal{P}_i, Z^{i_1 \dots i_k}] = -i \sum_j \frac{1}{k} \delta_i^j Z^{i_1 \dots \hat{j} \dots i_k}, \quad [Z^{i_1 \dots i_k}, Z^{j_1 \dots j_\ell}] = 0,$$

where \hat{j} means that the index j is omitted.

The commutators above given by the generators $\mathcal{P}_0, \mathcal{P}_i, J^{ij}, Z$ and $Z^{i_1 \dots i_k}, k = 1, \dots, P$ define the Lie algebra of a Lie group G , and \mathcal{P}_0 and J^{ij} correspond to the unbroken normal subgroup H . Take left invariant differential N -forms on G/H to be N -cochains, and take the coboundary operator $d^{(k)}$ to be the exterior derivative of differential forms. Denote the group of N -cocycles by $\mathcal{Z}^k = \text{Ker } d^{(k)}$, and the group of k -coboundaries by $\mathcal{B}^k = \text{Im } d^{(k-1)}$. The Chevalley-Eilenberg cohomology group $\mathcal{E}^k(G/H)$ is defined to be

$$\mathcal{E}^k(G/H) = \mathcal{Z}^k / \mathcal{B}^k,$$

which is isomorphic to the Lie algebra cohomology $\mathcal{H}_0^k(G/H; \mathbb{Z})$. (See [29] for details.)

We associate the generator Z with the Goldstone field ϕ . To each generator $Z^{i_1 \dots i_k}, k = 1, \dots, P$ we associate a symmetric k -tensor field $\phi_{i_1 \dots i_k}$. Indices can be lowered or raised by Kronecker delta symbols. The coset space is parametrized by

$$g = \exp(i\mathcal{P}_i x^i) \exp\left(iZ\phi + i \sum_{k=1}^P Z^{i_1 \dots i_k} \phi_{i_1 \dots i_k}\right).$$

The Maurer-Cartan form is

$$-ig^{-1}dg = \mathcal{P}_i dx^i + Z(d\phi + \phi_i dx^i) + \sum_{n=1}^{P-1} Z^{i_1 \dots i_n} (d\phi_{i_1 \dots i_n} + \phi_{i_1 \dots i_n i} dx^i) + Z^{i_1 \dots i_P} d\phi_{i_1 \dots i_P}.$$

Therefore, the basis dual to the generators is

$$\begin{aligned} \omega_{\mathcal{P}}^i &= dx^i, & \omega_{i_1 \dots i_P} &= d\phi_{i_1 \dots i_P}, \\ \omega &= d\phi + \phi_i dx^i, & \omega_{i_1 \dots i_k} &= d\phi_{i_1 \dots i_k} + \phi_{i_1 \dots i_k i} dx^i, \quad k = 1, \dots, P-1. \end{aligned} \quad (\text{C.1})$$

Moreover,

$$\begin{aligned} d\omega_{\mathcal{P}}^i &= 0, & d\omega_{i_1 \dots i_P} &= 0, \\ d\omega &= d\phi_i \wedge dx^i, & d\omega_{i_1 \dots i_k} &= d\phi_{i_1 \dots i_k i} \wedge dx^i, \quad k = 1, \dots, P-1. \end{aligned}$$

The inverse Higgs constraints [30, 31] imply the vanishing of ω and $\omega_{i_1 \dots i_k}$ ($k < P$) in (C.1):

$$\phi_{i_1 \dots i_k} = (-1)^k \partial_{i_1} \dots \partial_{i_k} \phi, \quad k = 1, \dots, P. \quad (\text{C.2})$$

Having reviewed the coset construction, we now present examples for $P = 2$ and 3 (the $P = 1$ scenario is essentially the same as the Galileon case [28]).

$P=2$ Case: For $N = 3$, the cohomology group is trivial for $D < 2$. Therefore, let us start with the simplest nontrivial case, $D = 2$. We are looking for a closed form involving the

wedge of three ω 's, which are not $\omega_{\mathcal{P}}$. There is one independent cohomology element, with the lowest number of indices on ω 's:

$$\Omega_3 = \epsilon_{ij} \omega_{ab} \wedge \omega_{ia} \wedge \omega_{jb} = d(\epsilon_{ij} \phi_{ab} d\phi_{ia} \wedge d\phi_{jb}) \equiv d\beta_2.$$

These expressions can be extended to $D \geq 2$:

$$\begin{aligned} \Omega_{D+1} &= \epsilon_{ijs_3 \dots s_D} \omega_{ab} \wedge \omega_{ia} \wedge \omega_{jb} \wedge \omega_{\mathcal{P}}^{s_3} \wedge \dots \wedge \omega_{\mathcal{P}}^{s_D}, \\ \beta_D &= \epsilon_{ijs_3 \dots s_D} \phi_{ab} d\phi_{ia} \wedge d\phi_{jb} \wedge dx^{s_3} \wedge \dots \wedge dx^{s_D}. \end{aligned}$$

Taking the pullback of β_D to the spacetime manifold and then applying the inverse Higgs constraints in (C.2) gives a term proportional to

$$\epsilon_{ijs_3 \dots s_D} \epsilon_{kls_3 \dots s_D} \partial_a \partial_b \phi \partial_i \partial_k \partial_a \phi \partial_j \partial_\ell \partial_b \phi,$$

which is already contained in [18]. One can verify that this is equivalent up to integration by parts and overall prefactor to the invariant in (4.10). That term was found to be invariant for $P = 3$, and is therefore also invariant for $P = 2$.

Next, consider $N = 4$. The simplest nontrivial case is $D = 3$. We seek a closed 4-form given as the wedge of four ω 's, which are not $\omega_{\mathcal{P}}$. There is one independent cohomology element, with the lowest number of indices on ω 's:

$$\begin{aligned} \Omega'_4 &= \epsilon_{ijk} \omega_a \wedge \omega_{ia} \wedge \omega_{jb} \wedge \omega_{kb} \\ &= d \left[\epsilon_{ijk} \phi_{ac} \left(\frac{1}{2} \phi_{ac} d\phi_{jb} + \phi_{bc} d\phi_{ja} \right) \wedge d\phi_{kb} \wedge dx_i \right] \equiv d\beta'_3 \end{aligned}$$

These expressions can be extended to $D \geq 3$:

$$\begin{aligned} \Omega'_{D+1} &= \epsilon_{ijk s_4 \dots s_D} \omega_a \wedge \omega_{ia} \wedge \omega_{jb} \wedge \omega_{kb} \wedge \omega_{\mathcal{P}}^{s_4} \wedge \dots \wedge \omega_{\mathcal{P}}^{s_D}, \\ \beta'_D &= \epsilon_{ijk s_4 \dots s_D} \phi_{ac} \left(\frac{1}{2} \phi_{ac} d\phi_{jb} + \phi_{bc} d\phi_{ja} \right) \wedge d\phi_{kb} \wedge dx^i \wedge dx^{s_4} \wedge \dots \wedge dx^{s_D}. \end{aligned}$$

Taking the pullback of β'_D to the spacetime manifold and then applying the inverse Higgs constraints in (C.2) gives a term proportional to

$$\epsilon_{ijs_3 \dots s_D} \epsilon_{kls_3 \dots s_D} \partial_{(a} \partial_b \phi \partial_c) \partial_j \partial_\ell \phi \partial_a \partial_b \phi \partial_c \partial_i \partial_k \phi.$$

One can verify that this is equivalent up to integration by parts and an overall prefactor to the invariant in (4.7).

P=3 Case: Let us focus on $N = 3$. Again, we start with $D = 2$. There is one independent cohomology element:

$$\begin{aligned} \Omega_3 &= \epsilon_{ij} (\omega_{ab} \wedge \omega_{ia} \wedge \omega_{jb} + 2\omega_a \wedge \omega_{ib} \wedge \omega_{jab} - 2\omega_a \wedge \omega_{ia} \wedge \omega_{jbb} \\ &\quad - \omega \wedge \omega_{iab} \wedge \omega_{jab} + \omega \wedge \omega_{iaa} \wedge \omega_{jbb}). \end{aligned}$$

It is quite a challenge to determine the potential, β_2 , for this Ω_3 . One can appreciate the power of the graphical method at this point: We have already determined that there is

one independent 3-invariant with $N = 3$. Therefore, we can immediately conclude without calculation that the pullback of β_2 must be proportional to the invariant in (4.3) up to total derivatives. Again, Ω_3 can be generalized to $D \geq 2$ by wedging the appropriate number of $\omega_{\mathcal{P}}$'s on the end:

$$\Omega_{D+1} = \epsilon_{ijs_3\dots s_D} (\omega_{ab} \wedge \omega_{ia} \wedge \omega_{jb} + 2\omega_a \wedge \omega_{ib} \wedge \omega_{jab} - 2\omega_a \wedge \omega_{ia} \wedge \omega_{jbb} - \omega \wedge \omega_{iab} \wedge \omega_{jab} + \omega \wedge \omega_{iaa} \wedge \omega_{jbb}) \wedge \omega_{\mathcal{P}}^{s_3} \wedge \dots \wedge \omega_{\mathcal{P}}^{s_D}.$$

References

- [1] G. 't Hooft, *Naturalness, chiral symmetry, and spontaneous chiral symmetry breaking*, *NATO ASI Series B* **59** (1980) 135.
- [2] P. Hořava, *Quantum gravity at a Lifshitz point*, *Phys.Rev.* **D79** (2009) 084008, [[arXiv:0901.3775](#)].
- [3] P. Hořava, *Membranes at quantum criticality*, *JHEP* **0903** (2009) 020, [[arXiv:0812.4287](#)].
- [4] S. Mukohyama, *Hořava-Lifshitz cosmology: A review*, *Class.Quant.Grav.* **27** (2010) 223101, [[arXiv:1007.5199](#)].
- [5] J. Ambjørn, A. Görlich, S. Jordan, J. Jurkiewicz, and R. Loll, *CDT meets Hořava-Lifshitz gravity*, *Phys.Lett.* **B690** (2010) 413–419, [[arXiv:1002.3298](#)].
- [6] P. Hořava, *General covariance in gravity at a Lifshitz point*, *Class.Quant.Grav.* **28** (2011) 114012, [[arXiv:1101.1081](#)].
- [7] C. Anderson, S. J. Carlip, J. H. Cooperman, P. Hořava, R. K. Kommu, et al., *Quantizing Horava-Lifshitz gravity via causal dynamical triangulations*, *Phys.Rev.* **D85** (2012) 044027, [[arXiv:1111.6634](#)].
- [8] S. Janiszewski and A. Karch, *String theory embeddings of nonrelativistic field theories and their holographic Hořava gravity duals*, *Phys.Rev.Lett.* **110** (2013), no. 8 081601, [[arXiv:1211.0010](#)].
- [9] S. Janiszewski and A. Karch, *Non-relativistic holography from Hořava gravity*, *JHEP* **1302** (2013) 123, [[arXiv:1211.0005](#)].
- [10] T. Griffin, P. Hořava, and C. M. Melby-Thompson, *Lifshitz gravity for Lifshitz holography*, *Phys.Rev.Lett.* **110** (2013) 081602, [[arXiv:1211.4872](#)].
- [11] T. Griffin, K. T. Grosvenor, P. Hořava, and Z. Yan, *Multicritical symmetry breaking and naturalness of slow Nambu-Goldstone bosons*, *Phys.Rev.* **D88** (2013) 101701, [[arXiv:1308.5967](#)].
- [12] H. Watanabe and H. Murayama, *Unified description of Nambu-Goldstone bosons without Lorentz invariance*, *Phys.Rev.Lett.* **108** (2012) 251602, [[arXiv:1203.0609](#)].
- [13] A. Nicolis, R. Rattazzi, and E. Trincherini, *The Galileon as a local modification of gravity*, *Phys.Rev.* **D79** (2009) 064036, [[arXiv:0811.2197](#)].
- [14] T. Griffin, K. T. Grosvenor, P. Hořava, and Z. Yan, *Cascading multicriticality in nonrelativistic spontaneous symmetry breaking*, (2015) [[arXiv:1507.06992](#)].
- [15] P. Hořava and C. M. Melby-Thompson, *General covariance in quantum gravity at a Lifshitz point*, *Phys.Rev.* **D82** (2010) 064027, [[arXiv:1007.2410](#)].

- [16] P. Hořava and C. M. Melby-Thompson, *Anisotropic conformal infinity*, *Gen. Rel. Grav.* **43** (2010) 1391, [[arXiv:0909.3841](#)].
- [17] S. Kachru, X. Liu, and M. Mulligan, *Gravity duals of Lifshitz-like fixed points*, *Phys.Rev.* **D78** (2008) 106005, [[arXiv:0808.1725](#)].
- [18] K. Hinterbichler and A. Joyce, *Goldstones with extended shift symmetries*, *Int.J.Mod.Phys.* **D23** (2014) 1443001, [[arXiv:1404.4047](#)].
- [19] N. Mermin and H. Wagner, *Absence of ferromagnetism or antiferromagnetism in one-dimensional or two-dimensional isotropic Heisenberg models*, *Phys.Rev.Lett.* **17** (1966) 1133–1136.
- [20] P. Hohenberg, *Existence of long-range order in one and two dimensions*, *Phys.Rev.* **158** (1967) 383–386.
- [21] S. R. Coleman, *There are no Goldstone bosons in two dimensions*, *Commun.Math.Phys.* **31** (1973) 259–264.
- [22] H. Watanabe and H. Murayama, *Effective Lagrangian for Nonrelativistic Systems*, *Phys.Rev.* **X4** (2014), no. 3 031057, [[arXiv:1402.7066](#)].
- [23] J. A. Bondy and U. Murty, *Graph theory (graduate texts in mathematics)*, Springer, 2008.
- [24] S. R. Coleman, J. Wess, and B. Zumino, *Structure of phenomenological Lagrangians. 1.*, *Phys.Rev.* **177** (1969) 2239–2247.
- [25] J. Callan, Curtis G., S. R. Coleman, J. Wess, and B. Zumino, *Structure of phenomenological Lagrangians. 2.*, *Phys.Rev.* **177** (1969) 2247–2250.
- [26] D. V. Volkov, *Phenomenological lagrangians*, *Fiz.Elem.Chast.Atom.Yadra* **4** (1973) 3–41.
- [27] V. Ogievetsky, *Nonlinear realizations of internal and space-time symmetries*, *Proc. of X-th Winter School of Theoretical Physics in Karpacz* **1** (1974).
- [28] G. Goon, K. Hinterbichler, A. Joyce, and M. Trodden, *Galileons as Wess-Zumino terms*, *JHEP* **1206** (2012) 004, [[arXiv:1203.3191](#)].
- [29] J. A. de Azcárraga and J. M. Izquierdo, *Lie groups, Lie algebras, cohomology and some applications in physics*. Cambridge University Press, 1998.
- [30] E. A. Ivanov and V. I. Ogievetskii, *Inverse Higgs effect in nonlinear realizations*, *Theor. Math. Phys.* **25** (1975), no. 2 1050.
- [31] T. Brauner and H. Watanabe, *Spontaneous breaking of spacetime symmetries and the inverse Higgs effect*, *Phys.Rev.* **D89** (2014) 085004, [[arXiv:1401.5596](#)].